NASA CONTRACTOR REPORT

NASA CR-2819

NASA CR-2819

VORTICITY IMBALANCE AND STABILITY IN RELATION TO CONVECTION

William L. Read and James R. Scoggins

NATIONAL AERONAUTICS AND SPACE ADMINISTRATION • WASHINGTON, D. C. • MARCH 1977

1. REPORT NO. NASA CR-2819	2. GOVERNMENT ACCESSION NO.	3. RECIPIEN.
4. TITLE AND SUBTITLE Vorticity Imbalance and Stability in Relation to Convection		5. REPORT DATE March 1977
		6. PERFORMING ORGANIZATION CODE
7. AUTHOR(S) William L. Read and James R. Scoggins		8. PERFORMING ORGANIZATION REPORT # M-215
9. PERFORMING ORGANIZATION NAME AND ADDRESS Center for Applied Geosciences College of Geosciences Texas A&M University College Station, Texas 77843		10. WORK UNIT NO.
		11. CONTRACT OR GRANT NO. NAS8-31773
		13. TYPE OF REPORT & PERIOD COVERED
12. SPONSORING AGENCY NAME AND ADDRESS National Aeronautics and Space Administration Washington, D. C. 20546		Contractor
		14. SPONSORING AGENCY CODE

15. SUPPLEMENTARY NOTES

16. ABSTRACT

A complete synoptic-scale vorticity budget has been related to convective storm development in the eastern two-thirds of the United States during NASA's fourth Atmospheric Variability Experiment (AVE IV). The 3-h sounding interval permitted a study of time changes of the vorticity budget in areas of convective storms. Results of analyses revealed significant changes in values of terms in the vorticity equation at different stages of squall line development. Average budgets for all areas of convection indicate systematic imbalance in the terms in the vorticity equation. This imbalance resulted primarily from sub-grid scale processes.

Potential instability in the lower troposphere was analyzed in relation to the development of convective activity. Instability was related to areas of convection; however, instability alone was inadequate for forecast purposes. Combinations of stability and terms in the vorticity equation in the form of indices succeeded in depicting areas of convection better than any one item separately.

17. KEY WORDS	18. DISTRIBUTION STATEMENT
	47

19. SECURITY CLASSIF. (of this report)	20. SECURITY CLASSIF. (of this page)	21. NO. OF PAGES	22. PRICE
Unclassified	Unclassified	118	$5.50

*For sale by the National Technical Information Service, Springfield, Virginia 22161

FOREWORD

This report is one of several to be published from research conducted under NASA Contract NAS8-31773 entitled, "Relationships Between Severe Storms and Their Environment." This effort is sponsored by the NASA Office of Applications under the direction of Marshall Space Flight Center's Aerospace Environment Division. The results presented in this report represent only a portion of the total research effort. Data used in the report were taken from the AVE IV Experiment conducted during the period beginning at 0000 GMT on 24 April 1975 and ending at 1200 GMT on 25 April 1975.

TABLE OF CONTENTS

LIST OF FIGURES

LIST OF TABLES

VORTICITY IMBALANCE AND STABILITY IN RELATION TO CONVECTION

by

William L. Read[1]

and

James R. Scoggins[2]

Center for Applied Geosciences
Texas A&M University

1.   INTRODUCTION

a.   Statement of problem

Operational and research branches of meteorology require an understanding of the physical processes involved in systems of thunderstorms. Studies ranging from the global circulation to the small-scale forecast problem are all in some way concerned with convection. Palmén and Newton (1969) give a summary of the studies which clearly point up convection as an important mechanism for transfer of energy from the boundary layer to the upper troposphere. Synoptic-scale extratropical cyclones undergo considerable development due to the release of latent heat by organized convection within their circulations (Danard, 1964). For the forecaster in the eastern two thirds of the United States, thunderstorms are a major concern in synoptic and local forecasts.

Numerical forecasts that accurately depict the large-scale flow patterns often fail to produce adequate forecasts of parameters related to thunderstorm development. Conversely, the effect of areas of organized convection on the large-scale flow pattern is also inadequately handled by these numerical models. There are two factors usually presented to explain why these numerical forecasts fail, namely, an incomplete knowledge of the physical processes involved, and inaccurate initialization of the models due to limitations in the observational data. The first problem involves an understanding of the interrelationships

---

[1] Graduate Assistant

[2] Professor of Meteorology

between large- and small-scale processes. To assume that forecasts of large-scale systems can accurately predict areas favorable for thunderstorm development implies that relationships exist between systems of different scale. The second factor includes measurement errors and incomplete resolution of small-scale systems. These limitations have an effect on determining physical relationships between scales, as well as on the accuracy of numerical forecasts. The principal problem then, is to investigate processes relating the large-scale flow to the development of thunderstorm systems within the limitations of the observational network.

In this study synoptic-scale processes related to thunderstorm development will be investigated using the fourth Atmospheric Variability Experiment (AVE IV) data. These data were obtained over the standard National Weather Service upper air network by the National Aeronautics and Space Administration (NASA) on 24 and 25 April 1975. The 3- and 6-h sounding intervals used in the experiment give an opportunity for better determining changes in time of synoptic-scale features than would standard 12-h soundings.

b. Objectives

The primary objective of this research is to investigate from 3-h rawinsonde data the synoptic-scale kinematic and thermodynamic properties of the atmosphere preceding and accompanying thunderstorms. First, individual terms of the complete vorticity equation will be evaluated in order to determine the synoptic-scale vorticity budget in a thunderstorm environment. Next, a measure of convective instability in the lower troposphere and low-level moisture will be added to determine the relationship of these large-scale atmospheric properties to intense convection. Third, time changes of the above quantities will be investigated for their relationship to thunderstorms. Finally, parameters of kinematics, moisture, and stability will be combined in a single parameter to serve as an index to aid in analyzing and forecasting the thunderstorm environment.

2. REVIEW OF PREVIOUS STUDIES

It is generally accepted that there are three basic conditions required for thunderstorm development: an adequate moisture supply, a potentially unstable lower troposphere, and a mechanism for releasing this instability (Newton, 1963). Synoptic studies that utilize 12-h rawinsonde data frequently have to extrapolate conditions of kinematics, moisture, and stability for extended time periods to establish relationships between these parameters and convection. House (1963) describes the physical theory behind most forecasts of stability and kinematic parameters related to thunderstorm development. He describes the development of organized convective activity in terms of vorticity changes and divergence production. Most of the techniques utilized by Miller (1967) involve synoptic-scale measurements of moisture, stability, and kinematics with graphical movement applied for later time periods. Organized systems of thunderstorms occur in areas or lines on a space scale resolvable within the standard rawinsonde network; however, these systems rarely have a life cycle that is resolved adequately by the 12-h interval of observations.

To fill the gap between 12-h soundings, forecasters have resorted to two sources; surface data and statistical forecasts based on numerical model output. Mogil (1975) used surface pressure tendency to detect subsynoptic-scale development that led to severe weather in the southeast United States. Darkow (1975) computed surface static energy from hourly data to delineate small areas of increased instability which were found to correlate well with subsequent severe weather. Much of the recent advances in severe weather forecasting in the National Weather Service and Air Weather Service is based on statistically combining measured and forecast quantities that best predict thunderstorm development.

Reap and Foster (1975) have made successful statistical forecasts using _forecast_ parameters from the National Meteorological Center numerical products. Basically, they correlated derived parameters of moisture, stability, and dynamics with digitized

radar data to obtain predictor equations for general and severe
thunderstorm activity. Miller (1975) combines an upper air statis-
tical equation with a surface equation to produce short-range local
forecasts of severe weather. All of these methods depend on an ac-
curate determination of what events on the synoptic scale are impor-
tant in severe weather occurrences.

An accurate understanding of the influence of the synoptic-
scale processes involves knowledge of the physical nature of
convective-scale processes. Fankhauser (1969) studied the dynamics
and thermodynamics of a system of thunderstorms as they developed
and passed through the National Severe Storms Laboratory mesonet-
work. His findings indicated that although individual thunderstorm
circulations could not be resolved, the interactions between meso-
and synoptic-scale systems could be. His work and that of Lewis
et al. (1974) emphasize the function of mesoscale circulations in
producing favorable conditions for thunderstorm development such
as locally strong instability and vertical motions within synoptic-
scale regions having some thunderstorm potential. The inability
to accurately determine the meso- and synoptic-scale interactions
from synoptic data is a primary reason why thunderstorm forecasts
based on large-scale analysis and forecasts have had low verifi-
cation.

Research by Pain et al. (1975) has indicated that successful
mesoscale numerical prediction can be achieved by not filtering out
small-scale wave phenomena produced due to imbalances in the initial
motions. Their forecasts predict local areas of strong changes in
divergence that correlate well with observed severe weather. Again,
this requires an imbalance on a scale large enough to be resolved
in the initial observations.

The vorticity equation has been a useful research tool in
atmospheric kinematics and dynamics. It has been used in studies
on the development of cyclones and anticyclones (Bosart, 1975;
Bjerknes, 1951). In recent years, studies of synoptic-scale con-
vective systems have used terms in the vorticity equation to explain
observed circulation features. Danard (1964) found excess produc-

tion of synoptic-scale vorticity in areas where a large release of latent heat had occurred in conjunction with convective activity. Williams (1970) and Reed and Johnson (1974) computed vorticity budgets for categories of tropical cloud clusters and easterly waves. In areas of widespread convection they observed large imbalances in the vorticity equation both at the surface and near the tropopause. Elliot and Hovind (1965) computed a vorticity budget for convective frontal bands using data taken over a meso-scale network. Their findings point to a systematic imbalance in areas of convection. The above studies treat the imbalance as an effect of unresolved small-scale systems on the environment and assumes that these small-scale systems act to restore balance on the large scale.

On the scale of individual severe thunderstorms, Fujita (1963) uses the vorticity equation at the surface to study the effect of individual thunderstorms on the environment. He shows how the imbalance in the computed terms represent production or dissipation of vorticity by strong downdrafts and updrafts and how this leads to development of mesoscale highs and lows observed in the surface data. On the same scale, in-cloud production of vorticity has been presented as a factor leading to the development of tornados and waterspouts (Danielson, 1975; Leverson et al., 1975). Although the individual thunderstorm circulations are deemed responsible for the development of the tornado, these authors point out the need for production of vorticity on the synoptic scale to initiate the convective systems.

Miller (1967) states that few, if any, severe thunderstorms develop in areas of negligible convective instability. Each of the average severe weather soundings that he presents is found to contain a significant layer of convective instability in the lower troposphere. Miller reviews the various stability indices that have been developed and concludes that although most thunderstorms occur in areas of synoptic-scale instability, the most unstable areas are generally free of thunderstorms. Barber (1975) and Wilson and Scoggins (1976) reach similar conclusions from climato-

logical and case studies of stability indices.

Wilson and Scoggins show that by combining a stability index with an indicator of vertical motion, considerable improvement in depiction of thunderstorm activity can be achieved. Endlich and Mancuso (1968) also developed indicators of severe weather by combining various stability, moisture, and kinematic parameters into a single parameter. A single numerical field so obtained aided in analysis and helped show the interrelationships between the individual parameters and convection.

3.   DATA

a.   AVE IV experiment

The basic data for this research consists of upper air sound-
ings taken during the National Aeronautics and Space Administra-
tion's (NASA) fourth Atmospheric Variability Experiment (AVE IV),
which covered the period 0000 GMT on 24 April 1975 to 1200 GMT on
25 April 1975.   Soundings were taken at 42 upper air stations in the
eastern two thirds of the United States (Fig. 1) at the following
nine times: 0000, 0600, 1200, 1500, 1800, and 2100 GMT on 24 April
1975, and 0000, 0600, and 1200 GMT on 25 April 1975.
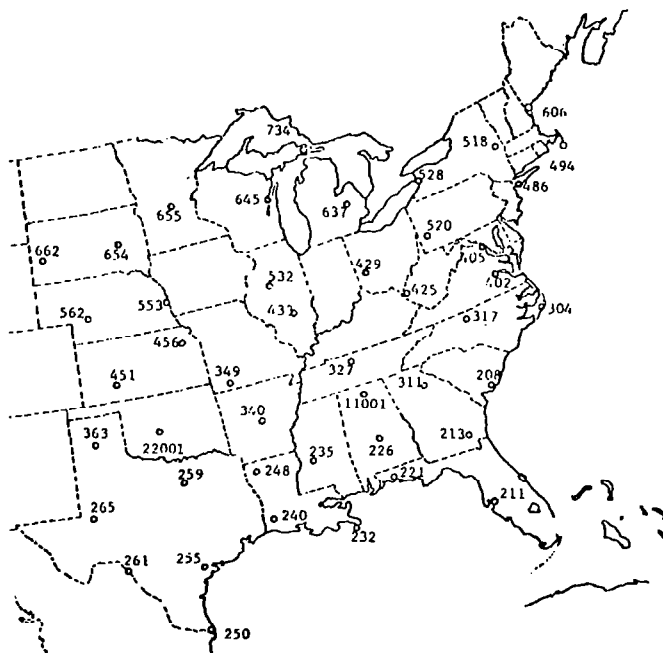
Fig. 1.   Location of rawinsonde stations for AVE IV.

The pressure contact and wind data were reduced to 25-mb
intervals as described by Fuelberg (1974) and presented by Fucik
and Turner (1975).   The reduction technique gives far more detail
in the data than does data received operationally from the National
Weather Service.   Azimuth and elevation angles were measured every

8

30 s instead of the usual 1-min interval, while pressure, temper-
ature, and humidity data were taken at every contact. The resulting
data is thought to retain the most detail realistically available
within the accuracy of the radiosonde. An error analysis conducted
by Fuelberg (1974) establishes standard error estimates in the
rawinsonde data as shown in Table 1. While the reduction technique
should significantly smooth some of the measurement errors, no
attempt is made here to establish the effect quantitatively.

b.   Surface observations

Hourly surface observations taken over the National Weather
Service's airways network were provided by the National Climat
Center for the time span of AVE IV. The network of surface stations
used is shown in Fig. 2. The surface data were used to augment the
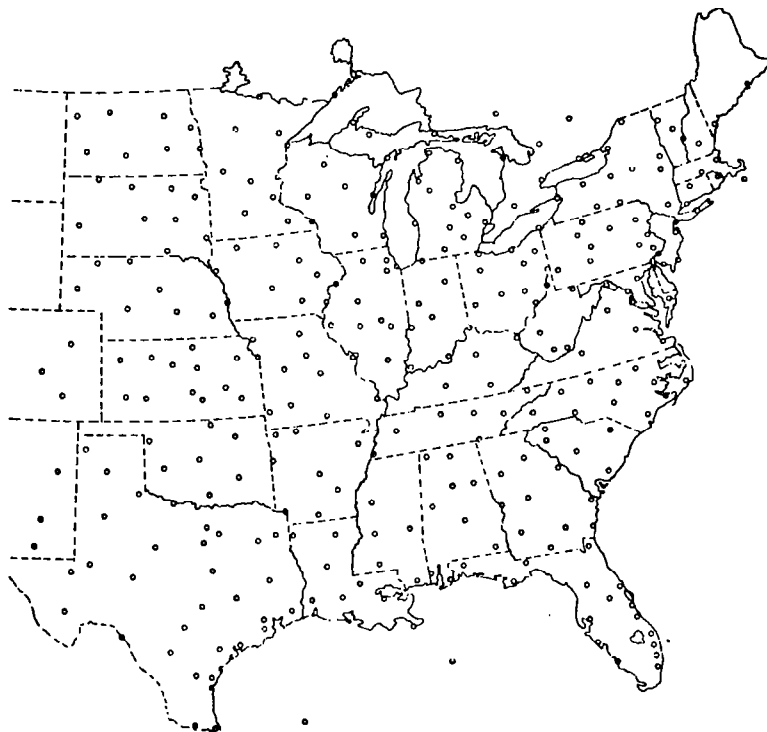
Fig. 2. Locations of surface stations in AVE IV.

Table 1. RMS errors in the rawinsonde data

a. Thermodynamic

Parameter	Approximate RMS Error
Temperature	1°C
Pressure	1.3 mb from surface to 400 mb; 1.1 mb between 400 and 100 mb; 0.7 mb between 100 and 10 mb.
Humidity	10 percent
Pressure Altitude	10 gpm at 500 mb; 20 gpm at 300 mb; 50 gpm at 50 mb.

b. Wind

Level	Elevation Angle		Elevation	
	40°	20°	40°	20°
	RMS Direction Error		RMS Speed Error	
700	1.8°	3.8°	0.5 m s^{-1}	1.0 m s^{-1}
500	2.5°	5.6°	0.8 m s^{-1}	2.0 m s^{-1}
300	3.1°	7.5°	1.0 m s^{-1}	3.8 m s^{-1}
100	6.2°	15.0°	2.0 m s^{-1}	5.7 m s^{-1}

upper air data and, due to the smaller spacing between stations,
a finer resolution of detail is available than in the rawinsonde
network.

c. Manually Digitized Radar (MDR) data

In order to compare objectively computed quantities of kine-
matics and stability to thunderstorm activity, a numerical measure
of convection is needed. In this study Manually Digitized Radar
(MDR) data provided by the Techniques Development Laboratory (TDL)
of the National Oceanic and Atmospheric Administration (NOAA) have
been used as a quantitative measure of convection. Reap (1975)
describes the relationship between MDR data and rainfall rates in
a coded form reproduced in Table 2. MDR values $\geq$ 4 are considered

Table 2. Explanation of Manually Digitized Radar (MDR) code

Code No.	Maximum Observed VIP[1] Values	Coverage In Box	Maximum Rainfall Rate (in./hr)	Intensity Category
0	No Echoes			
1	1	Any VIP1	< .1	Weak
2	2	$\leq$ 50% of VIP2	.1- .5	Moderate
3	2	> 50% of VIP2	.5-1.0	Moderate
4	3	$\leq$ 50% of VIP3	1.0-2.0	Strong
5	3	> 50% of VIP3	1.0-2.0	Strong
6	4	$\leq$ 50% of VIP3 and 4	1.0-2.0	Very Strong
7	4	> 50% of VIP3 and 4	1.0-2.0	Very Strong
8	5 or 6	$\leq$ 50% or VIP3, 4, 5, and 6	> 2.0	Intense or Extreme
9	5 or 6	> 50% or VIP3, 4, 5, and 6	> 2.0	Intense or Extreme

[1]Video Integrator Processor

to represent general thunderstorm activity while severe thunder-storms are indicated by MDR ≥ 8 (Reap and Foster, 1975).

MDR data are available on a gridded network over the eastern two-thirds of the United States as shown in Fig. 3. Maximum observed values are reported each hour for each block of the grid. Due to frequently missing hourly MDR observations and the synoptic-scale nature of this study, 3-h composites of MDR data were prepared centered on the rawinsonde observation times. The maximum observed MDR values over the 3-h period was used as the plotted value. Figure 3 shows an example of the composited MDR data. MDR fields for other times are shown in Appendix A.

Fig. 3. MDR grid and composited field for 0000 GMT on 25 April 1975.

4.   SYNOPTIC CONDITIONS

During AVE IV, severe weather developed along a quasi-stationary polar front through the midwest in response to two relatively weak short wave perturbations in the upper levels. The first short wave was centered in the Midwest at the start of the experiment and a squall line, henceforth referred to as squall line one, had already formed on the front (Fig. 4). This squall line and associated short wave moved to a position off the East Coast by the end of the experiment.
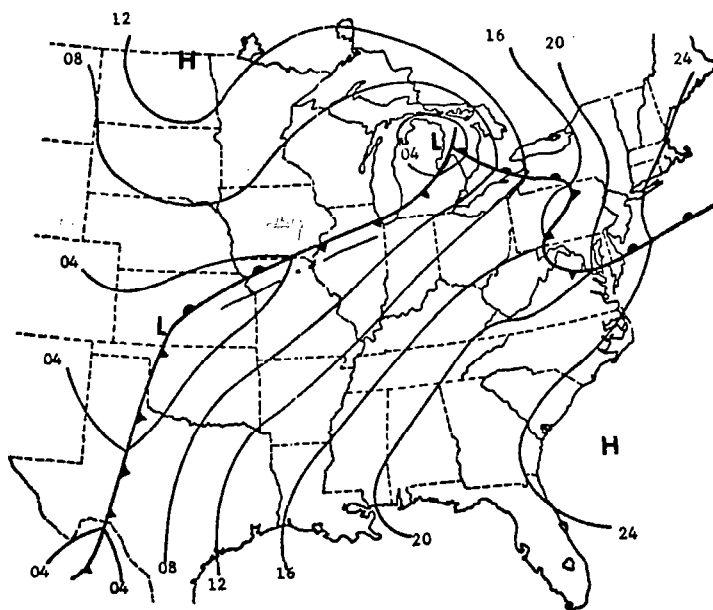
Fig. 4.   Surface chart for 0000 GMT, 24 April 1975.

Another squall line, referred to as squall line two, formed along the frontal zone, shown in Fig. 5., in Kansas and Oklahoma at 0000 GMT on 25 April 1975 in response to a second short wave moving through the central plains. This squall line was responsible for much of the severe weather reported during AVE IV.
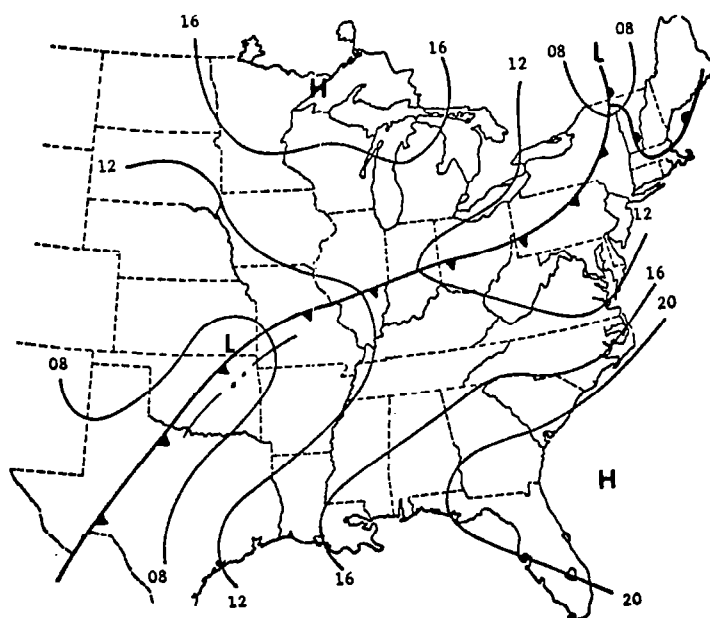
Fig. 5. Surface chart for 0000 GMT, 25 April 1975.

The synoptic situation during AVE IV proved interesting in that the circulation features such as a strong jet stream and a high amplitude short wave normally associated with severe thunderstorms were not well defined; however, considerable low level heat and moisture were observed in the areas of convective activity.

A detailed discussion of the synoptic conditions and selected upper air charts are given in Appendix B.

5.   ANALYTICAL METHODS

a.   Objective analysis technique

A key to any study utilizing observational data is the method of analysis. Research on synoptic conditions that lead to convective storms requires a technique that will retain the most detail resolvable from the observed data. In this study the technique developed by Barnes (1964) will be used. His method is based on the assumption that atmospheric variables can be represented as a sum of an infinite series of waves. In general, values of a parameter are interpolated to grid points from the original data as a first guess field with successive corrections applied to the gridded field on following iterations. A grid spacing of approximately 160 km was chosen based on work by Barr et al. (1971), Fuelberg (1974), and Wilson and Scoggins (1976). These studies show that a shorter grid interval will not retrieve any greater detail from data taken over the standard rawinsonde network. With this grid spacing a scan radius of 3 grid distances was used to ensure adequate data for interpolation to each grid point. Four iterations were performed on the gridded data followed by a nine point smoothing as described by Shuman (1957) to further remove unresolvable features from the gridded fields. The final gridded fields retain the following approximate amplitudes for systems with selected wavelengths: 90% of 1600 km, 60% of 800 km, and 15% of 400 km systems.

In order to compute kinematic and thermodynamic parameters, fields of wind, temperature, and humidity were analyzed over the 18 x 18 grid shown in Fig. 6. Values of u, v, T, T_d, and q were analyzed at all nine time periods for 50-mb intervals from 900 to 100 mb. Vertical averaging was used on the u- and v-components over a 50-mb layer centered at the level being analyzed.

The above technique of analysis was extended to surface data but with a scan radius of only two grid distances because of the shorter distance between surface stations. The same parameters were analyzed at the surface as at the upper levels.
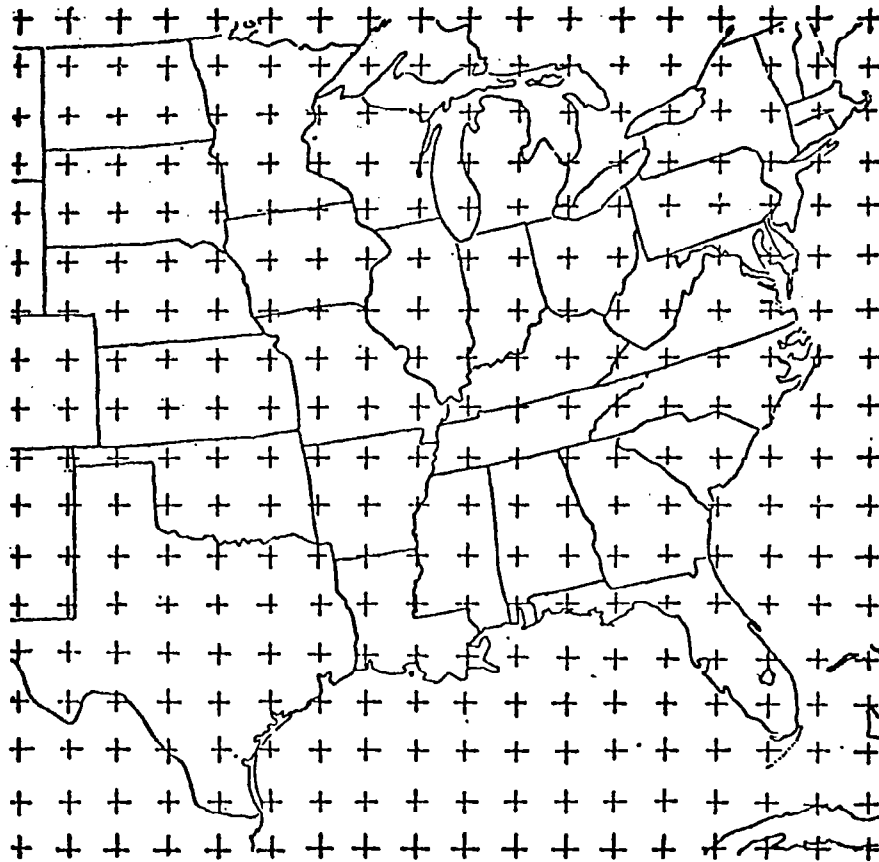
Fig. 6. Grid used for numerical computations.

b. Vorticity equation

Many researchers have found that systems of thunderstorms form shortly after development of a cyclonic circulation in the troposphere. The 3-h and 6-h sounding intervals in AVE IV give much better time resolution of development on the synoptic scale than is normally available.

The development of synoptic-scale cyclonic circulations during the AVE IV experiment was studied through a computation of the vorticity budget. The equation for the vertical component of the curl of velocity is (see, for example, Panofsky [1959])

$$\underset{1}{\frac{\partial \zeta}{\partial t}} + \underset{2}{\vec{V}_p \cdot \vec{\nabla}_p (\zeta + f)} + \underset{3}{\omega \frac{\partial \zeta}{\partial p}} = \underset{4}{-(\zeta + f)\vec{\nabla}_p \cdot \vec{V}_p} + \underset{5}{\frac{\partial \omega}{\partial y} \frac{\partial u}{\partial p} - \frac{\partial \omega}{\partial x} \frac{\partial v}{\partial p}} + \underset{6}{\vec{k} \cdot \vec{\nabla} x \vec{F}}, \qquad (1)$$

where term 1 is the local time rate of change of relative vorticity, term 2 the advection of absolute vorticity on isobaric surfaces, term 3 the vertical advection of vorticity, term 4 the concentration or dilution of absolute vorticity through convergence, term 5 represents the transfer of vorticity between horizontal and vertical axes and is called the twisting term, and term 6 represents friction. In this study term 6 will be solved for as a residual and will represent imbalance between the total derivative and synoptic-scale sources of vorticity in Eq. 1. Terms 1-5 represent contributions by mean quantities and the residual will represent a combination of perturbation quantities, viscous friction, measurement error, and computational error (truncation).

1) Error analysis

Errors in wind observations at upper levels are frequently cited as a major problem in upper air analysis. These errors may have a significant effect on computed terms in the vorticity equation. If computational errors are of the same order of magnitude or greater than expected values of a term, then the representativeness of fields of that term would be questionable. An error analysis of terms in the vorticity equation was done to determine which terms are most sensitive to errors in the rawinsonde data. In this study the only errors considered quantitatively are random errors in the measured winds.

For the error analysis the technique of Young (1962) was used. He gives

$$\sigma_Q = \left[\left(\frac{\partial Q}{\partial a}\right)^2 \sigma_a^2 + \left(\frac{\partial Q}{\partial b}\right)^2 \sigma_b^2 \right]^{1/2}, \qquad (2)$$

where σ_Q is the standard deviation of the derived quantity, Q, which is a function of observations of a and b, and σ_a and σ_b are the known standard deviations of a and b. For the present study

linear relationships were assumed for partial derivatives of Q, and errors in wind for an elevation angle of 20° were used for σ_a and σ_b. Since the above assumptions do not account for the smoothing effect of either the data reduction technique or the objective analysis method, the error estimates shown in Table 3 are approximate values for errors in the analyzed terms.

The table shows that errors for the individual terms increases with height due to increased error in wind measurement. Since ω is computed by integrating the continuity equation, terms involving ω and its gradients are very sensitive to errors in the wind, but scale analysis (Holton, 1972) indicates that these terms are generally small if not negligible compared to the other terms in Eq. 1.

The effect of the analysis technique in either smoothing out or introducing error is unknown. Vincent and Chang (1975) introduced random errors in rawinsonde data used to compute energy budgets for tropical and extratropical cyclones and then compared results to that obtained from the original data. Some terms were more sensitive than others to the error introduced; the maximum effect was by a factor of two. Their results indicate that maximum errors after smoothing by analysis are less than or equal to standard deviations computed using Eq. 2. This implies that the smoothing introduced in analyzing the data acts to reduce the effect of errors. Vincent and Chang point out that although the errors did change numerical values of terms, the relationships developed were the same for the original and the altered data.

2)   Computational procedures

The vorticity budget was computed for the surface, 850-, 700-, 500-, and 300-mb levels. All terms in the equation were computed at each level except at the surface where terms involving ω were neglected. Terms in Eq. 1 were evaluated at each grid point from the analyzed fields of u and v wind components. Vertical motion was computed using the kinematic method with an adjustment technique developed by O'Brien (1970) applied to smooth the effect of errors that accumulate when integrating the continuity equation. Boundary values used were terrain-induced vertical motion at the

Table 3.   Estimated RMS errors of terms in the vorticity equation

Quantity	Scale Value (λ = 100 km)	RMS Error			
		$\sigma_{850\ mb}$	$\sigma_{700\ mb}$	$\sigma_{500\ mb}$	$\sigma_{300\ mb}$
u, v components	$10\ m\ s^{-1}$	1	1.7	3.0	5.0
ω	$1\ \mu bar\ s^{-1}$	.4	2.0	4.0	7.0
$\frac{\partial u}{\partial x} + \frac{\partial v}{\partial y}$	$10^{-5}\ s^{-1}$	$.5 \times 10^{-5}$	1.0×10^{-5}	1.5×10^{-5}	2.0×10^{-5}
$\frac{\partial v}{\partial x} - \frac{\partial u}{\partial y}$	$10^{-5}\ s^{-1}$	$.5 \times 10^{-5}$	1.0×10^{-5}	1.5×10^{-5}	2.0×10^{-5}
$\frac{\partial \zeta}{\partial t}$	$10^{-10}\ s^{-2}$	1.0×10^{-10}	5.0×10^{-10}	10.0×10^{-10}	15.0×10^{-10}
$\vec{V}_p \cdot \vec{\nabla}_p (\zeta + f)$	$10^{-10}\ s^{-2}$	5.0×10^{-10}	10.0×10^{-10}	15.0×10^{-10}	20.0×10^{-10}
$\omega \frac{\partial \zeta}{\partial p}$	$10^{-11}\ s^{-2}$	1.0×10^{-10}	5.0×10^{-10}	10.0×10^{-10}	15.0×10^{-10}
$-(\zeta + f)\ \vec{\nabla}_p \cdot \vec{V}_p$	$10^{-9}\ s^{-2}$	10.0×10^{-10}	20.0×10^{-10}	30.0×10^{-10}	40.0×10^{-10}
$\frac{\partial \omega}{\partial x} \frac{\partial u}{\partial p} - \frac{\partial \omega}{\partial y} \frac{\partial v}{\partial p}$	$10^{-11}\ s^{-2}$	2.5×10^{-10}	10.0×10^{-10}	20.0×10^{-10}	40.0×10^{-10}

surface and the adiabatic vertical motion at 100 mb, as given by Panofsky (1959).

It is unknown what quantitative effect the adjustment of ω has on errors. Various authors have used the method with encouraging results. Smith (1971) found the method to give accurate results for synoptic-scale studies, while Fankhauser (1969), and Wilson and Scoggins (1976) achieved realistic patterns in mesoscale and synoptic-scale analyses of convective activity. A most compelling argument for using the technique comes from a study by Williams (1970) where kinematic quantities were composited for a large number of tropical cloud clusters. Kinematic vertical motions computed for the composited wind data with no vertical adjustment gave a smooth profile with small values at the top level. These profiles resembled profiles from other studies computed using the O'Brien technique. Compositing of wind data from many cases apparently has a smoothing effect on errors that acts in the same manner as the O'Brien technique.

The time derivative in Eq. 1 was approximated by centered finite differences except at the initial time, where a forward difference was applied, and the last time where a backward difference was applied. All horizontal and vertical spatial derivatives were approximated by centered finite differences. The depth interval used to approximate vertical derivatives was 200 mb.

3) Method of presentation of results

The error analysis indicated that individually analyzed fields of terms in the vorticity equation could contain significant error. In order to develop relationships between the terms of Eq. 1 and convection, and to reduce the effect of random errors, parameters were averaged over all nine times for several categories of convection.

The categories of convection were based on the MDR code with MDR $\leq$ 1 representing no convection, MDR $\geq$ 2 representing all convection, MDR $\geq$ 4 representing thunderstorms, and MDR $\geq$ 8 representing severe thunderstorms. First, grid point values of MDR data had to be determined for each time. From the composited MDR charts

the maximum MDR values within a scan radius of one grid distance from each grid point was chosen to be the MDR value at that grid point. Averages of each term were then computed for each MDR category. Averages were computed for each level and graphs were prepared showing the vertical distribution of average values of terms in the vorticity equation.

Operational 12-h sounding intervals rarely allow one to study atmospheric conditions prior to initial development of thunderstorms. With 12-h data extrapolation of conditions over an unacceptable length of time frequently is done. The 3- and 6-h intervals in AVE IV provide the opportunity to examine synoptic conditions before thunderstorms develop. To test these conditions, average values of the terms in the vorticity equation were computed for a 3- and 6-h lag in MDR fields. This was done by simply comparing the gridded fields of terms in the vorticity equation at each time with the observed convection 3- and 6-h later. Differences between these profiles and the ones for zero lag give an indication of how long favorable conditions on the synoptic scale exist prior to the development of thunderstorms. This also indicates what large scale changes take place, if any, in areas of convection after thunderstorm development.

In order to determine the usefulness of general relationships between convection and terms in the vorticity equation, individually analyzed fields were examined. Examples are presented and discussed below.

c. Stability

1) Computational procedure

As stated above, a convectively unstable layer of air is required for thunderstorm development. The average tornado sounding presented by Miller (1967) indicates the presence of a dry, subsidence inversion in the lower troposphere with convective instability being greatest in the layer containing the inversion. In this research three layers, one generally below the inversion, one containing the inversion, and one above the inversion, were used

to compute convective instability. Stability in each layer was compared to radar-observed convective activity.

The three layers used were the surface to 850 mb, 850 to 700 mb, and 700 to 500 mb. In addition, convective instability in the layer from the surface to 500 mb was computed to see if a deep layer measurement adequately described the stability requirement. Convective instability, σ_e, was defined by $-\frac{\partial \Theta_e}{\partial p}$, where Θ_e is equivalent potential temperature. Grid point values of σ_e were computed at the top and bottom of each layer using gridded fields of temperature and dew point temperature. σ_e was evaluated by finite differences from grid point values of Θ_e with Δp equal to the difference between the pressures at the top and bottom of each layer.

2) Method of presentation of results

General relationships between convective instability and thunderstorms were developed in the same fashion as the vorticity budget. Averages for zero lag were computed to investigate synoptic-scale instability in areas of observed convective activity while averages for 3- and 6-h lags in MDR data were used to study conditions prior to thunderstorm development.

Individually analyzed fields were used to establish whether the general relationships hold for specific time periods, and to study changes in stability during the life cycle of convective systems.

d. Thunderstorm Potential Indices

1) Rationale

As shown in previous studies, neither stability nor kinematic parameters alone provide a very good analysis or forecast tool for severe weather. Wilson and Scoggins (1976) showed that by combining an index of stability with vertical motion a substantial improvement in depicting severe thunderstorms could be achieved. Statistical techniques used by the weather services combine many observed and forecast parameters in making a severe weather forecast. Endlich and Mancuso (1968) have developed indicators for severe weather by combining scaled parameters of mois-

ture, stability, and kinematics into a single parameter. Analyzed fields of these indicators correlated better with convection than did the individual parameters that made up the indicator.

In this study an index was developed to combine, in a simple manner, the effects of moisture, stability, and vorticity development when related to convection. Since this is only one case study no attempt is made to develop exact statistical relation-ships of the type used by the National Weather Service (Charba, 1975). The combinations were chosen based on physical reasoning with essentially equal weight placed on input parameters.

A direct measure of moisture was required since the vorticity equation is independent of moisture and σ_e considers only the vertical distribution of moisture. Wilson and Scoggins (1976) found boundary layer moisture to correlate best with observed thunderstorms; therefore, in this study the average mixing ratio $\bar{q}$, from the surface to 850 mb was used as a moisture parameter.

Terms in the vorticity equation indicating development of circulation systems are expected to correlate best with areas of convection. In the lower levels, terms involving ω and its gradients are generally negligible on the synoptic-scale. Horizontal advection should be smaller than the divergence term due mainly to smaller wind speeds. In the lower levels the dominating terms are the local derivative, divergence term, and friction. For use in an index, the divergence term was preferred since it relates to a source of vorticity in the lower layers.

In the middle and upper troposphere, the dominant terms in the vorticity equation are the horizontal advection term, divergence term, and the local derivative of vorticity. From scale analysis, terms involving ω should be small compared to the other terms. If the equation is applied at the level of non-divergence, usually near 500 mb, development of circulation is primarily due to vorticity advection $[\vec{V}_p \cdot \vec{\nabla}p(\zeta + f)]$. In the presence of vorticity production by convergence such development would be enhanced. However, error analysis as shown in Table 3, indicates that at the upper levels the divergence term is considerably more

in error than the horizontal advection term. Hence, vorticity advection at 500 mb is the preferred vorticity development input to the index.

As stated earlier, instability is an essential criterion for thunderstorm development. The exact layer in which this instability should exist for maximum development is not known and probably varies for different cases. In many cases, boundary layer instability is probably most important, while with strong lifting, upper level instability may be important. The depth of the layer of instability is certainly of importance and the indices developed include this as well as the instability observed in the boundary layer and aloft.

2) <u>Definitions</u>

Three initial indices were formed, two representing lower tropospheric synoptic conditions and one representing upper-level conditions. Two thunderstorm potential indices were formed by adding each of the low-level indices separately to the upper-level index.

The low-level indices (LLI) were computed using the following formulas:

$$\text{LLI } 1 = [\sigma^*_{e_{Sfc-850}} + \overline{(\zeta + f)(\vec{V}_p \cdot \vec{V}_p)}^*] \bar{q}, \text{ and} \tag{3}$$

$$\text{LLI } 2 = [\sigma^*_{e_{850-700}} + \overline{(\zeta + f)(\vec{V}_p \cdot \vec{V}_p)}^*] \bar{q}, \tag{4}$$

where an overbar indicates an average from the surface to 850 mb, and * indicates that the quantities have been scaled by their standard deviation as was done by Endlich and Mancuso (1968). Scaling was required due to the different orders of magnitudes of the stability and vorticity terms. In order to obtain the proper effect of moisture, average specific humidity (or mixing ratio) was used as a multiplier instead of being added to the index. Simply adding the term to the index would not effectively reduce the potential for thunderstorm development in areas where insufficient moisture was observed.

High negative values of either index indicate moist, unstable

air and vorticity production occurring at the same point. Where these factors occur simultaneously, environmental conditions in the lower troposphere are excellent for thunderstorm development.

The upper level index (ULI) was defined by

$$\text{ULI} = [\sigma_{e_{700-500}}^{*} + \vec{V}_p \cdot \vec{\nabla}_p (\zeta + f)^{*}]\bar{q}, \tag{5}$$

where symbols have the same meaning as for the low-level index. Since dry, low-level regions often exhibit unstable conditions between 700 and 500 mb as well as positive vorticity advection at 500 mb, the low-level average mixing ratio $\bar{q}$, was used to reduce the effect of strong advection in areas of low moisture content. Again, areas that have large negative values of the upper index are areas of upper-level instability and positive vorticity advection above a moist boundary layer.

The two Thunderstorm Potential Indices (TPI) are given by

$$\text{TPI 1} = \text{LLI 1} + \text{ULI, and} \tag{6}$$
$$\text{TPI 2} = \text{LLI 2} + \text{ULI.} \tag{7}$$

Minimum values of each occur where moist, unstable air with production of vorticity in the lower troposphere is located beneath regions of mid-tropospheric instability and positive vorticity advection.

3) Method of presentation of results

Fields of the Low Level, Upper Level, and Thunderstorm Potential Indices were examined for correlation with thunderstorm activity to assess the improvements compared with the use of individual parameters of stability and vorticity production. Comparison between upper-level and lower-level indices was done to determine which was better at depicting severe weather development.

Analyzed fields are presented to show the effectiveness of the indices for outlining areas of convective activity. Subjective comparison between index fields and observed MDR values will be used to test the effectiveness of the indices.

6. RESULTS

a. Budget of vorticity

The evaluation of terms in the vorticity equation gives insight
into processes taking place in the large scale wind field that tend
to produce or inhibit circulations capable of triggering convective
activity. Average quantities of the terms show the general rela-
tionship between development of circulation in the wind field and
convection, while specific analyzed fields depict evolution of
these quantities during the life cycle of thunderstorm systems.

1) General relationships between vorticity and convection

The profiles for the local rate-of-change of vorticity shown
in Fig. 7 confirms the hypothesis that in areas of convection there
is large-scale development of cyclonic circulation. A maximum
rate of increase occurs in the mid- and upper-troposphere while
areas of no convection have slight negative tendencies. Except
at 500 mb, the profile of $\frac{\partial \zeta}{\partial t}$ exhibits little difference for dif-
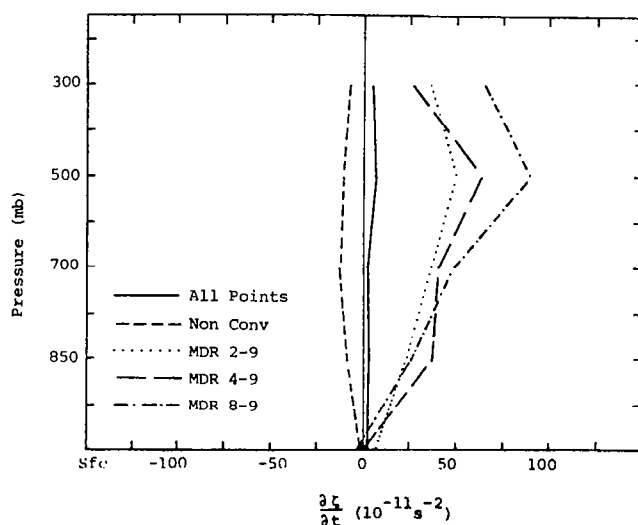ferent categories of thunderstorm intensity.

Fig. 7. Average values for the local derivative of vorticity.

The profiles of horizontal vorticity advection shown in Fig. 8 were as expected. Positive vorticity advection $[\vec{V}_p \cdot \vec{\nabla}_p (\zeta + f) \geq 0]$ occurs in the mid- to upper-troposphere in areas where convection is occurring, while slightly negative advection is associated with convection-free areas. As with the local derivative, advection seems to differentiate poorly between convection of varying intensity.
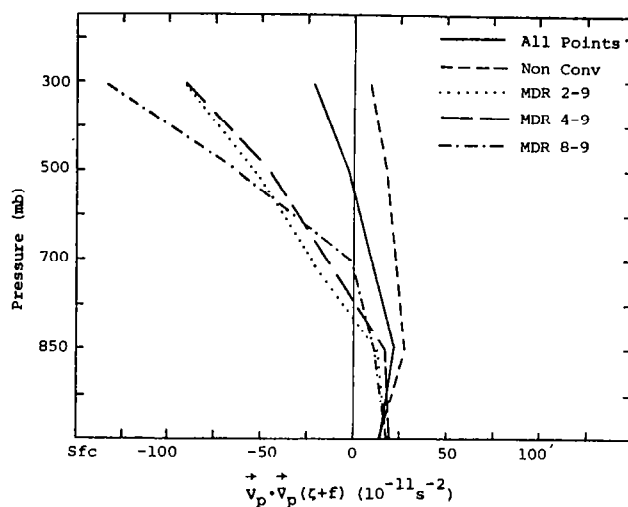

Fig. 8. Average profiles for horizontal vorticity advection.

Average profiles of vertical advection of vorticity are shown in Fig. 9. Scale analysis indicates that the term should be negligible for large-scale motions, and the results show this is basically correct. At 500 mb, however, the term approaches the order of magnitude of the more dominant terms of the equation in areas of convection. This would indicate that numerical forecasts that neglect the vertical advection term could be in error in areas where convective activity is present. The term tends toward increasing negative values for increasing thunderstorm intensity.
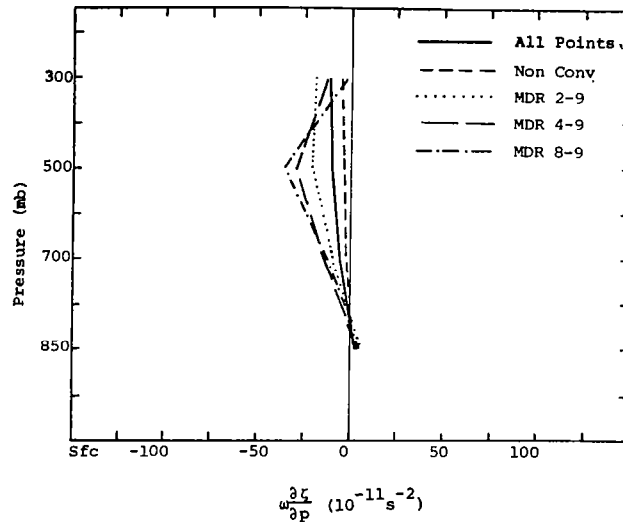
Fig. 9. Average profiles for vertical advection of vorticity.

Profiles of the divergence term show large positive values in lower levels and large negative values aloft in areas of convection (Fig. 10). Since ζ_a is almost always positive, the maximum values at 300 mb indicate divergence. This term shows a strong relationship between increasing positive values of low level vorticity production with increasing MDR values.

The average values of the twisting term, shown in Fig. 11, have profiles similar to the vertical advection term, being negligible except in the middle troposphere. The twisting term seems to increase slightly with increasing thunderstorm intensity in the same manner as the vertical advection term. Since, on the average, this term approaches the order of magnitude of other terms in the middle troposphere, neglect of the twisting term could introduce significant error. However, the vertical advection and twisting terms tend to cancel each other out in areas of convection.

Figure 12 shows the average profiles for the total derivative of vorticity, $\frac{d\zeta_a}{dt}$, and Fig. 13 shows the sum of the divergence and twisting terms. The total derivative profiles show that parcels
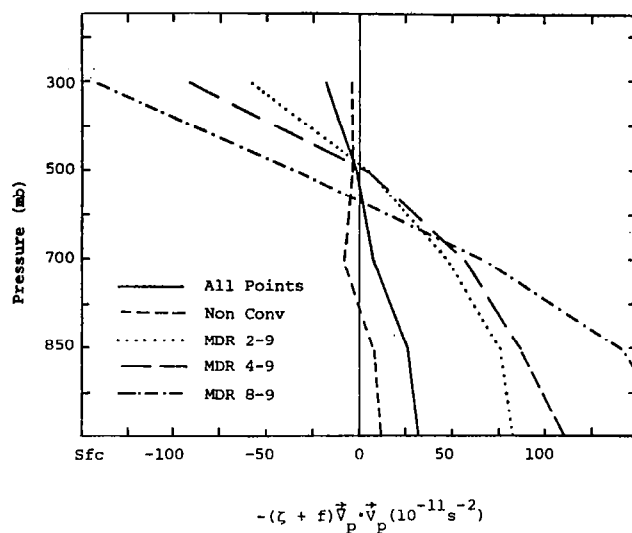
Fig. 10.   Average profiles for the divergence term in the vorticity equation.
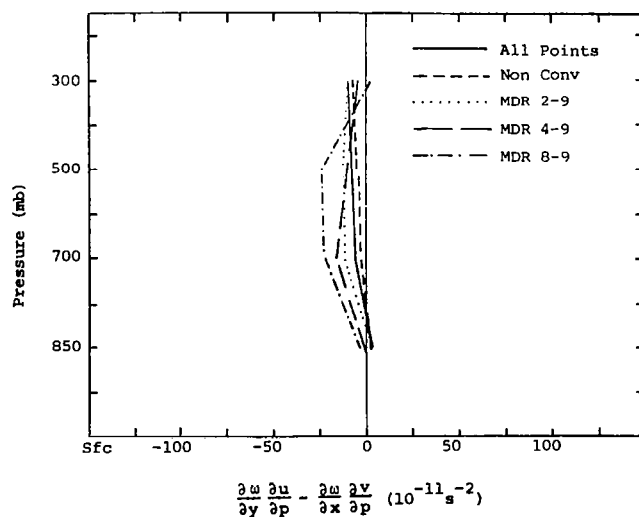

Fig. 11.   Average profiles for the twisting term in the vorticity equation.
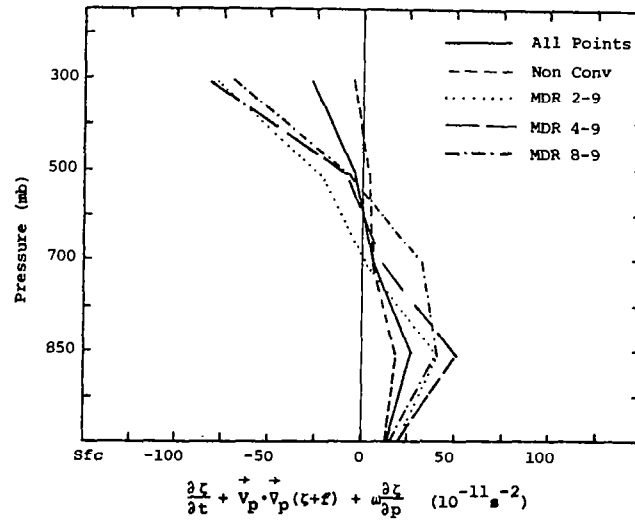
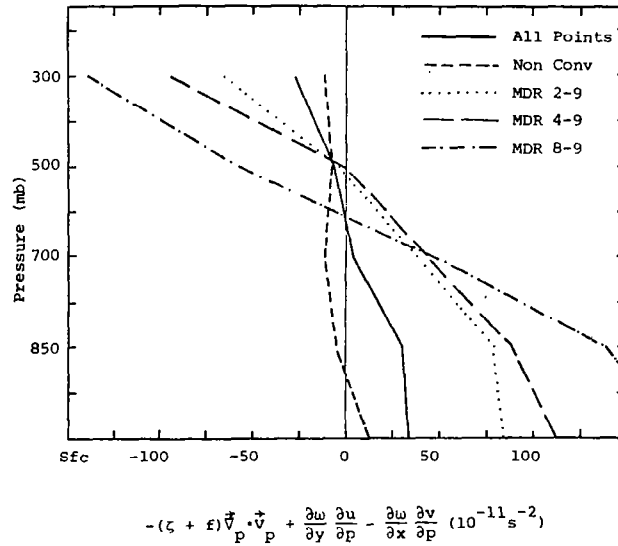Fig. 12. Average profiles for the total derivative of
vorticity.

Fig. 13. Average profiles for the sum of the divergence
and twisting terms.

gain vorticity in the lower levels and lose vorticity aloft in areas
of convection. Negative values aloft are due to the advection term
being much larger in magnitude than the local derivative, while in
the lower levels, positive values are a result of both advection
and the local derivative being greater than zero. The profiles in
Fig. 13 are very similar to the divergence term indicating the
dominance of divergence production over the twisting term.

From a comparison of the profiles in Figs. 12 and 13 it is
obvious that imbalance exists in the vorticity budget, even when
averaged over many points. Figure 14 shows the profiles of the
residual term computed by subtracting the divergence and twisting
terms from the total derivative. In general, the profiles show
a systematic imbalance in the mean values of terms in the vor-
ticity equation. The low levels have increasing negative imbalance
with increasing MDR values and the upper levels have increasing
positive imbalance with increasing MDR values. For areas free of
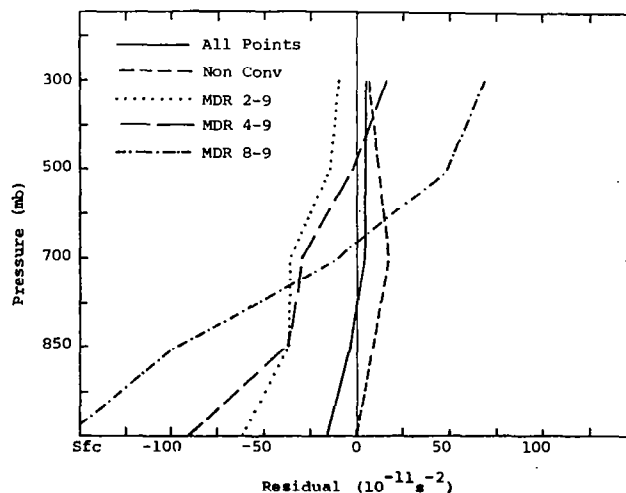convection the imbalance is small and opposite in sign from con-
vective areas.

Fig. 14. Average profiles for the residual in the
vorticity equation.

The effect responsible for this imbalance is not immediately evident. Reexamination of Figs. 12 and 13 indicate that the magnitude of the sum of the divergence and twisting terms of Eq. 1 is always greater than that of the total derivative in areas of convection. At the surface and 850-mb levels, advection is small due to low wind speeds, while the vertical motion terms are negligible. Large positive values of the divergence term would indicate, neglecting friction, that large increases in vorticity should be observed. The local derivative does not usually reflect this in the low levels (Fig. 7).

Imbalance at 300 mb is not as clearly defined as in the lower levels. Significant imbalance at 300 mb exists only for the severe thunderstorm category (MDR $\geq$ 8). The divergence term is more negative than horizontal advection, which should give a local change less than zero. The observed tendency is positive (Fig. 7) giving the large imbalance.

Why is there a systematic imbalance in mean quantities of Eq. 1 and what is responsible for restoring balance? As previously stated, the residual should be interpreted as a combination of error and eddy friction. The time averaging of the results should have reduced the effect of rawinsonde measurement errors and the space smoothing the magnitude of truncation errors.

In the low levels, the imbalance seems to be caused by large positive values of the divergence term that are not reflected in equally large local tendencies. Frictional dissipation may be a dominant source for maintaining balance in the boundary layer but seems less likely at 850 mb. Danard (1964) found a similar imbalance at the surface in a study involving large-scale systems. He proposed that frictional dissipation accounts for maintaining balance in the vorticity equation at the surface. He did not say whether friction as he used it was to include unresolved scales of motion as well as viscous friction. At 850 mb, it is unlikely that the viscous friction effect would be as large as the divergence term. Small-scale motions must account for some of the residual at that level.

The systematic imbalance in convective areas at 300 mb is also hard to explain by friction alone. Small-scale circulations could again act in opposition to the large-scale forcing (by advection or divergence) to restore balance.

Large thunderstorms may act to create the imbalance aloft. Severe thunderstorms are thought to exert a considerable effect on the synoptic-scale flow. Fankhauser (1971) and Ninomiya (1971) show observational evidence of changes in synoptic flow patterns in areas of severe thunderstorms. The storms act as an obstacle to the flow, creating divergent flow in the wind field around them. This could explain why for severe (MDR $\geq$ 8) cases the divergence term was more negative than the advection term. Since the storms were not severe for a long time period, the local derivative computed by finite differences over a 6-h interval does not reflect this excess negative vorticity production by divergence. Circulation within the system of thunderstorms may account for dissipation of this negative production.

Systems of thunderstorms act as turbulence in the mean flow, giving rise to significant values of the perturbation quantities in the residual. Rewriting the vorticity equation in terms of mean motions and fluctuations, averaging over time, and assuming no correlation between mean and fluctuation quantities, yields the following small-scale terms in the residual:

$$\overline{-\zeta'(\vec{\nabla}_p \cdot \vec{v}_p)'} \; \underset{2}{-} \; \overline{\vec{v}'_p \cdot \vec{\nabla}_p \zeta'} \; \underset{3}{-} \; \overline{\omega'\frac{\partial \zeta}{\partial p}} + \overline{\frac{\partial \omega'}{\partial y}\frac{\partial u'}{\partial p}} - \overline{\frac{\partial \omega'}{\partial x}\frac{\partial v'}{\partial p}} \tag{8}$$

These terms represent contributions to the mean vorticity field by sub-grid scale processes. Term 1 is production of vorticity by divergence, term 2 is small-scale horizontal advection of vorticity, term 3 is small-scale vertical advection, and term 4 is the small-scale twisting term. Since the correlations involved in each of the perturbation terms is unknown, actual scale analysis is difficult to compute. Vertical velocities in thunderstorm circulations are frequently two orders of magnitude larger than synoptic-scale vertical motion, indicating that the perturbation quantities in-

volving ω are probably larger than the other terms. Reed and John-
son (1974) explain the restoration of balance in the vorticity
budget in tropical waves through small-scale vertical advection.
The term acts within the updraft-downdraft circulation of the
thunderstorms with the storms acting as a sink of vorticity in
the low levels and a source aloft, balancing the opposing effects
of the large-scale divergence term. They neglected the effect of
the other perturbation terms although large gradients of ω in
thunderstorms indicate that the twisting terms may also be sig-
nificant. The effect of the small-scale twisting term when averaged
over time is unknown.

Elliot and Hovind (1965) do not specify any one term for re-
storing balance in their study of mesoscale convective bands. They
refer to the residual as a mixing of vorticity encompassing all
effects. Without direct observations or convincing results from
numerical models of scale interaction, the residual should be
considered as a combined effect of all terms.

One problem in using 12-h rawinsonde data that many researchers
have faced has been separating cause and effect when relating de-
rived synoptic-scale parameters to thunderstorm activity. The
unique 3- and 6-h sounding intervals in AVE IV provided data for
studying conditions prior to the occurrence of convection. In AVE
IV, few areas outside of the southeastern United States are free
of convection for the entire experiment. With few exceptions,
however, most blocks with MDR $\geq$ 4 were free of convection 3- and
6-h prior to the observation.

Figure 15a shows the average profiles for $\frac{\partial \zeta}{\partial t}$ computed over a
6-h interval and associated with MDR values at the end of the time
interval (3-h lag in MDR values), while Fig. 15b shows the profiles
for a 6-h lag. Overall there is a tendency for increasing vor-
ticity both 3- and 6-h prior to observed thunderstorm activity,
with the maximum increase in the middle troposphere. The profiles
indicate that the local derivative does not differentiate between
severe and non-severe thunderstorms either prior to or after de-
velopment.
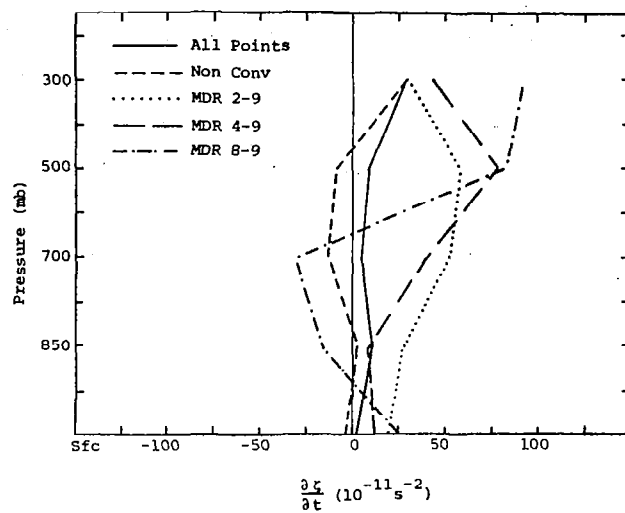
(a)   3-h lag in MDR.
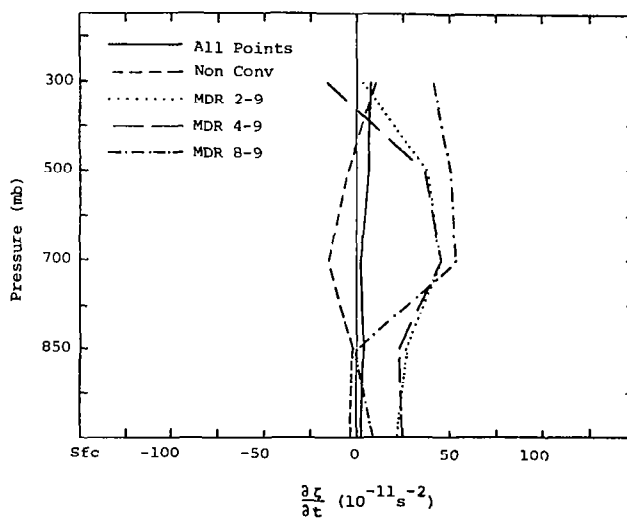
(b)   6-h lag in MDR.

Fig. 15.   Average profiles for the local derivative
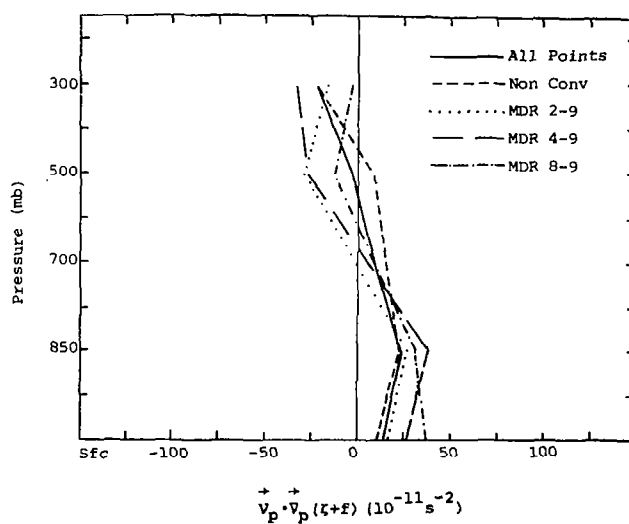with time lags in MDR.

The profile for average values of $\vec{V}_p \cdot \vec{\nabla}_p (\zeta + f)$ for 3-h lag
in MDR data are similar to the profiles for zero lag (Fig. 8) with
maximum values at 500 mb (Fig. 16a). This indicates that synoptic-
scale advection of vorticity at upper levels develops prior to the
formation of systems of thunderstorms. The 6-h lag profiles (Fig.
16b) show a marked change from zero and 3-h lag profiles. The 6-h
profiles indicate almost no relationship between horizontal vor-
ticity advection and convection. This result points to the possible
importance of cyclonic development in the middle and upper tropo-
sphere in the initiation of severe thunderstorms, since thunder-
storms were observed a relatively short period after the positive
vorticity advection appeared.

Averages for the divergence term for 3-h lag in MDR (Fig. 17a)
indicate significant differences between convective and non-
convective areas 3-h prior to observed thunderstorms. The surface
and 850-mb levels are essentially unchanged from the zero lag
profiles (Fig. 10) but significant changes are evident aloft. The
profile for the severe category (MDR $\geq$ 8) indicates that the level
of non-divergence (LND) is between 850 and 700 mb, forcing a
maximum upward vertical motion in the layer which usually contains
the capping subsidence inversion. The other convection categories,
MDR $\geq$ 2 and MDR $\geq$ 4, also exhibit a lower LND than for the zero lag
profiles. Negative vorticity production, which was pronounced at
300 mb for zero lag (Fig. 10) is not clearly evident at 300 mb
for the 3-h lag. This would indicate that strong upper-level
divergence observed with zero lag is caused by thunderstorms and
does not contribute significantly to their initial development.

The average profiles for the divergence term with a 6-h lag
in MDR data shown in Fig. 17b show the same features as the 3-h
lag. Low-level production differentiates between convective and
non-convective areas at least 6 h prior to initial development while
no clear relationship exists aloft. On the synoptic scale, it
would appear that favorable kinematic conditions exist in the lower
troposphere for a considerable period prior to development of
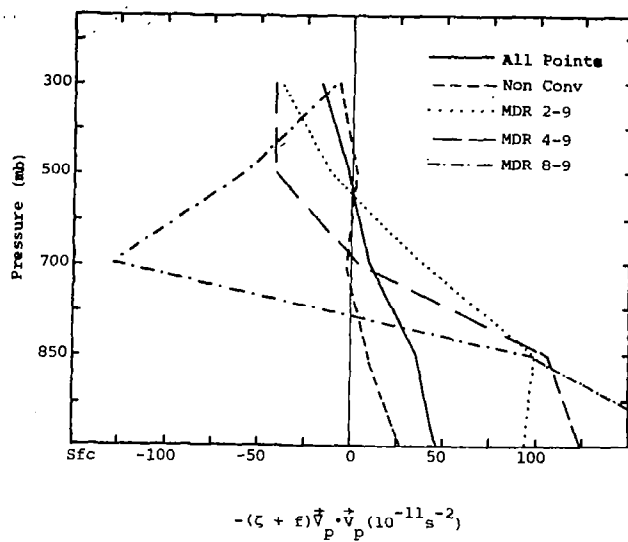thunderstorms. Development of severe thunderstorms appears to be
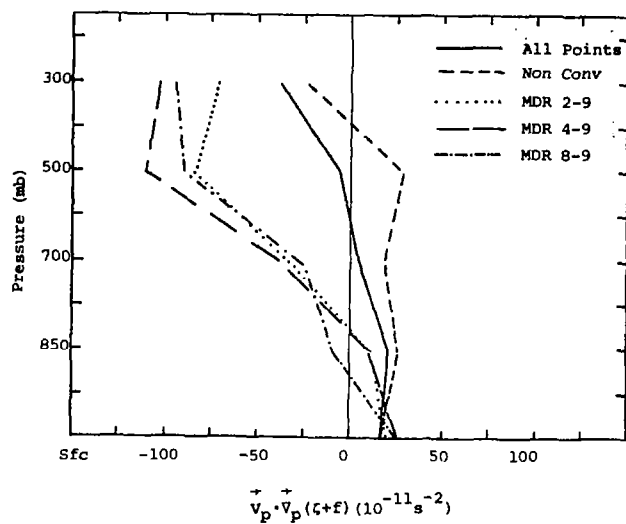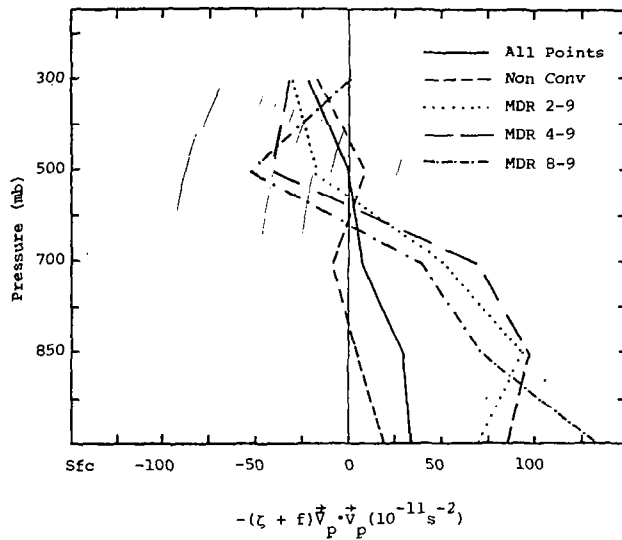
(a) 3-h lag in MDR.

(b) 6-h lag in MDR.

Fig. 16. Average profiles for horizontal vorticity advection
with time lags in MDR.

(a) 3-h lag in MDR.

(b) 6-h lag in MDR.

Fig. 17. Average profiles of the divergence term with time lags in MDR.

directly related to the coincidence of low-level vorticity produc-
tion with upper-level positive vorticity advection.

Average profiles for the vertical advection and twisting terms
for 3- and 6-h lags (not shown) indicated that the terms were
negligible when compared to their values at zero lag (Figs. 9 and
11.) Larger synoptic-scale values of these terms seem to be
caused by the systems of thunderstorms and show little if any
relation to initial development.

Figure 18 shows profiles of the total derivative for 3- and
6-h lags. The profiles of the sum of the divergence and twisting
terms in Eq. 1 for 3- and 6-h lags is essentially identical to those
of the divergence term (Fig. 17). The total derivative does not
clearly distinguish between convective and non-convective areas
for either 3- or 6-h lags. When comparing Fig. 18a to Fig. 17a,
it is obvious that an imbalance in the mean quantities in Eq. 1
exists prior to convection being observed.

The average profiles of the residual for 3- and 6-h lags show
that systematic imbalance occurs in the lower troposphere mainly
due to large values of the divergence term (Fig. 19). The imbalance
in middle levels shows the effect of a lower LND at 3-h lags. These
figures indicate that small-scale vertical advection alone is
probably not responsible for restoring balance and that other terms
must be considered since no convective circulations are evident
3 and 6 h prior to initial thunderstorm formation.

Overall, average profiles for 3- and 6-h lags indicate that
low-level, synoptic-scale events favorable for the development of
thunderstorms occur up to 6 h prior to development. Apparently the
development of positive vorticity advection at the mid- and upper-
levels is required over favorable regions in the lower levels to
initiate thunderstorms. Other possible explanations for development
include synoptic-scale changes in stability and moisture or actions
on a smaller scale than observed in AVE IV.

Table 4 summarizes the results of the vorticity equation dis-
cussed above for zero and 3-h lags in observed MDR values. The
last three columns of the table, $\frac{d\zeta_a}{dt}$, RHS (sum of the divergence
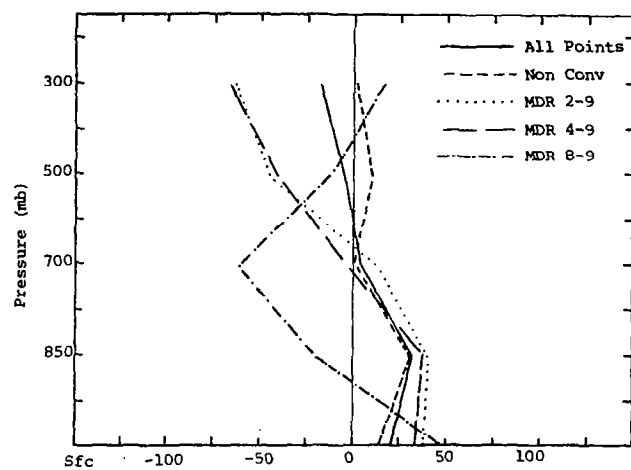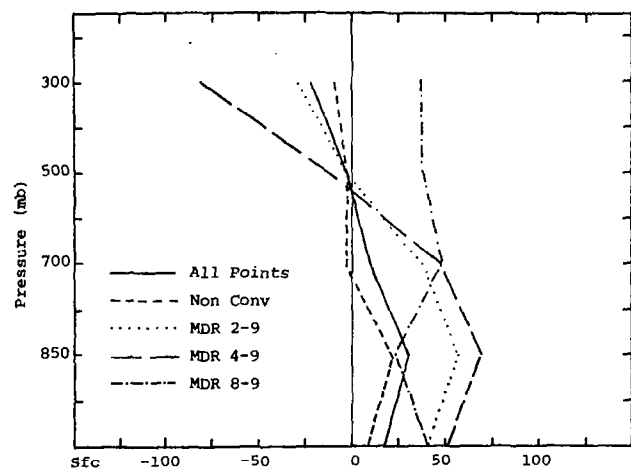
(a)   3-h lag in MDR.

(b)   6-h lag in MDR.

Fig. 18.   Average profiles for the total derivative of
vorticity with time lags in MDR.
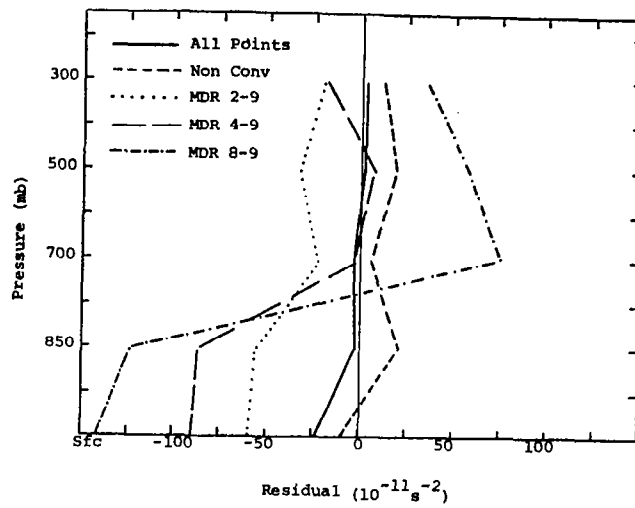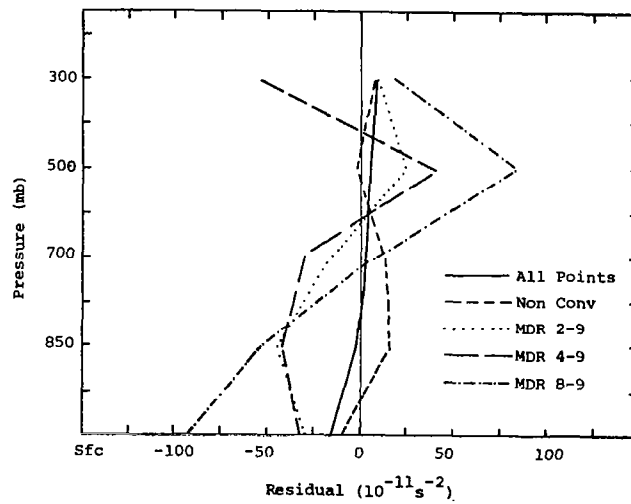
(a) 3-h lag in MDR.

(b) 6-h lag in MDR.

Fig. 19. Average profiles for the residual with
time lags in MDR.

Table 4. Averages for terms in the vorticity equation ($10^{-11}\sec^{-2}$).

Zero Lag

	Level	$\frac{\partial \zeta}{\partial t}$	$\vec{V}_p \cdot \nabla_p(\zeta_a)$	$\omega \frac{\partial \zeta}{\partial p}$	$-\zeta_a(\vec{\nabla}_p \cdot \vec{V}_p)$	Twisting Terms	$\frac{d\zeta_a}{dt}$	RHS	Residual
No Conv	Sfc	-0.6	14.1	0.0	12.4	0.0	13.5	12.4	1.1
	850	-8.2	26.2	2.0	8.5	2.5	20.0	11.0	9.0
	700	-12.8	21.5	-2.7	-7.9	-3.3	6.1	-11.2	17.3
	500	-11.2	18.5	-3.7	-2.9	-5.8	3.6	-8.8	12.4
	300	-7.3	7.6	-5.0	-3.8	-7.5	-4.6	-11.2	6.6
MDR≥8	Sfc	-2.2	16.5	0.0	170.8	0.0	14.3	170.8	-156.5
	850	26.4	11.4	3.4	143.4	-3.1	41.1	140.3	-99.1
	700	48.3	-0.8	-13.5	67.6	-21.3	33.9	46.3	-12.3
	500	90.9	-64.5	-33.8	-33.1	-23.5	-7.4	-56.6	49.1
	300	67.9	-133.6	-3.8	-141.0	2.4	-69.6	-138.7	69.0

3-h Lag in MDR Values

	Level	$\frac{\partial \zeta}{\partial t}$	$\vec{V}_p \cdot \nabla_p(\zeta_a)$	$\omega \frac{\partial \zeta}{\partial p}$	$-\zeta_a(\vec{\nabla}_p \cdot \vec{V}_p)$	Twisting Terms	$\frac{d\zeta_a}{dt}$	RHS	Residual
No Conv	Sfc	-2.5	17.4	0.0	25.1	0.0	14.9	25.1	-10.2
	850	3.5	24.9	1.7	8.6	-0.3	30.1	8.3	21.8
	700	-13.7	18.1	-3.1	-1.7	-3.2	1.2	-4.9	6.2
	500	-9.9	27.8	-6.3	2.3	-8.8	11.6	-6.5	18.0
	300	28.3	-24.0	-3.5	-7.0	-4.4	0.8	-11.4	12.2
MDR≥8	Sfc	26.7	24.2	0.0	191.3	0.0	50.9	191.3	-140.4
	850	-16.8	-10.1	8.7	95.0	9.1	-18.2	104.1	-122.3
	700	-31.9	-27.4	-2.1	-128.2	-8.4	-61.4	-136.6	75.2
	500	81.0	-91.2	-1.0	-57.1	-12.1	-11.2	-69.3	58.0
	300	91.8	-95.4	19.5	-9.1	-9.9	16.0	-19.0	35.0

and twisting terms), and the residual, emphasize the systematic
nature of the imbalance in the equation in areas of convection.
The surface and 850-mb levels exhibit an excess source of vorticity
while at 800 and 300 mb, there is an excess sink of vorticity.
Again, balance is assumed to be achieved primarily through eddy
friction.

2)   Relationships in time between vorticity and convection

The average profiles give a general picture of what the
synoptic-scale relationship between the various terms of the vor-
ticity·equation and convection should be at various levels in the
troposphere. The individually analyzed fields at each time must be
examined in order to determine changes in time and to see whether
or not the conditions at a particular time fit the general rela-
tionships developed through averaging.

At 0000 GMT on 24 April 1975, widespread and intense thunder-
storm activity was associated with the cold front in the central
plains. Figures 20 and 21 show all the terms of the vorticity
equation at 850 and 300 mb, respectively.

The field of $\frac{\partial \zeta}{\partial t}$ at 850 mb (Fig. 20a) subjectively fits the
synoptic conditions at 0000 GMT even though a ·forward difference
was used to compute the term. Ahead of the 850-mb frontal zone,
tendencies for increasing vorticity are evident with maximum
values ahead of two short wave troughs. Negative tendencies are
found behind the cold front and in a narrow band behind the short
wave trough over the Great Lakes region. Convective activity
(MDR ≥ 4) was occurring in areas of neutral tendency along the
front.

Horizontal vorticity advection at 850 mb (Fig. 20b) fits well
with the synoptic wind field at 0000 GMT. The narrow bands of
positive and negative advection in the Ohio Valley are a result of
the short wave·situated in that region. Average profiles indicate
no clear relationships between 850-mb vorticity advection and con-
vection. The analyzed field of vorticity advection at 0000 GMT
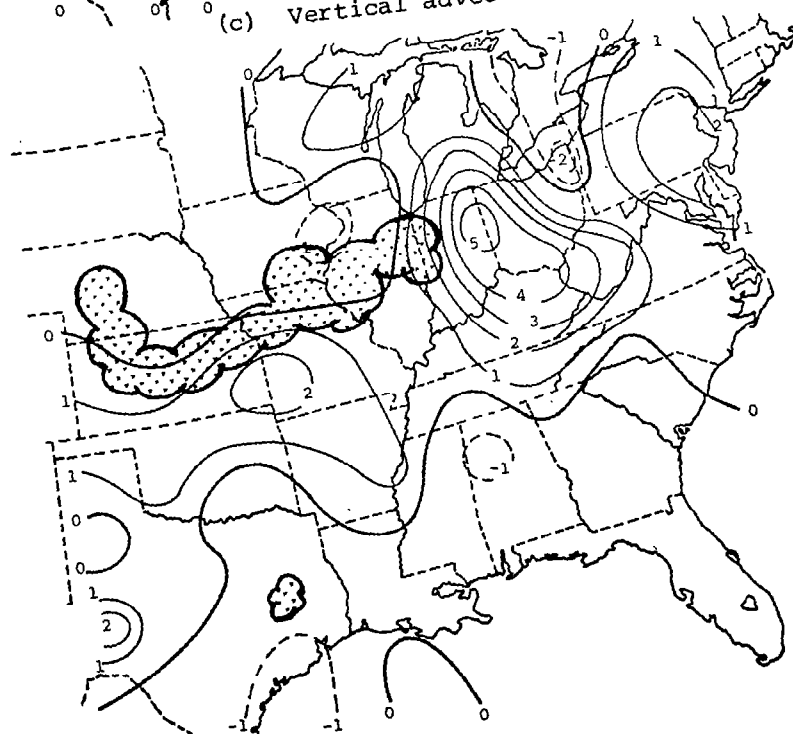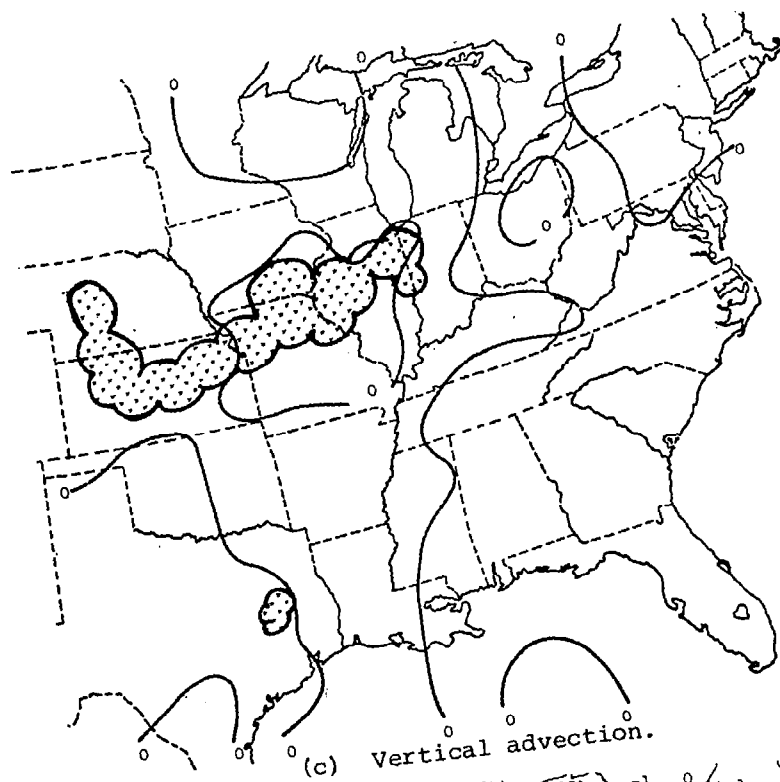reflects little or no correlation between areas of MDR ≥ 4 and the
advection pattern.
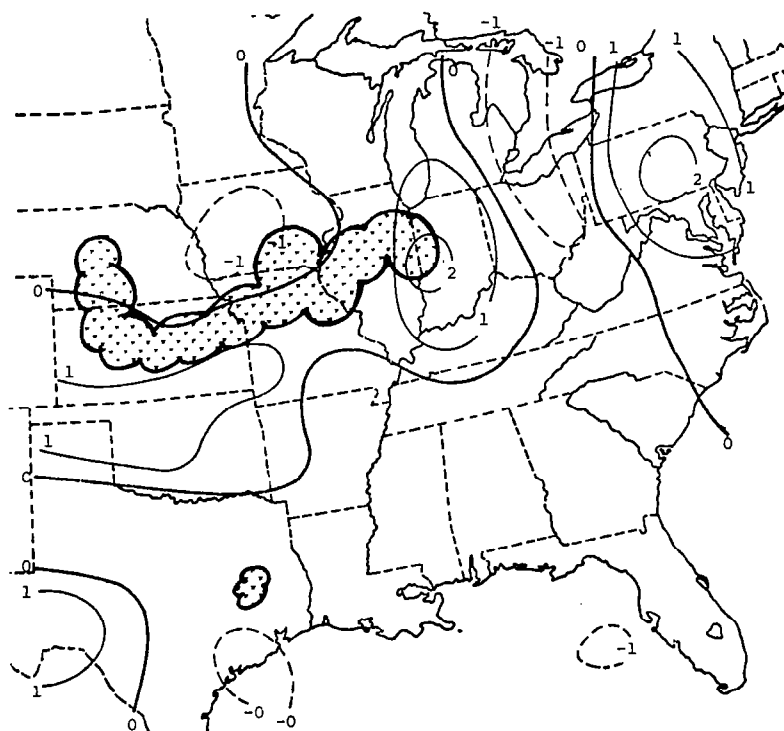
(a) Local derivative.
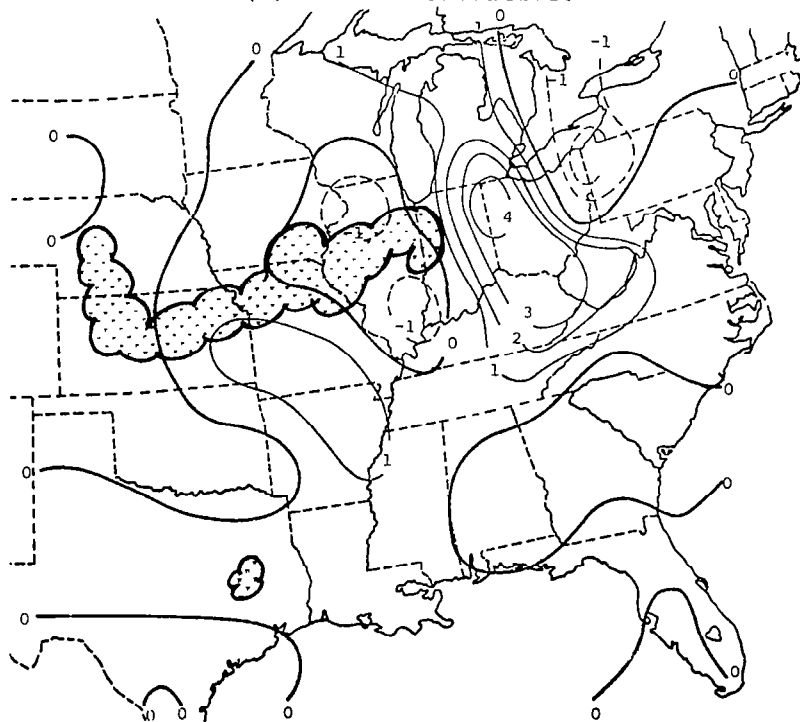
(b) Horizontal advection.

Fig. 20. Terms in the vorticity equation ($10^{-9} s^{-2}$) at 850 mb for
0000 GMT, 24 April 1975 (MDR $\geq$ 4 superimposed)

(c) Vertical advection.

(d) Total derivative.

Fig. 20. (Continued)

(e)   Divergence term.

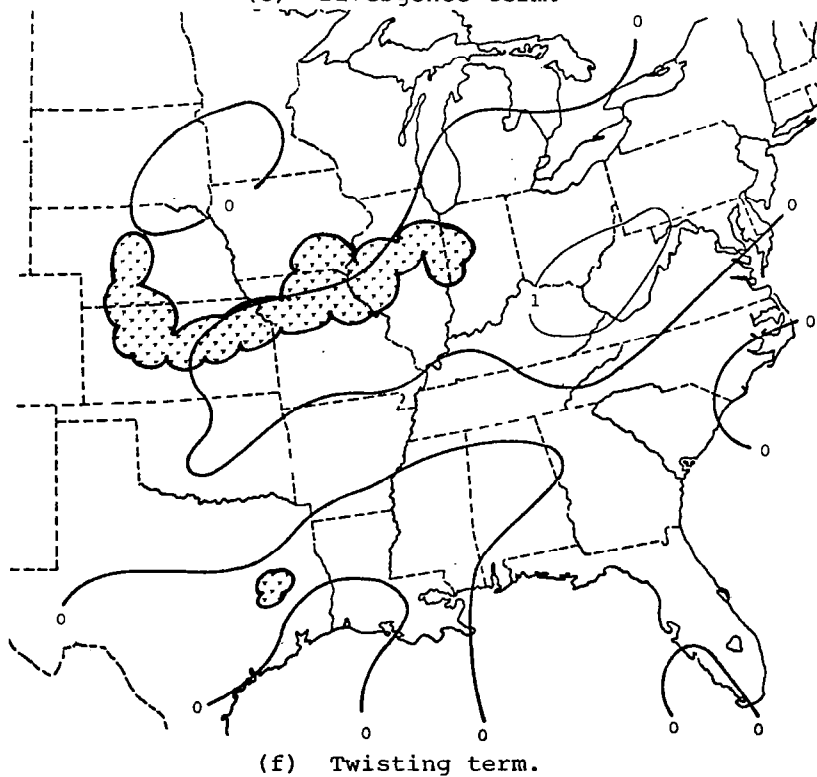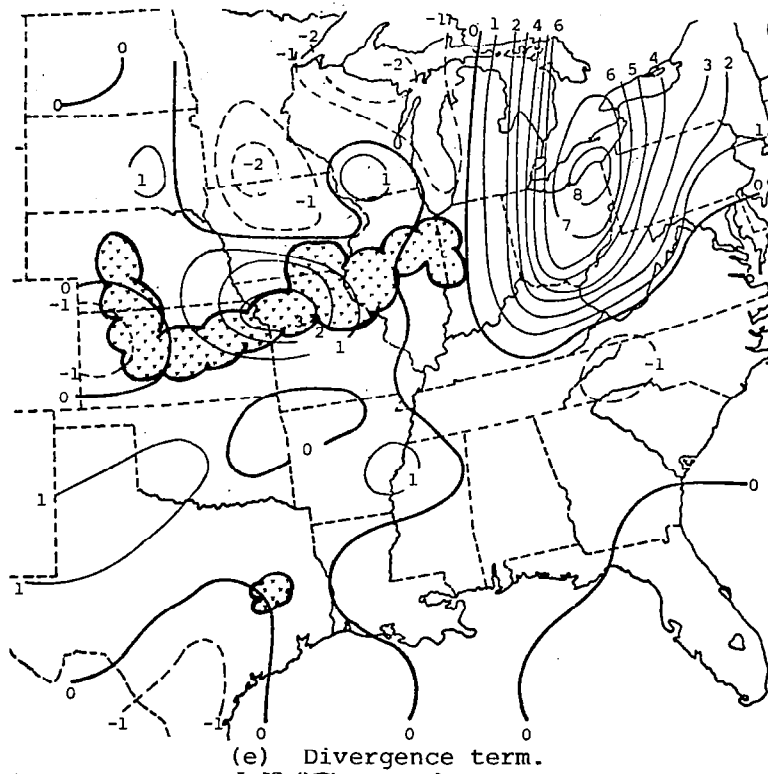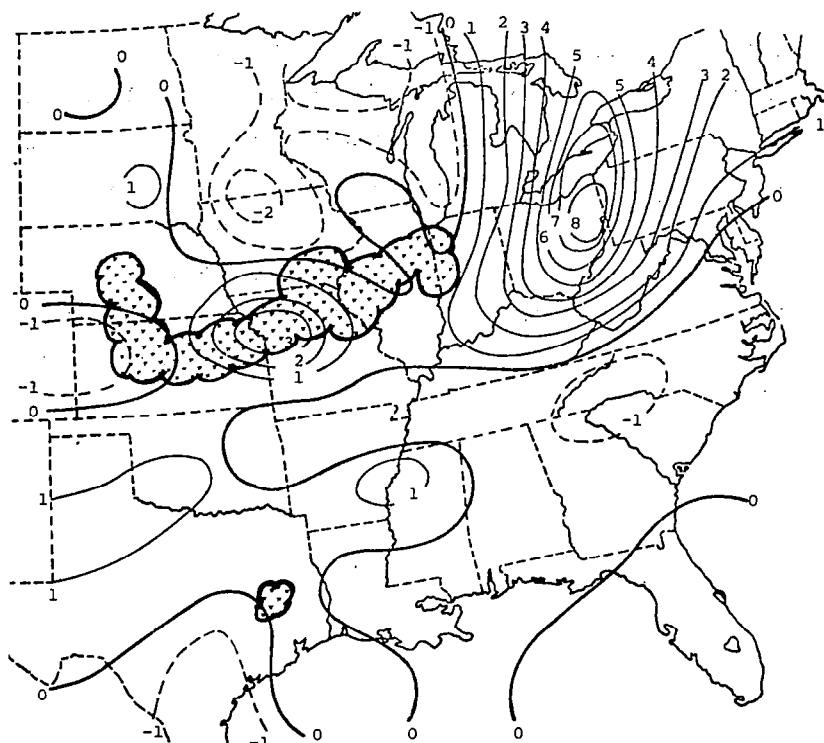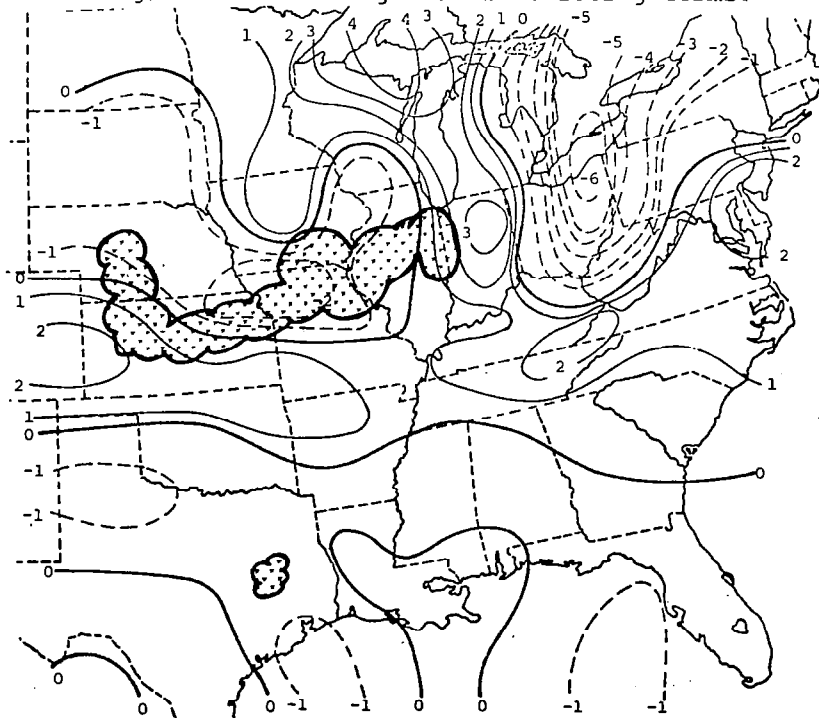(f)   Twisting term.

Fig. 20.   (Continued)

(g)   Sum of divergence and twisting terms.

(h)   Residual.

Fig. 20.   (Continued)

Scale analysis (Table 3, p. 19) indicated that the vertical advection term in the vorticity equation should generally be one order of magnitude less than the horizontal advection term. The analyzed field of $\omega \frac{\partial \zeta}{\partial p}$ (Fig. 20c) confirms that finding with most areas showing negligible values. However, one positive area associated with the short wave in the Ohio Valley approached the same order of magnitude as other terms. This was the largest value of the term found at 850 mb for the entire experiment, and neglect of the term would introduce approximately 25% error in the total derivative.

The total derivative of absolute vorticity shown in Fig. 20d indicates that parcels of air at 850 mb are gaining positive absolute vorticity ahead of the frontal system while losing it behind the front, in good agreement with the synoptic pattern. Convection was observed in both positive and negative areas at 850 mb showing no clear-cut relationship to convection.

The average profiles indicated a higher correlation between positive values of the divergence term and convection than any other term at 850 mb. The analyzed field of the divergence term at 0000 GMT supports this relationship. Maximum convergence, hence maximum values of the divergence term are located along the frontal zone. At this time, maximum convective activity was also located near the front giving good correlation between the divergence term and thunderstorm activity. Divergent flow begind the front and in the southeastern U. S. is associated with negative values of the term and an absence of thunderstorms.

Several authors have indicated values of the twisting term of the same order of magnitude as other terms in the vorticity equation in the vicinity of fronts, orographic barriers, and near low-level wind maxima (Barnes, 1970; Dallavalle and Bosart, 1975). In AVE IV the synoptic-scale, low-level wind shear was not strong in areas where gradients of ω were large, giving essentially negligible contributions of the twisting term at 850 mb. As was the case for vertical advection, the twisting term had maximum 850-mb values for the entire experiment at 0000 GMT. Maximum values were

associated with the frontal zone but were not clearly correlated with convection.

The residual term, or measure of imbalance in the mean terms of the equation, has greatest values at 850 mb for 0000 GMT near the frontal zone and also in the short wave in the upper Ohio Valley. Large changes in vorticity, which would be expected from the divergence term, are not observed over the time or space scales of the observational data so that the residual term essentially resembles a negative of the divergence term. The imbalance cor-relates fairly well with observed convection although minimum values are associated with light showers only.

The error analysis presented in Table 3 (p. 19) indicated that all terms of the vorticity equation were subject to considerable error at 300 mb, and that caution should be exercised when refer-ring to values of the terms at that level. In general, however, analyzed fields of the terms fit well with the observed wind field.

The local derivative at 300 mb for 0000 GMT on 24 April 1975, shown in Fig. 21a, depicts with marginal accuracy the passage of short waves over the map. These waves had small amplitudes and may have been approaching a scale below adequate resolution. A zero line separating maximum and minimum rates of change over the squall line in the central plains indicates the presence of a 300-mb ridge over the convection as expected from the synoptic charts.

Horizontal vorticity advection at 300 mb (Fig. 21b) seems to fit the synoptic wind field much better than did the local de-rivative, indicating resolution of the short waves may be worse in time than in space. Areas of positive vorticity advection $[\vec{V}_p \cdot \vec{\nabla}_p (\zeta + f) < 0]$ occur ahead of vorticity centers with negative advection upwind of the centers. The pattern clearly depicts the existence of short waves in the wind field. The advection patterns do not relate as clearly to the observed convection at this time as at future times, indicating that the first prefrontal squall line in AVE IV was primarily associated with low-level synoptic conditions.

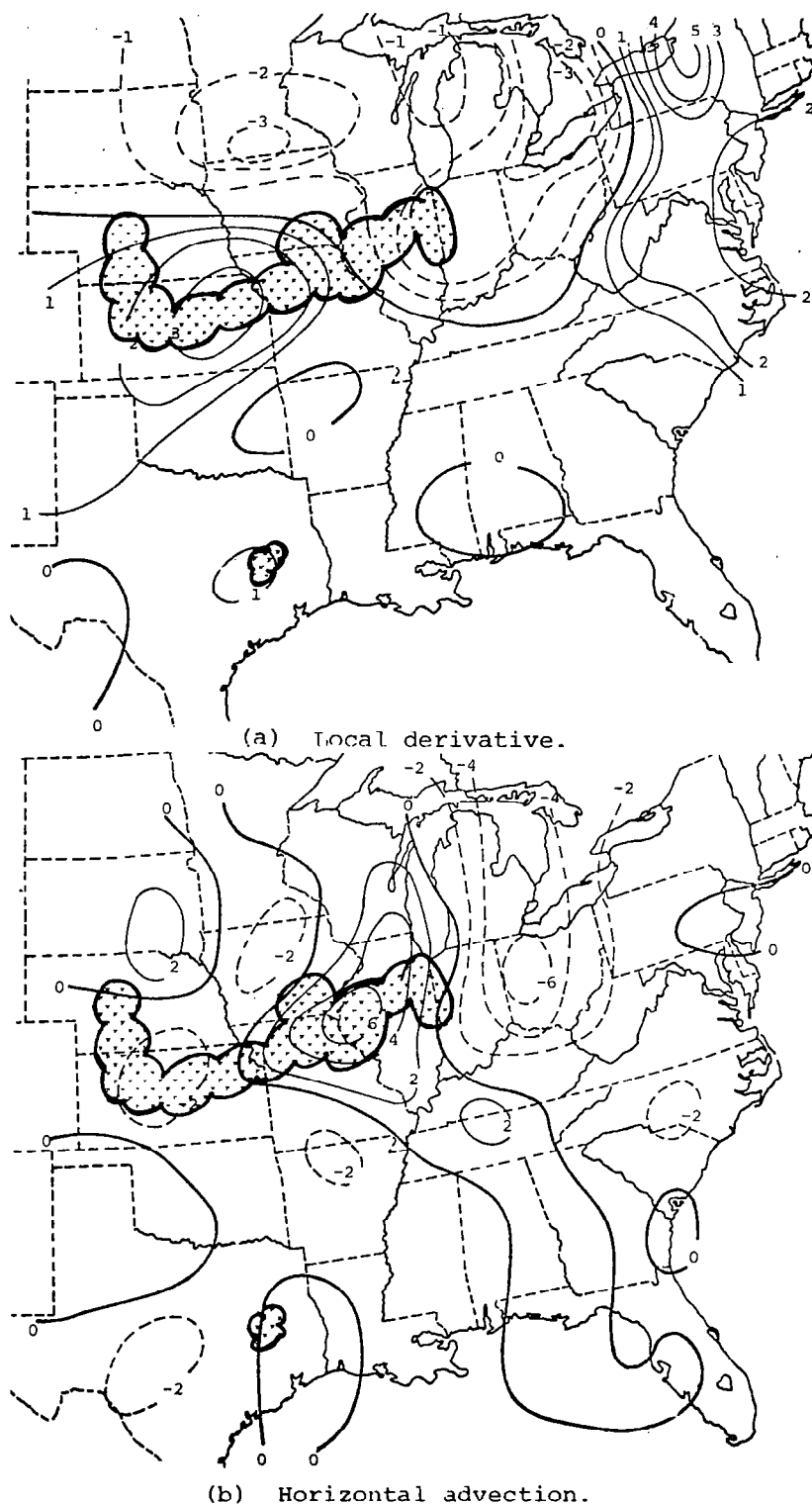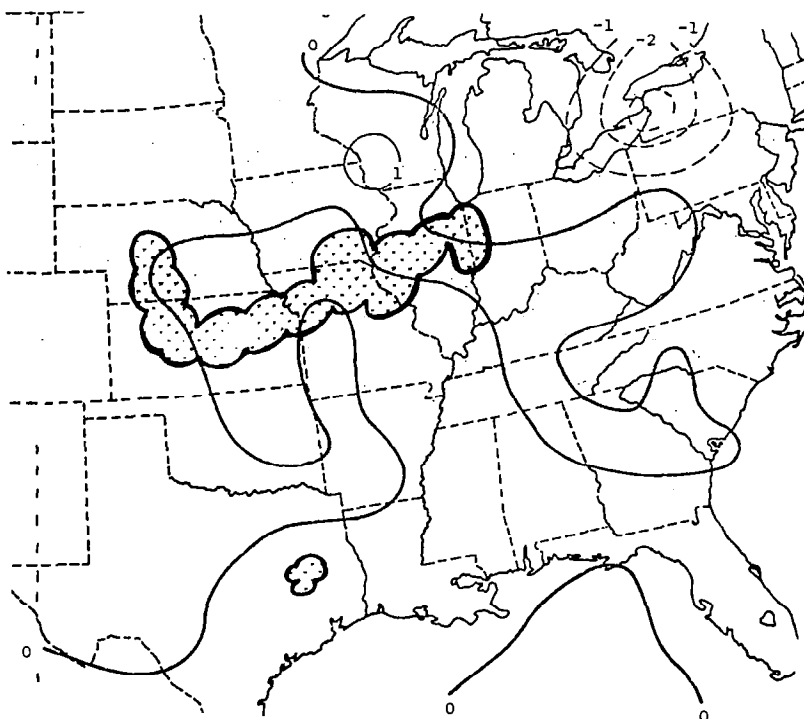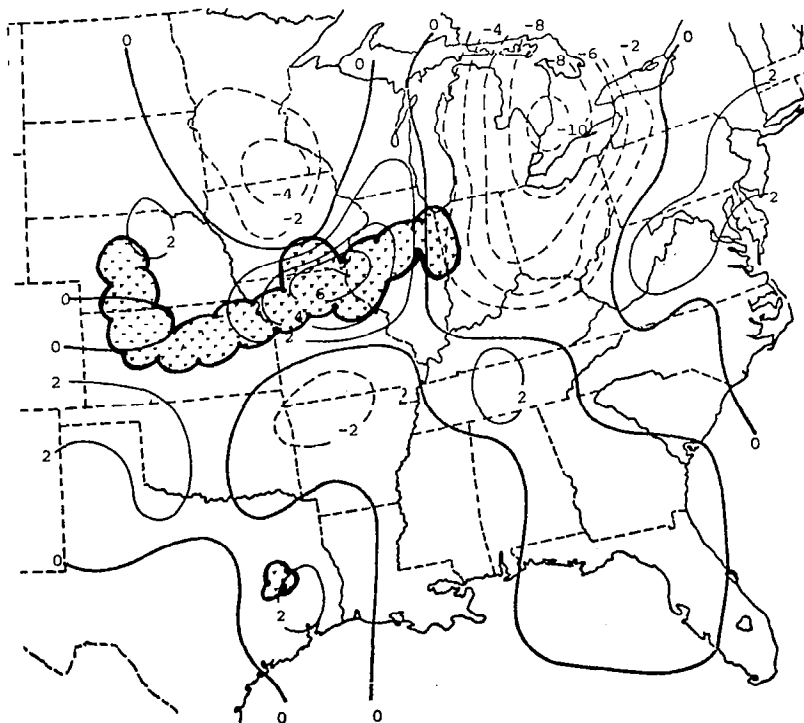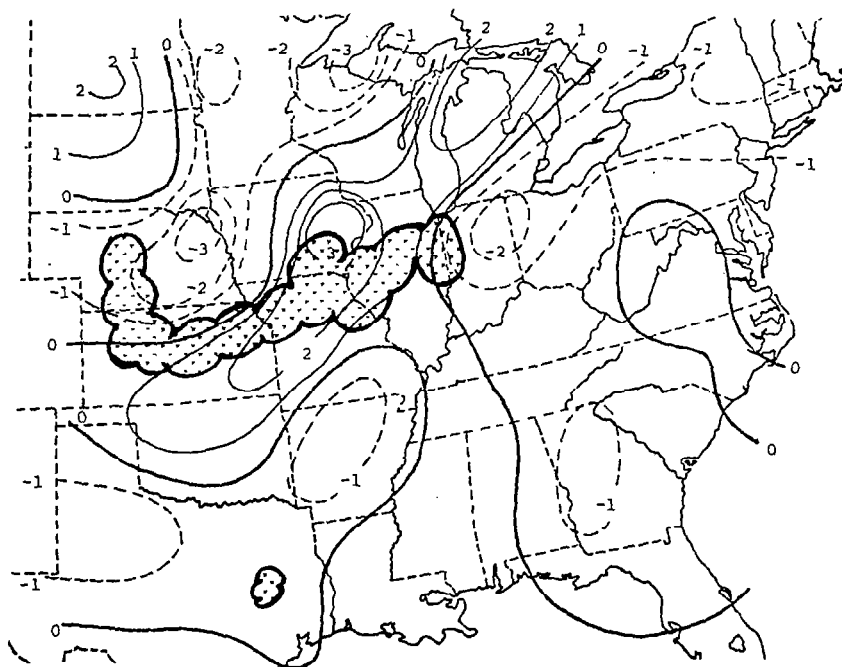The magnitude of the vertical advection of vorticity was larger

(a) Local derivative.

(b) Horizontal advection.

Fig. 21. Terms in the vorticity equation at 300 mb ($10^{-9}s^{-2}$) for 0000
GMT on 24 April 1975 (MDR $\geq$ 4 superimposed).

(c) Vertical advection.
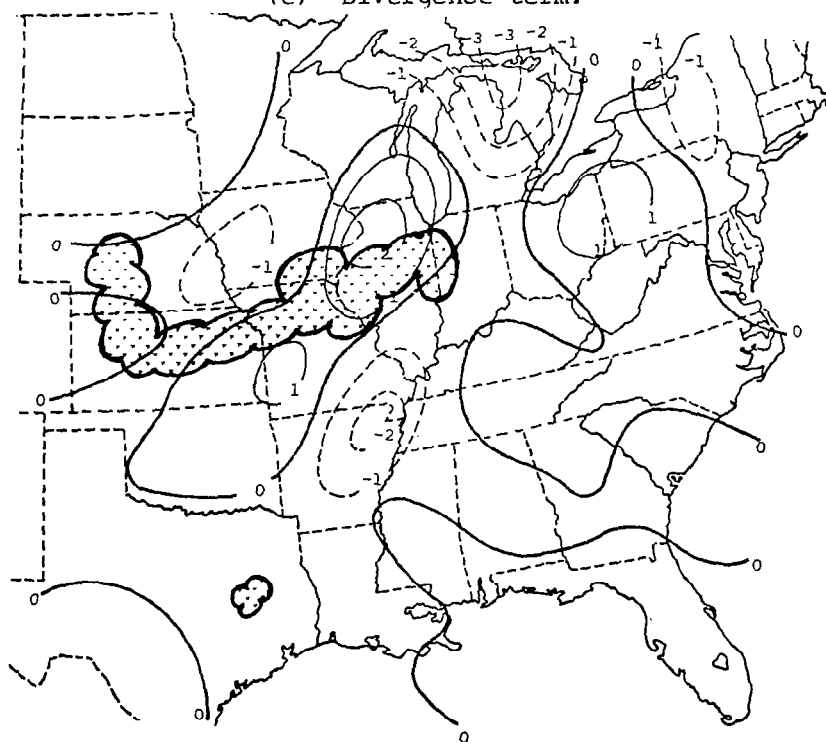

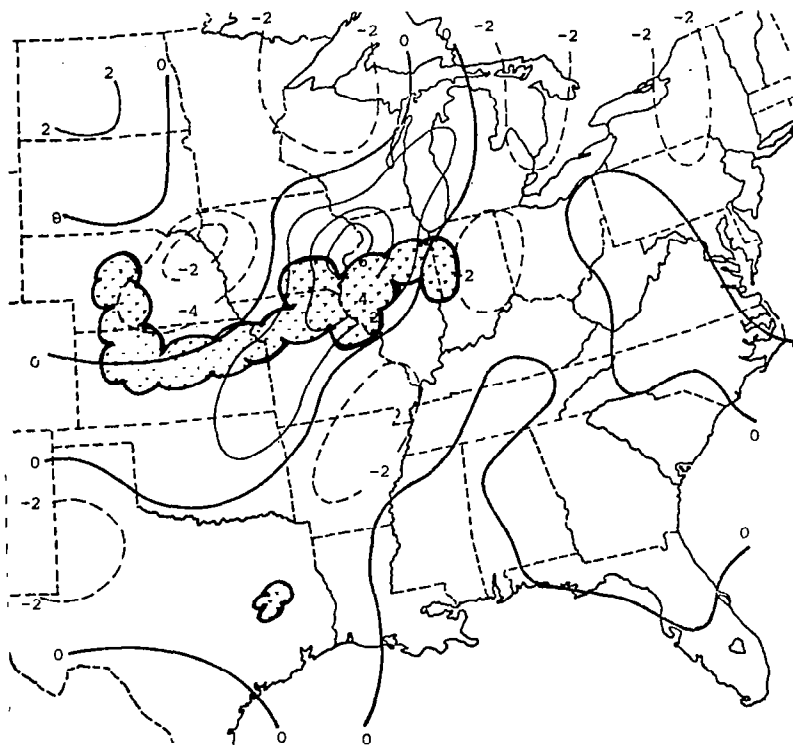(d) Total derivative.

Fig. 21. (Continued)
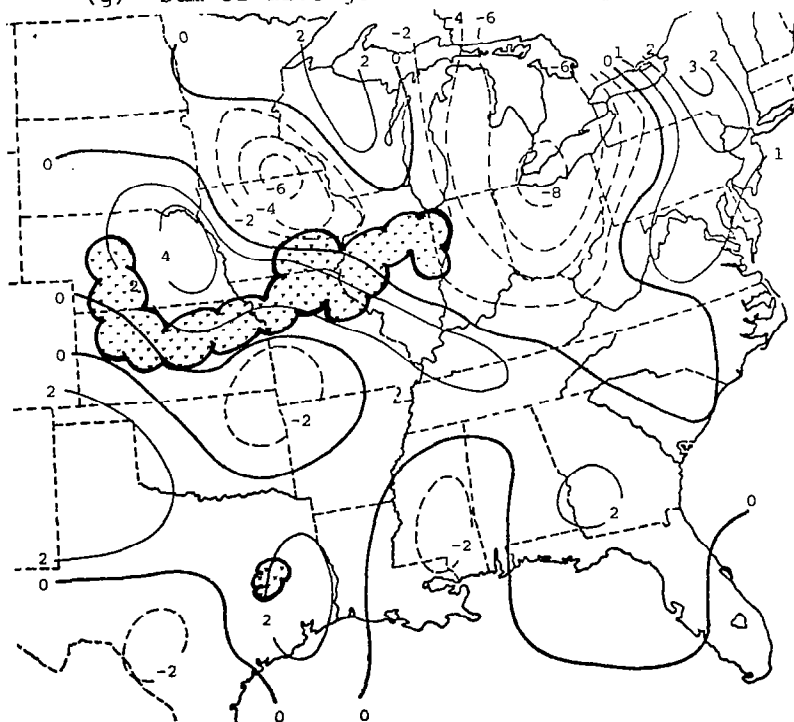
(e)   Divergence term.

(f)   Twisting term.

Fig. 21.   (Continued)

(g) Sum of divergence and twisting terms.

(h) Residual.

Fig. 21. (Continued)

at 300 mb than at 850 mb due mainly to larger values of ω, but since
the other terms in the equation also increased in magnitude the
relative importance of the term is still small. In Fig. 21c,
it is evident that vertical advection approached the same size as
horizontal advection only over the Great Lakes region.

The field of the total derivative of absolute vorticity at
300 mb fits well with the synoptic pattern with air parcels gaining
vorticity through troughs and losing it through ridges (Fig. 21d).
When related to observed convection, the large positive area over
the eastern part of the pre-frontal squall line is opposite what
would be expected from the average profiles.

The divergence term was expected to be a sensitive term based
on the error analysis, but the observed field seems to fit the
synoptic wind field fairly well (Fig. 21e). Convective activity
was associated with negative values of the term at 300 mb except
for the eastern part of the squall line. None of the terms at
300 mb fits the expected relationship to convection over this area.
Inspection of the 700- and 500-mb divergence terms at 0000 GMT
indicates strong divergence in these layers. This again, suggests
that lower-level conditions may be responsible for initiating
this activity.

At 300 mb it was expected that the twisting terms could reach
large values, since gradients of ω may be large and strong vertical
shears were present near the jet stream. Since four parameters
are used in computing the twisting terms, it is hard to visualize
what the synoptic field of the term should look like. Since the
u and v components were almost always increasing with height at
this level, the sign of the term is determined by the gradients of
ω. The computed field of the twisting term (Fig. 21f) seemed
reasonable when compared to the synoptic pattern, with centers of
maximum and minimum values associated with waves in the jet stream.
The average profiles indicated little relationship between convec-
tion and the twisting terms; the analyzed fields also showed this.
Since ω was usually a maximum in areas of convection, the twisting
terms were zero in the centers of convective systems. Also, since

ω reached large values <u>after</u> thunderstorms had developed, the twisting terms were usually negligible <u>prior</u> to initial development.

The sum of the divergence and twisting terms (Fig. 21g) gives a pattern very similar to the total derivative (Fig. 21d) with magnitudes being the major difference. In relation to the squall line, large positive values are observed over the eastern half of the squall line and large negative values over the western half.

The residual term at 300 mb for 0000 GMT (Fig. 21h) appears to show positive values over ridges in the wind field and negative values over troughs which would indicate that the residual is somewhat systematic. However, fields of the residual at other times and levels do not show the same relationship. All terms are sensitive at 300 mb to fluctuations in the wind field. Even though considerable smoothing of the data has been done before computation of the terms in the vorticity equation, considerable influence of perturbations of 400- to 1000-km wavelengths is still present. It is the effect of these unresolved scales of motion that are most likely producing large values of the residual. Most of these fluctuations occur on a space and time scale shorter than can be determined from the observations, which is unfortunate, since amplification of these minor fluctuations may be important in triggering severe thunderstorms.

The examples presented at 0000 GMT establish the important terms and possible causes for imbalance in the vorticity equation. Examples that follow will be used primarily to establish relationships in time between the occurrence of severe thunderstorms and the terms in the vorticity equation.

Between 0000 GMT and 2100 GMT on 24 April 1975, the prefrontal squall line moved ahead of the short wave trough with thunderstorm intensities generally decreasing after 0600 GMT. There were no major amplifications of short waves in the synoptic flow during this period and the fields of the terms in the vorticity equation reflected this. By 2100 GMT, however, thunderstorm activity had begun to develop along the frontal zone from Kansas through Oklahoma. In the upper levels, the second and

stronger short wave of AVE IV was entering the western edge of the grid.

By 2100 GMT the terms in the vorticity equation reflected the developing short wave in the west. Large values of vorticity production in the low levels were evident along the frontal zone, indicating both a forcing of increased circulation and lifting through convergence. Figure 22 shows the field of the surface divergence term at 2100 GMT. Maximum values of vorticity production were well correlated with observed thunderstorm activity, although large areas experiencing vorticity production were free of convection.
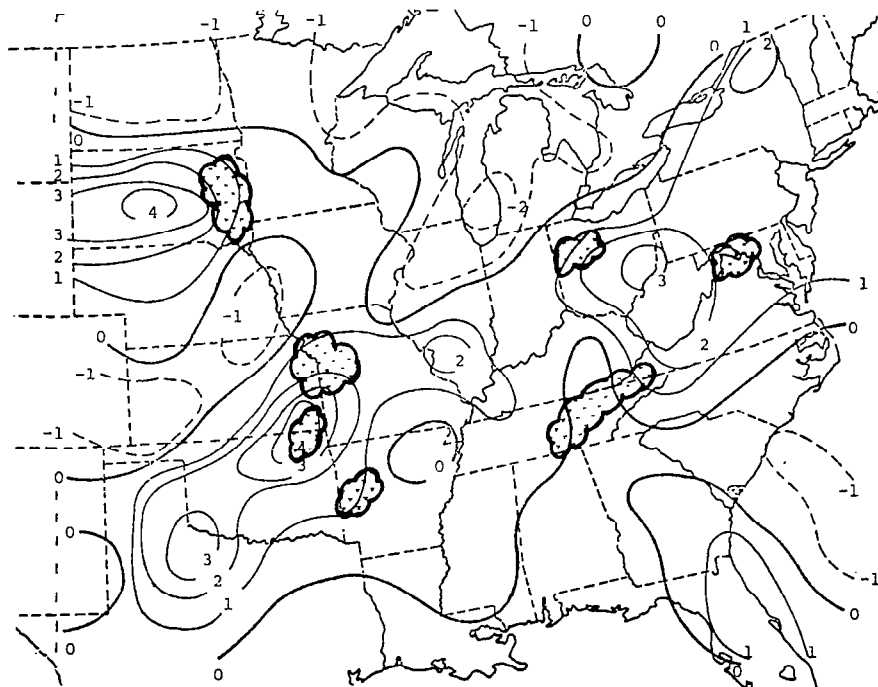

Fig. 22. Analyzed field of the divergence term ($10^{-9}s^{-2}$) at the surface for 2100 GMT on 24 April 1975 (MDR $\geq$ 4 superimposed).

At 300 mb major changes were appearing at 2100 GMT in the spatial fields of the terms in the vorticity equation in response to the developing short wave. A band of positive vorticity advection was located from North Dakota to Texas ahead of the short wave trough at 300 mb (Fig. 23a). All of the thunderstorms through the central plains were located within this band. Low-level conditions had been favorable for development within this region for 3 to 6 h prior to 2100 GMT, but thunderstorms did not occur until the approach or development of the upper-level trough. Further east, the area of scattered thunderstorms also correlated well with a band of positive vorticity advection at the upper level. The center of the advection had moved eastward from the main activity in Tennessee, possibly explaining the decrease in thunderstorm intensity observed there.

Imbalance in the vorticity equation has a maximum near the severe thunderstorms in Kansas and Missouri. The twisting terms and vertical advection term were negligible while the divergence term was positive (Fig. 23c). Production by divergence along with large values of positive vorticity advection should give large positive values of the local derivative over this region. The observed change is slightly negative (Fig. 23b), indicating large imbalance in Eq. 1 over Missouri. This points again to events on a smaller scale creating changes in the synoptic-scale flow patterns that are not measured in the space or time scale of AVE IV. The short wave amplified considerably between 2100 and 0600 GMT on 25 April 1975 with a sharp ridge developing over the thunderstorm activity. This lends support to the hypothesis that the residual may represent real effects of small-scale motions on the large-scale flow and not just the effect of rawinsonde measurement error and truncation error.

By 0000 GMT on 25 April 1975 the squall line from Oklahoma through Missouri had greatly intensified. Several tornadoes accompanied by hail and damaging winds had been reported along the entire length of the system. The synoptic-scale short wave was developing over the central plains in conjunction with the squall
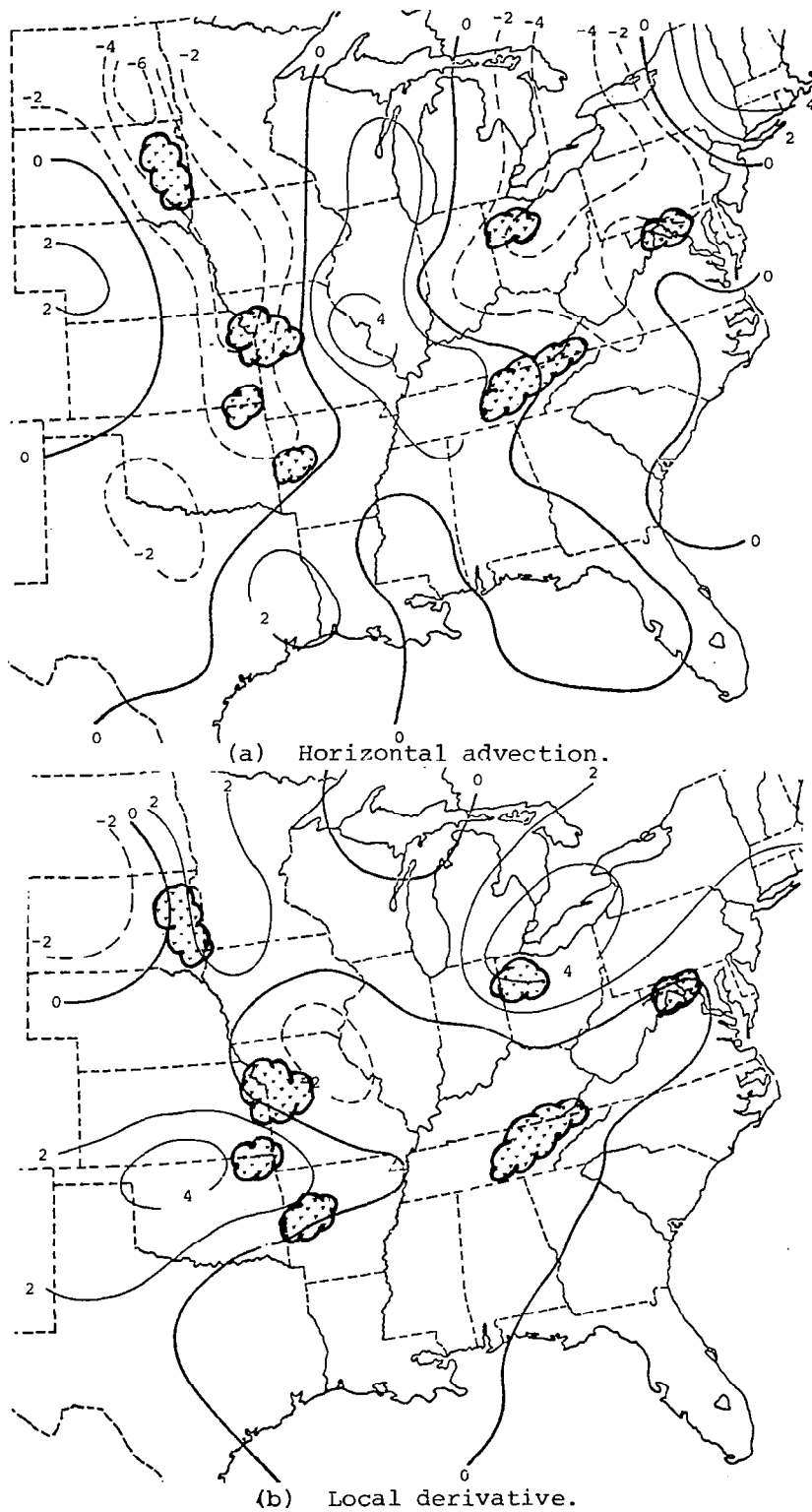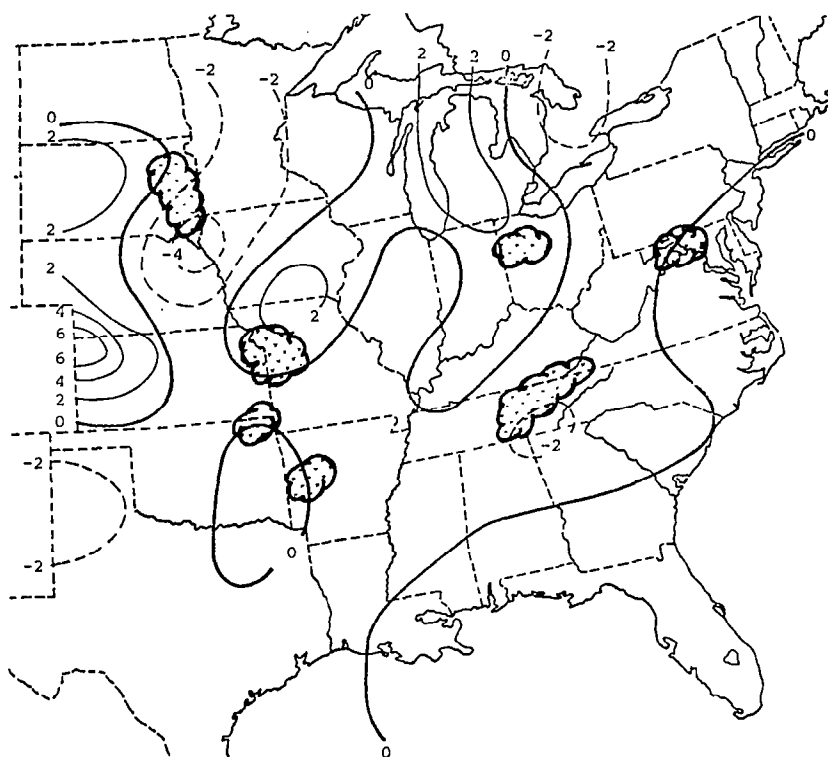
(a)   Horizontal advection.

(b)   Local derivative.

Fig. 23.   Analyzed fields of terms in the vorticity equation ($10^{-9} s^{-2}$) at 300 mb for 2100 GMT on 24 April 1975 (MDR $\geq$ 4 superimposed).
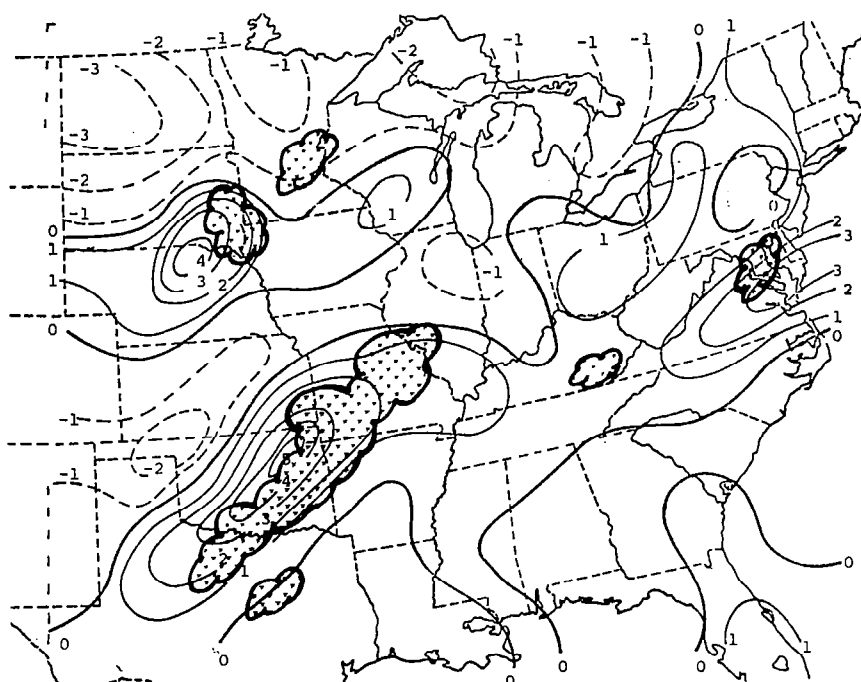
(c) Divergence term.

Fig. 23. (Continued)

line.

Surface vorticity production at 0000 GMT on 25 April 1975 (Fig. 24a) clearly showed areas of severe convection especially along the intensifying squall line. Secondary areas of convection in South Dakota and in the Middle Atlantic Region were also associated with centers of vorticity production. The residual had essentially the same pattern as Fig. 24a with the signs reversed since the other terms were an order of magnitude smaller than the divergence term. As expected from the average profiles, an excess production of vorticity correlated best with areas of thunderstorms. Dissipation through friction or small-scale circulations must have been occurring in order to prevent rapid cyclonic development at the surface.

The 300-mb vorticity advection field shown in Fig. 24b clearly indicates the amplification of the short wave over the central plains. The band of positive vorticity advection over the squall line has increased in area and in magnitude since 2100 GMT while moving slightly eastward. The divergence term was still quite small compared to the horizontal advection term over the squall line at 0000 GMT. Local increase of vorticity in response to the advection was evident but not nearly enough to achieve balance.

It appears that although vorticity production at the surface properly depicted where the squall line developed, the initial formation of thunderstorms did not occur until the upper-level, short-wave system had either moved or developed over the region of low-level vorticity production. Maximum intensity of the system of thunderstorms appears to occur when the correlation between lower-level production and upper-level positive vorticity advection is greatest.

At 0600 GMT on 25 April 1975 the second squall line had reached or surpassed its maximum intensity while moving slowly eastward. Low-level vorticity production was essentially the same as at 0000 GMT but of lesser magnitude. However, in the upper levels the terms of the vorticity equation reflected further intensification of the synoptic-scale short wave.

(a) Surface divergence term.
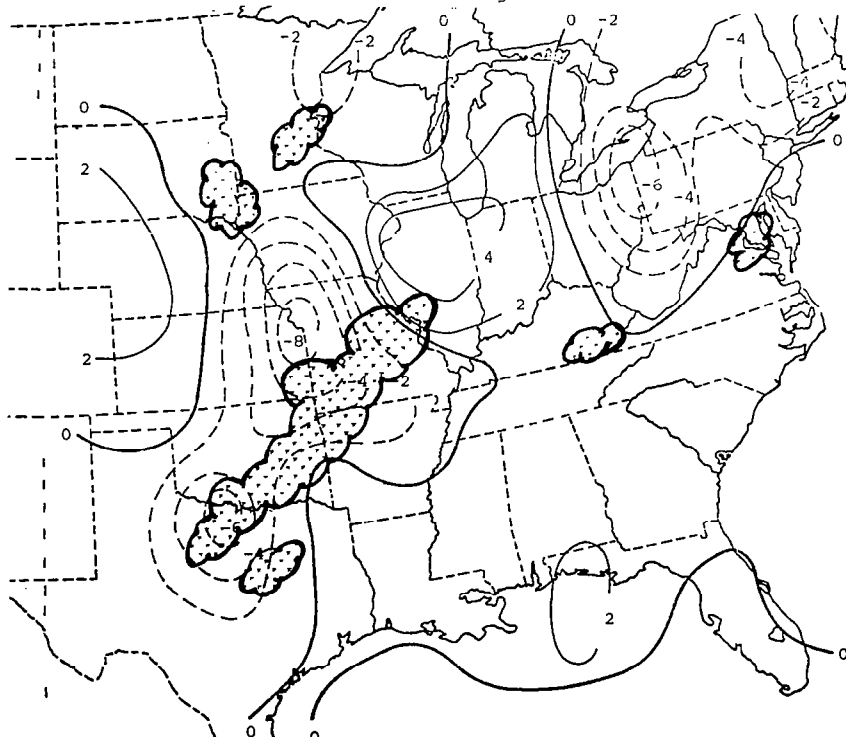
(b) 300 mb horizontal advection.

Fig. 24. Analyzed fields of terms in the vorticity equation ($10^{-9} s^{-2}$) at 0000 GMT on 25 April 1975 (MDR $\geq$ 4 superimposed).

Large values of positive vorticity advection preceded the sharp
trough in the wind field over the upper Mississippi Valley with
strong negative advection ahead of the sharp ridge over Illinois
and Michigan (Fig. 25a). Values over the squall line were not as
large as at 2100 or 0000 GMT, possibly due to interaction between
the squall line and the synoptic-scale flow. The sharp intensifi-
cation of the ridge in the wind field in Fig. 25b over the squall
line closely resembles the effect described by Fankhauser (1971)
and Ninomiya (1971). Large systems of thunderstorms are thought
to act as an obstacle to the synoptic-scale flow, forcing a diver-
gent current around the convective region while, at the same time,
reducing wind speeds in the area of activity.

This newly developed sharp ridge over the squall line created
large values of the divergence term over the squall line (Fig. 25c).
The field fits observed convection better at this time than at
previous times, indicating that development of a divergent zone
aloft in areas of thunderstorms may be caused by the thunderstorms
themselves.

The movement of the upper-air short wave system to the north-
east was followed by decreasing intensity of the thunderstorms at
1200 GMT on 25 April 1975. Relationships developed at previous
times between convection and terms in the vorticity equation re-
main unchanged in the spatial fields at 1200 GMT.

In summary, the individually analyzed fields of terms in the
vorticity equation have shown that general relationships developed
by the average profiles work best in the lower levels and that
features in the upper levels of the troposphere change with evolv-
ing systems of thunderstorms. Systematic imbalance when related
to convection was evident in the low levels while the upper-level
imbalance seemed more related to small-scale fluctuations in the
wind field than to thunderstorm activity.

b.   Stability

The results of the stability analysis are presented in the
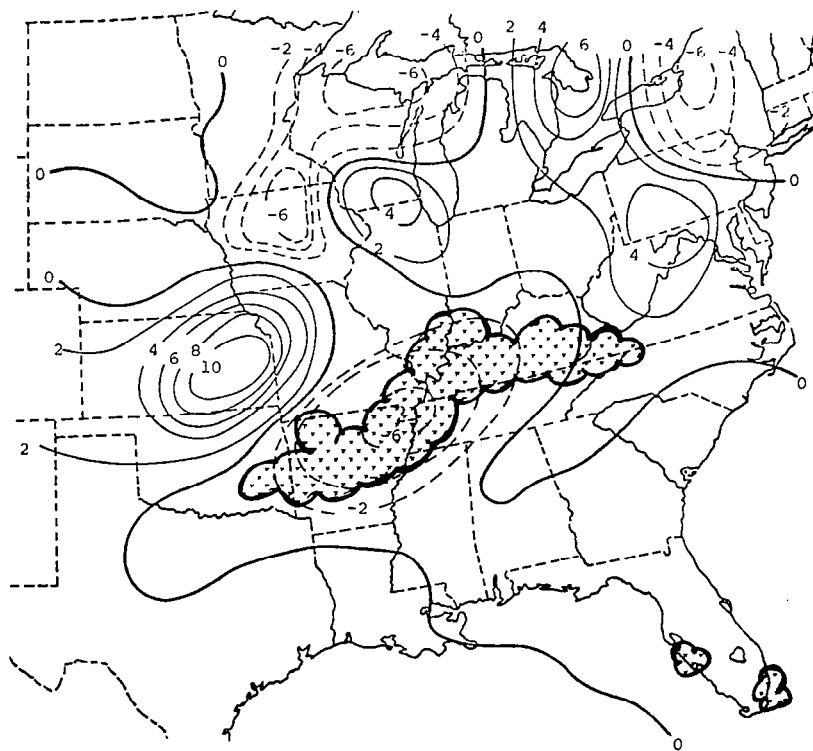same manner as the vorticity budget. Previous studies had indicated
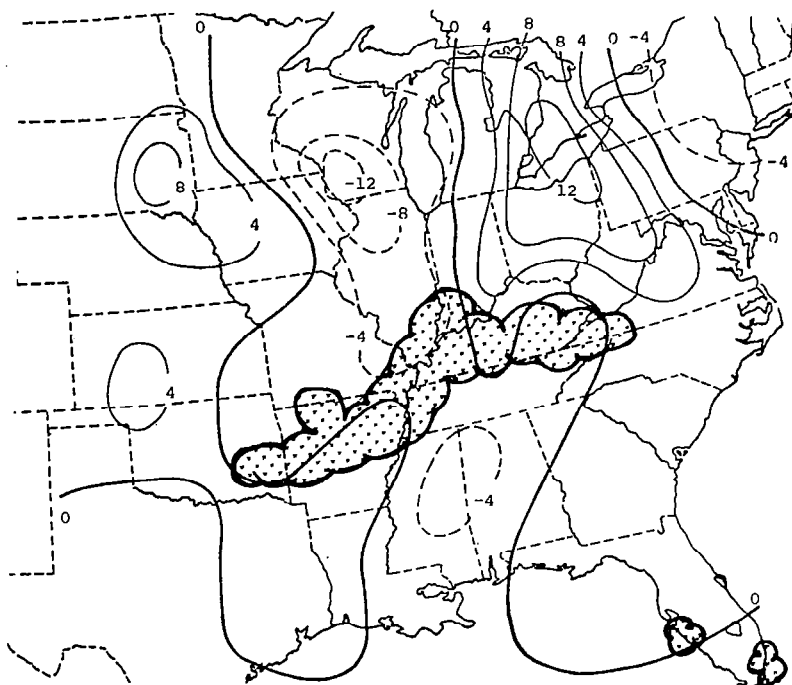
(a) Horizontal vorticity advection.
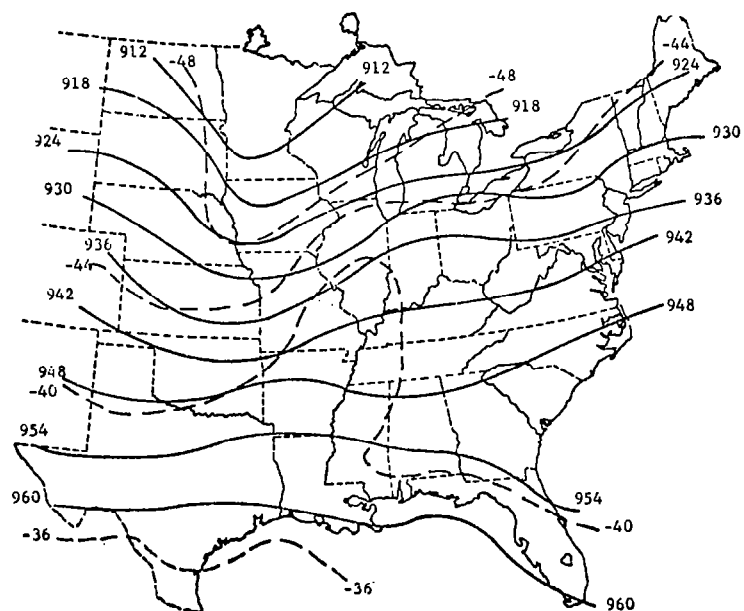
(b) 300 mb synoptic chart.

Fig. 25. Analyzed fields of terms in the vorticity equation and
synoptic chart at 300 mb for 0600 GMT on 25 April 1975.

(c)   Divergence term.

Fig. 25   (Continued)

that although instability is present in areas of convective activity

many non-convective areas are more unstable. This was tested for

AVE IV first through averages and then by examination of individual-

ly analyzed fields.

Figure 26 shows the average values of the four measures of σ_e

for different categories of observed MDR data. In all layers the

trend is for decreasing stability with increasing thunderstorm in-

tensity. The layer in which the subsidence inversion was usually

located, 850 to 700 mb, exhibited the largest instability.

Wilson and Scoggins (1976) found that some large areas without

thunderstorms were highly unstable for the AVE II experiment.

The averages for the MDR $\leq$ 1 category indicate the same results for

AVE IV for the surface- to 850-mb layer. Non-convective areas are

more unstable than convective areas on the average. Possible ex-

planations for this are that the thunderstorms have interacted

with the boundary layer to increase low-level stability, or that

the kinematics of the atmosphere in non-convective areas indicate
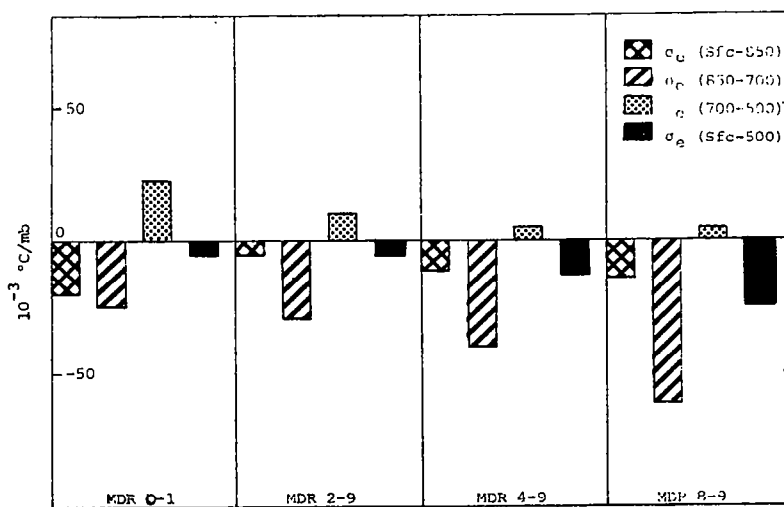
the suppression of convection.

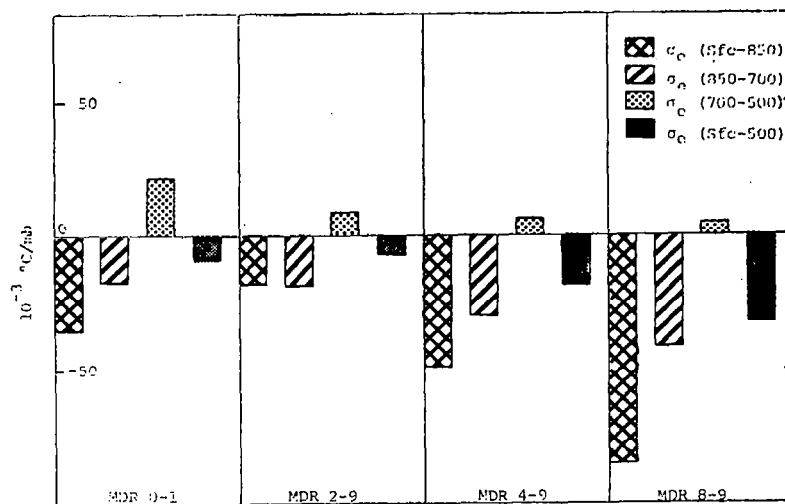Fig. 26. Averages of convective instability (10^{-3}°C mb^{-1}).

Average values for stability for 3- and 6-h time lags are shown in Fig. 27. Important points in these averages are the much more unstable boundary layer at 3- and 6-h lags compared to zero lag in areas of thunderstorms (MDR $\geq$ 4, MDR $\geq$ 8), and the systematic decrease in stability for increasing MDR as much as 6 h prior to initial thunderstorm development.

The fact that stability in the surface- to 850-mb layer was smaller prior to than during convection is evidence of the interaction of the thunderstorms with the environment. The other layers were essentially the same for 3- and 6-h lags as for zero lag. Apparently the interaction is more effective in the boundary layer than aloft. This observation fits well with results of the vorticity equation, where a larger imbalance existed in the lower levels than aloft, requiring more action by smaller-scale circulations in the boundary layer.

The average profiles of σ_e for 6-h lags in MDR values (Fig. 27b) indicate that areas of severe thunderstorm development have more unstable conditions than less severe areas well in advance of the occurrence of the thunderstorms. Darkow (1975) found similar results with his surface static energy index. Maximum values were located in advance of existing severe storms or prior to initial development.

The average profiles indicate that thunderstorms occur in an unstable environment but that the release of instability in the form of thunderstorms must be triggered by large-scale kinematic features or small-scale development undetected in the data.

Specific analyzed fields of stability showed the same relationships between σ_e and convection as was developed above through average profiles. Figure 28 shows σ_e for all four levels at 0000 GMT on 24 April 1975. Values of σ_e for the surface- to 850-mb layer in the vicinity of the squall line in the central plains are more stable than the surrounding area, indicating the possible effect of the thunderstorms acting to stabilize the boundary layer. Large areas of unstable air are present in this layer from west Texas to the southeastern U. S., a region in which very little

(a)   3-h lag.
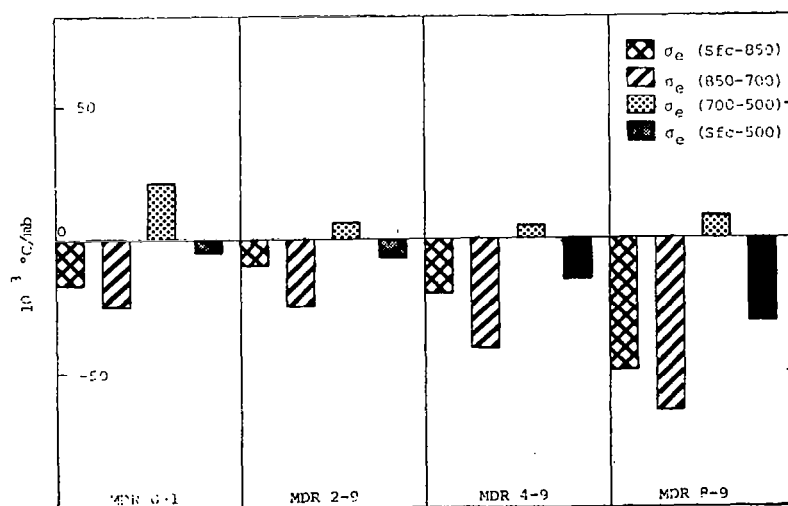
(b)   6-h lag.

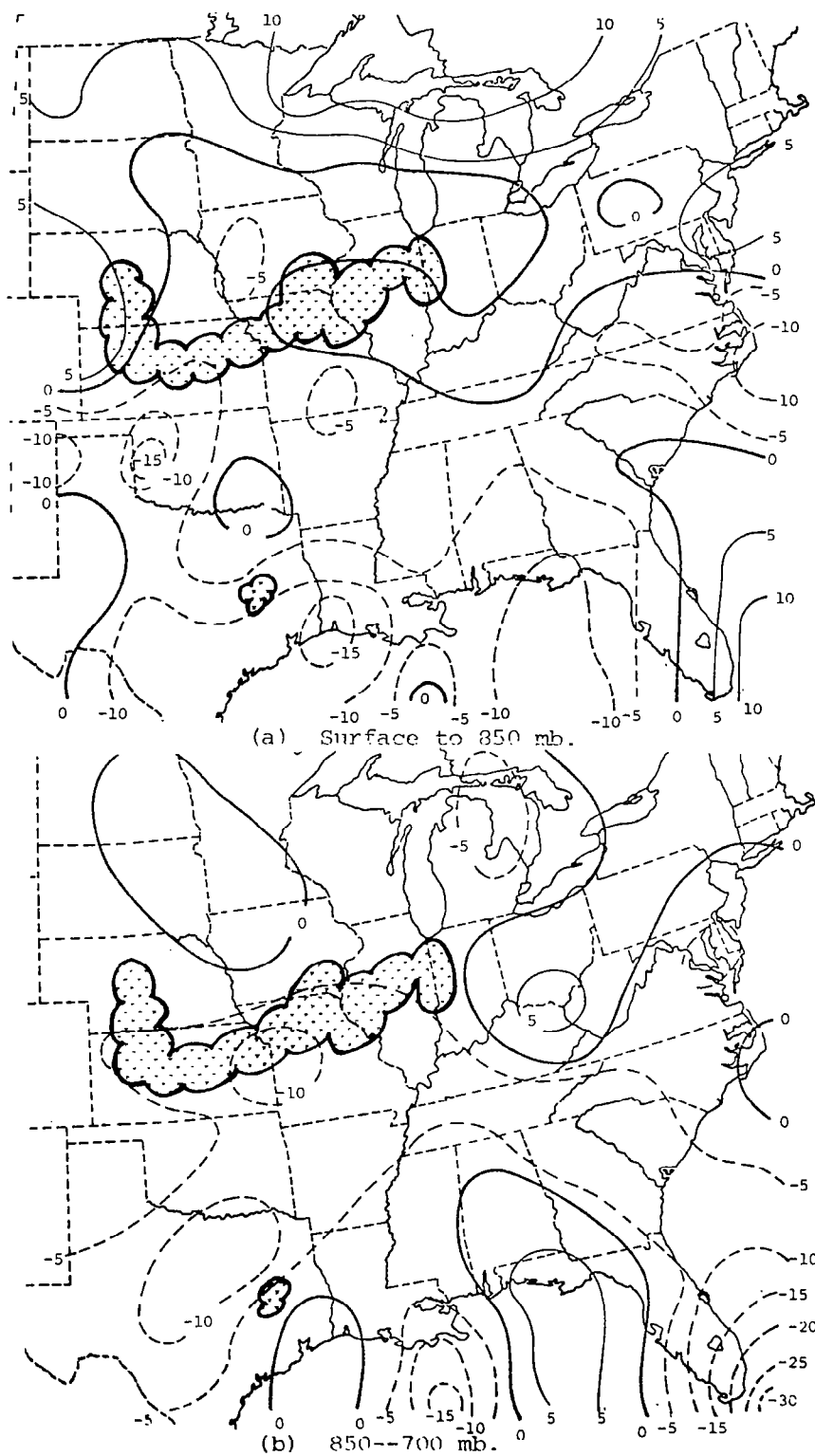Fig. 27.   Averages of convective instability (10^{-3}°C mb^{-1}) with time lags in MDR.

Fig. 28. Analyzed fields of convective instability $(10^{-2}\,°\text{C mb}^{-1})$ at 0000 GMT on 24 April 1975.

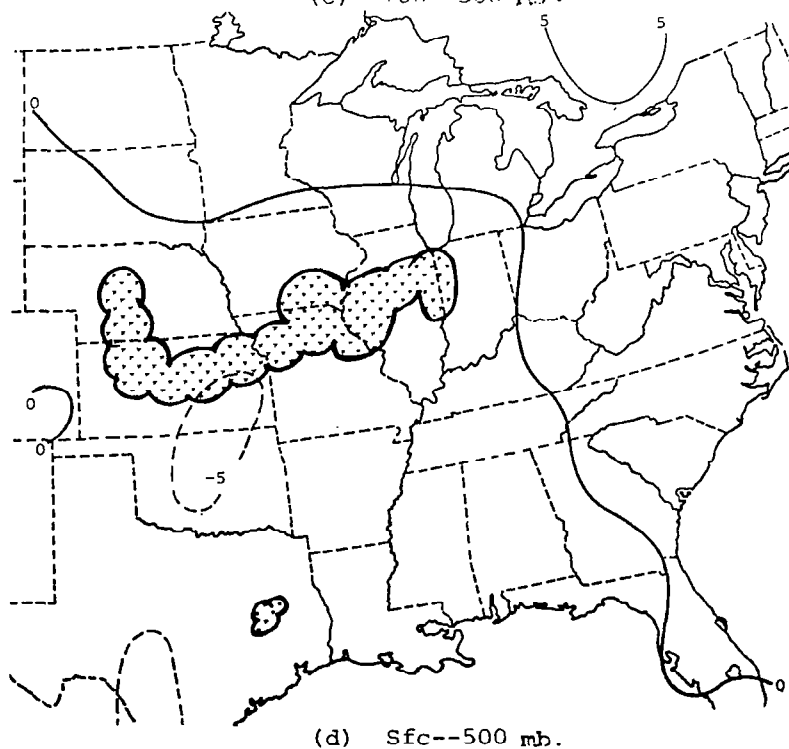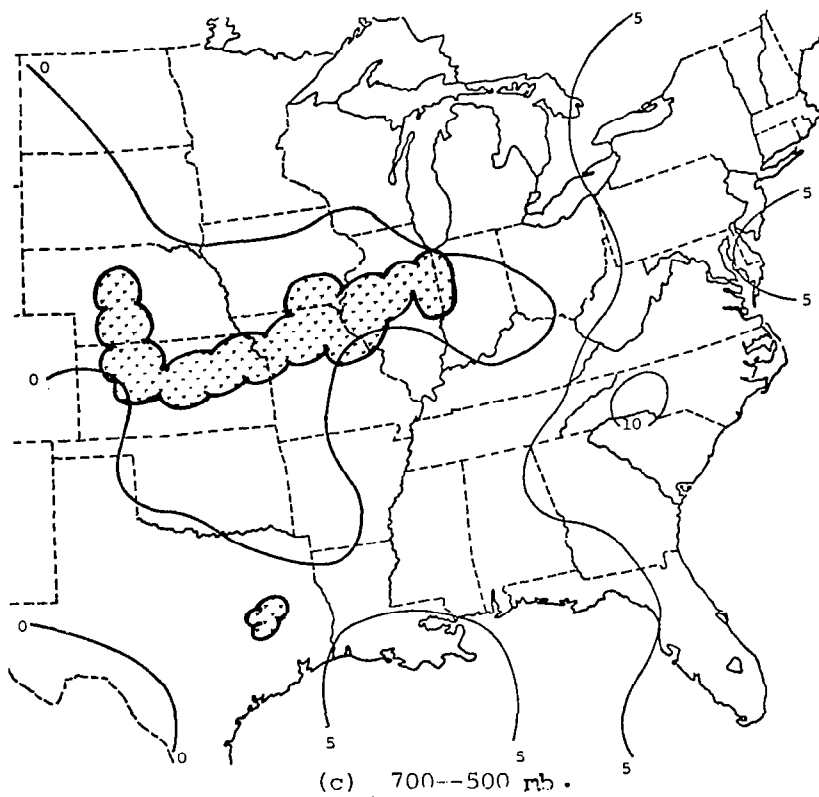(c) 700--500 mb.

(d) Sfc--500 mb.

Fig. 28. (Continued)

convective activity is observed.

The intrusion of dry air from the southwest into Missouri and Kansas at 700 mb is reflected in the field of σ_e for the 850- to 700-mb layer. The maximum instability occurs in conjunction with the dry intrusion. Although convection is occurring where instability in this layer exists, the most unstable regions are free of thunderstorms.

The area of instability present in the 700- to 500-mb layer shows the importance of instability through the middle troposphere in maintaining systems of thunderstorms. Unlike the lower layers, this layer appears to have less area of instability in convection-free regions.

The field of deep instability, $\sigma_{e\ sfc-500}$, while depicting most of the convection in unstable air, is too smooth a field to pin-point where convection will occur. This time period showed a better relationship between stability and convection for the deep layer than at other times in AVE IV.

The relationships between stability and convection observed at 0000 GMT were evident again at 0600 GMT on 24 April 1975. The surface- to 850-mb and 850- to 700-mb layers were generally more unstable in areas free of convection than in areas of observed thunderstorms. The 700- to 500-mb layer again had an area of maximum instability centered over the squall line.

At 1200 and 1500 GMT on 24 April 1975 convective activity was at a minimum for the AVE IV experiment. The relationships between stability and convection were still the same, but less pronounced, coinciding with the diminished activity.

At 1800 GMT on 24 April 1975 thunderstorms were beginning to develop along the frontal zone in eastern Kansas, but no severe activity was reported. Instability was observed in all three layers in a band from the Gulf Coast in Texas to the Northern Plains States, clearly indicating a preferred area for development of thunderstorms (Fig. 29).

At 2100 GMT on 24 April 1975 some severe thunderstorms were reported forming within the band of instability observed at 1800
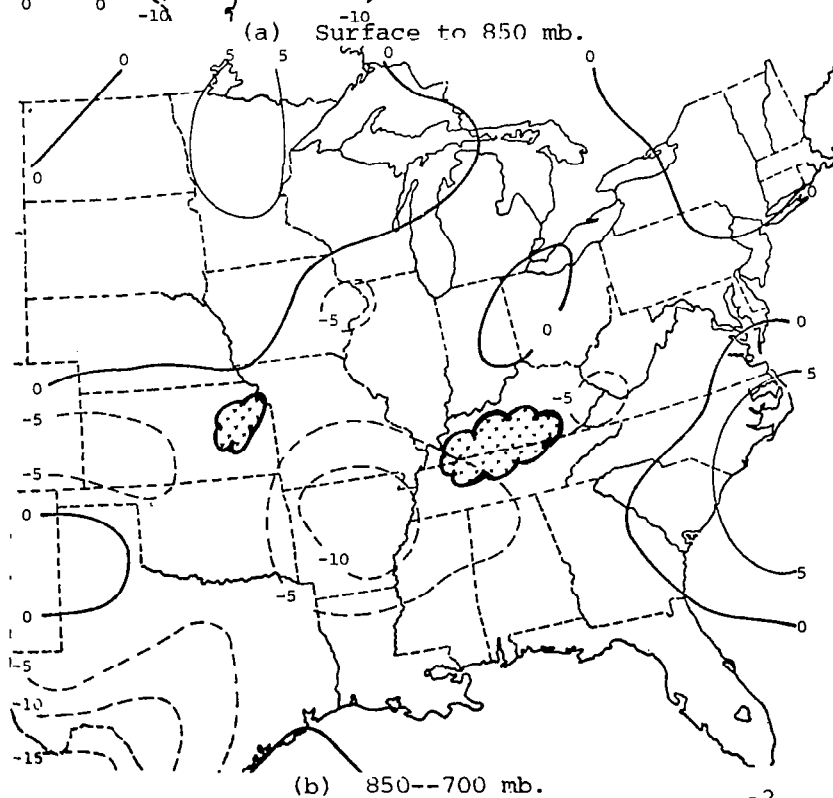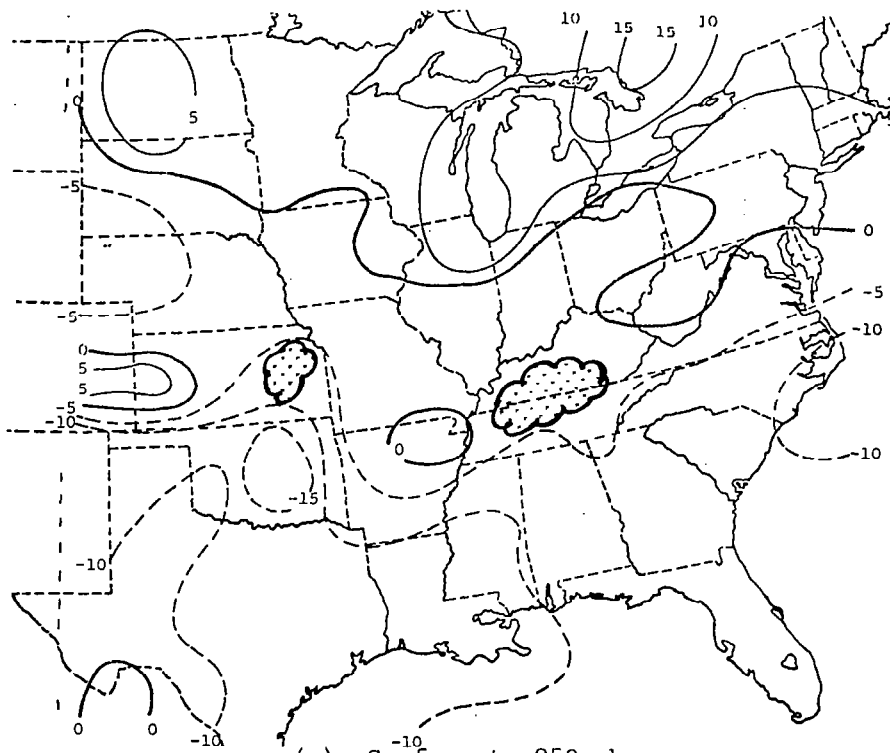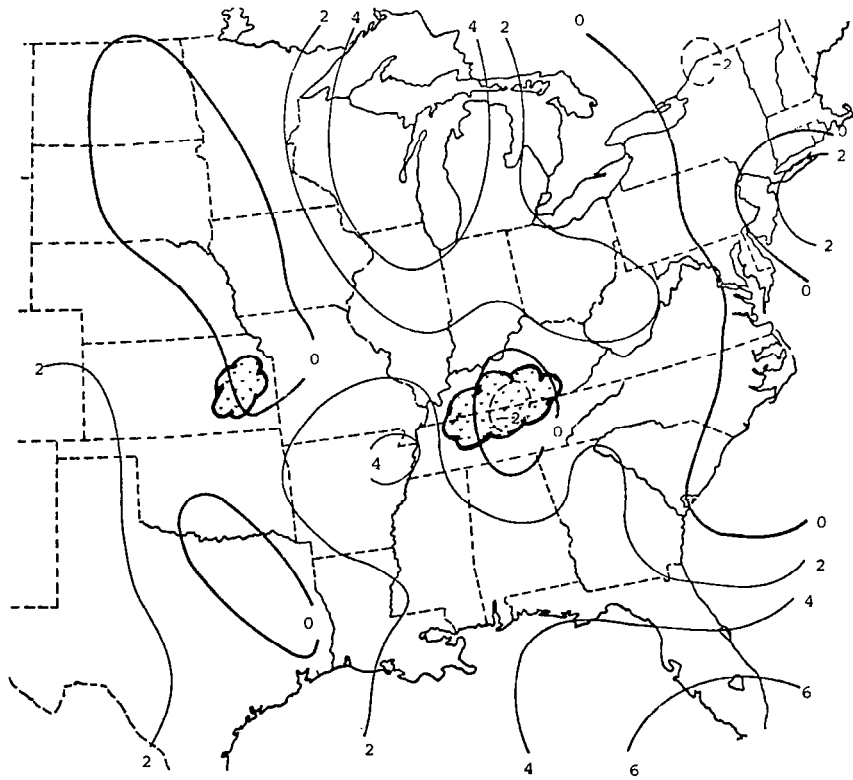
(a) Surface to 850 mb.

(b) 850--700 mb.

Fig. 29. Analyzed fields of convective instability (10^{-2}°C mb^{-1}) at 1800 GMT on 24 April 1975.

(c)   700--500 mb.

Fig. 29.   (Continued)

GMT in Eastern Kansas and Northwestern Missouri. The pattern of stability had changed little from 1800 GMT, with large areas of instability in all layers.

The second squall line during AVE IV was rapidly forming at 0000 GMT on 25 April 1975. The stability pattern in the surface-to 850-mb and 850- to 700-mb layers reflect the presence of a system of convection, with stability within the area of observed thunderstorms generally increasing (Fig. 30). In spite of this interaction, instability was found in at least one layer along the entire length of the squall line. Other areas of weaker convection also exhibit at least one layer of instability in the lower troposphere but the magnitude is not as great.

At 0600 GMT on 25 April 1975 the squall line had reached maximum intensity and the low level stability within the squall line had increased considerably. This process continued through 1200 GMT on 25 April 1975 when little instability was present and the thunderstorms were decreasing.

In summary, the fields show the same relationship between stability and convection as the average profiles. The large convection-free regions of instability show the need for considering other factors when examining causes for thunderstorm development.

c. Thunderstorm Potential Indices

In general, the indices defined by Eqs. 3-7 were better at depicting observed convection than any one of the parameters used to compute them. Most areas of intense convection occurred near minimum values of the indices. The average profiles of terms in the vorticity equation and convective instability indicated that some parameters had larger values at 3-h time lags than for zero lag. The zero lag profiles tended to show increased stability, slightly less vorticity production in the boundary layer, and slightly less vorticity advection at 500 mb, than did the 3-h lag profiles. This produced minimum values of the indices in advance of moving weather systems. Use of the indicator for forecast
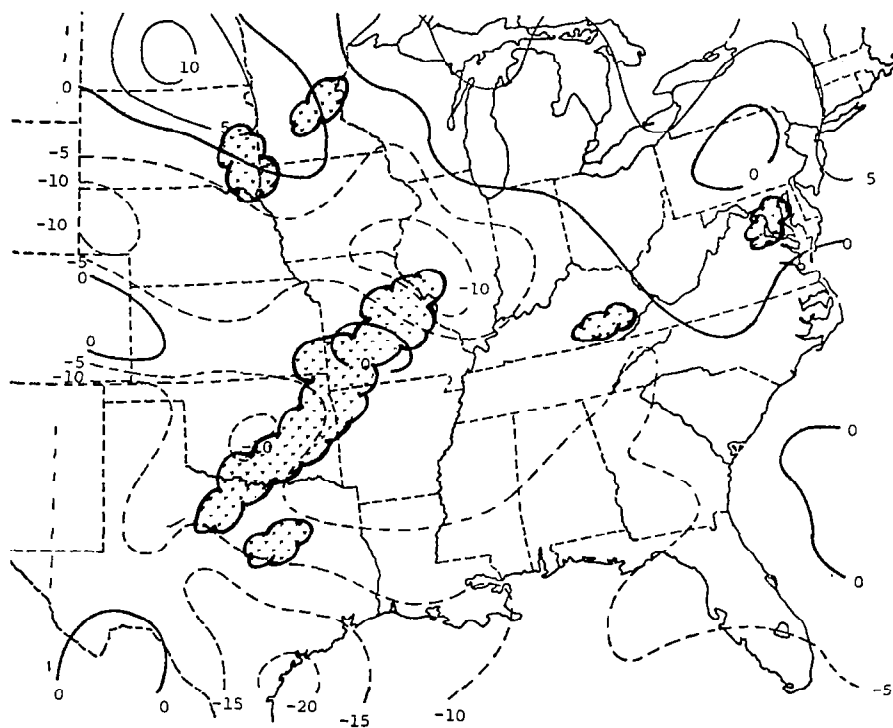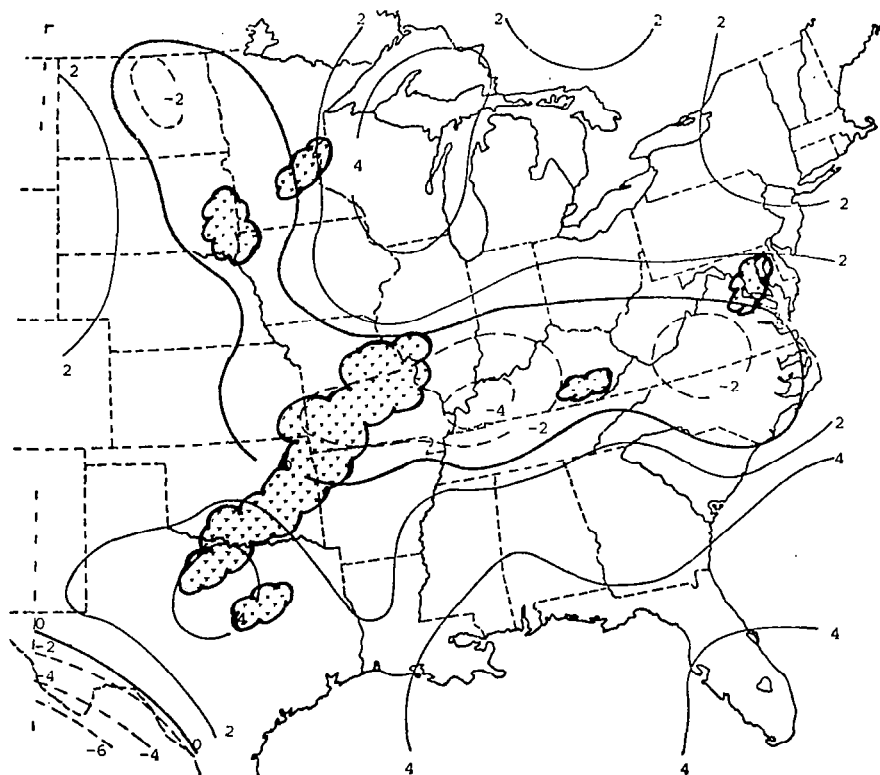
(a) Surface to 850 mb.
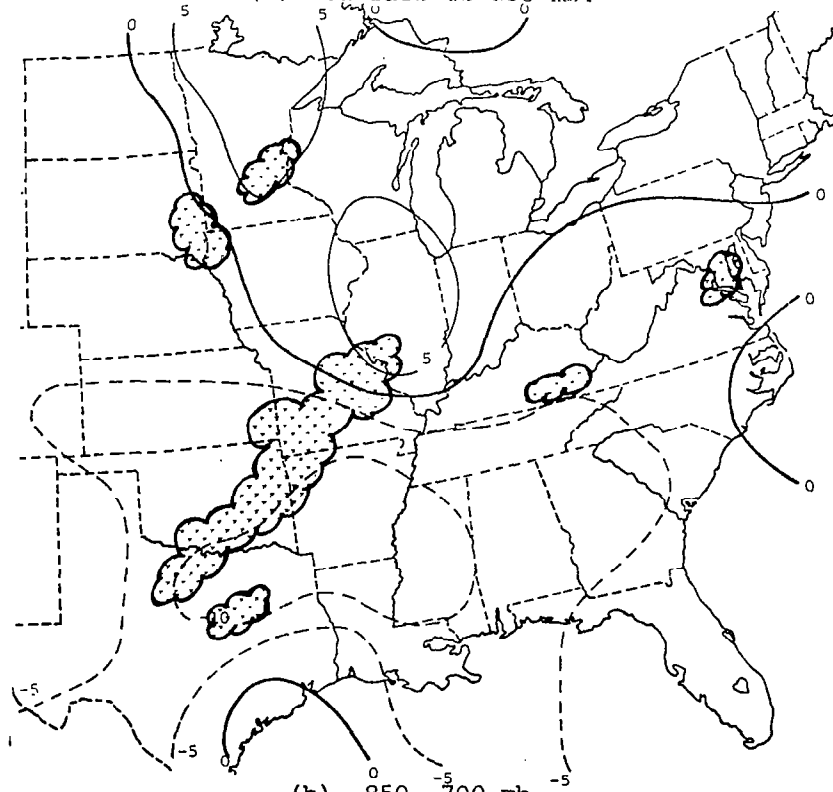
(b) 850--700 mb.

Fig. 30. Analyzed fields of convective instability (10^{-2}°C mb^{-1}) at
0000 GMT on 25 April 1975.

(c)   700--500 mb.

Fig. 30.   (Continued)

values of moisture, stability, and kinematic properties from models
such as those used by the National Weather Service should show bet-
ter definition at zero lag since the effect of thunderstorm systems
on the environment is not included in these forecasts.

Figure 31 shows the Low Level Index 1 (LLI 1), the Upper
Level Index (ULI), and the sum of these two, TPI 1, for 0000 GMT
on 24 April 1975 with observed MDR $\geq$ 4 at that time. While neither
LLI 1 nor ULI give a good forecast field for the major prefrontal
squall line in the Central Plains states, TPI 1 has an axis of min-
imum values through the major portion of the system. The most in-
tense areas of convection are associated with minimum values of
the index while areas of lesser convection in the Ohio Valley
and Northeast occur in areas of less negative values of the indices.

The heavy thunderstorms (MDR $\geq$ 8) in western Nebraska and
Kansas were not associated with large negative values of either
LLI 1, ULI, or TPI 1. Low-level moisture and stability were not
favorable here, nor was vorticity production very large. Con-
ditions at a higher level may have produced this activity or
smaller scale factors such as the effect of terrain features may
have been responsible. The weak synoptic-scale support for this
activity was probably the reason why all thunderstorms in western
Kansas had vanished by 0600 GMT.

These three indices overforecast badly in only one area, the
northern portion of Texas. All synoptic-scale factors necessary
for thunderstorm development were available; namely, high in-
stability in the lower troposphere, adequate moisture, and vorticity
production through convergence. Examination of the Stephenville,
Texas, sounding for 0000 GMT on 24 April 1975 indicated the presence
of a strong subsidence inversion between 850 and 700 mb. Ap-
parently not enough lifting was being produced to release the in-
stability. Soundings closer to the squall line did not have as
strong an inversion.

Figure 31d shows Low Level Index 2 (LLI 2) for 0000 GMT on
24 April 1975. A larger area of high negative values occur near
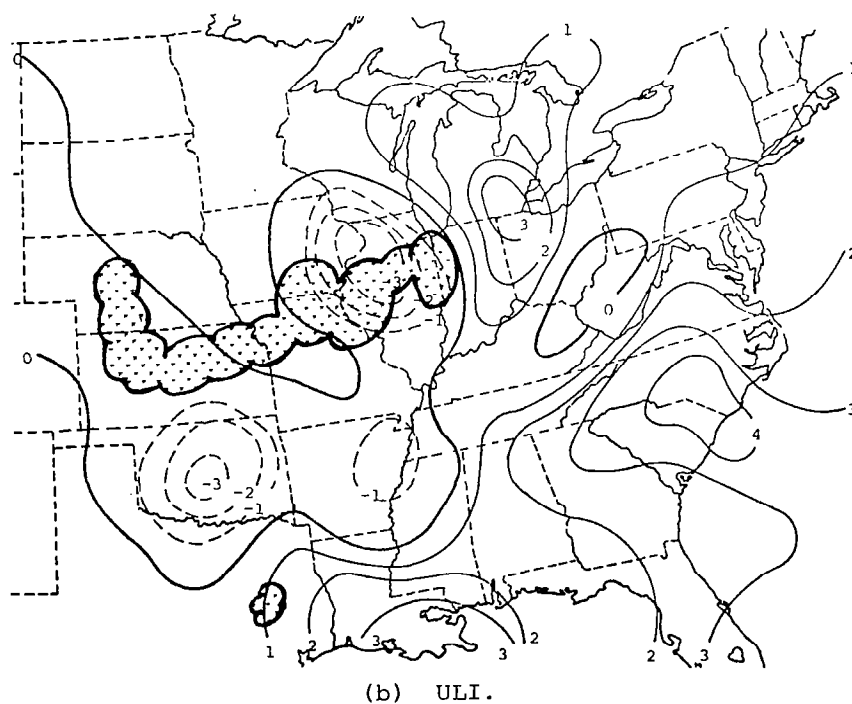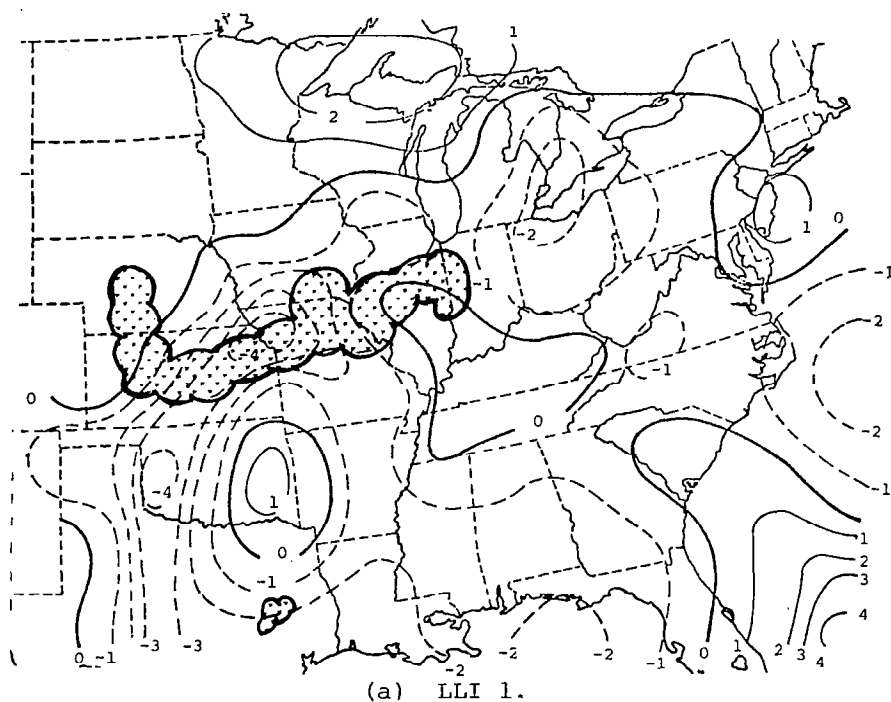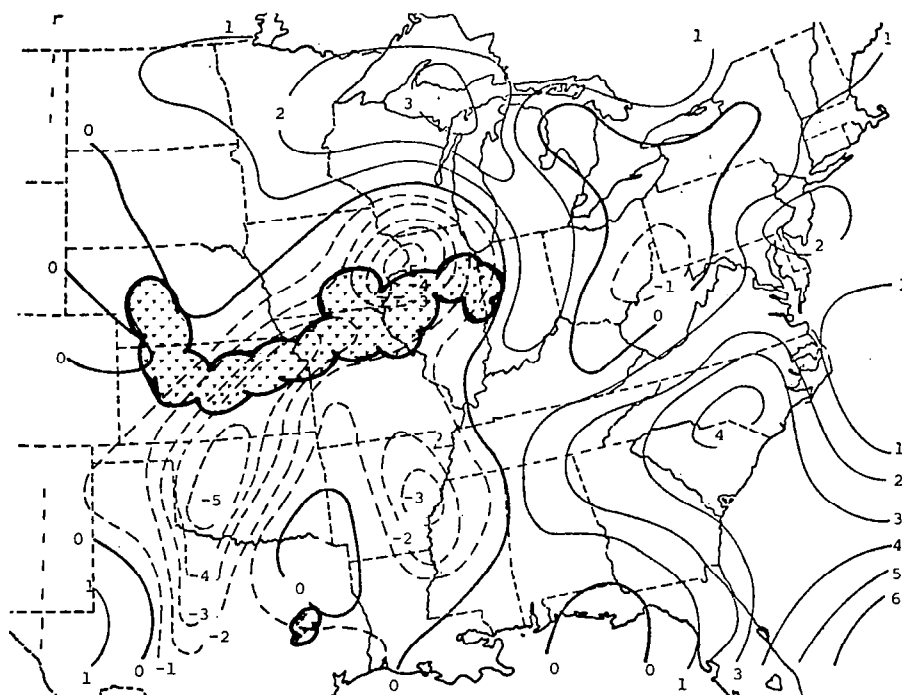the squall line in the Central Plains than for LLI 1, and the
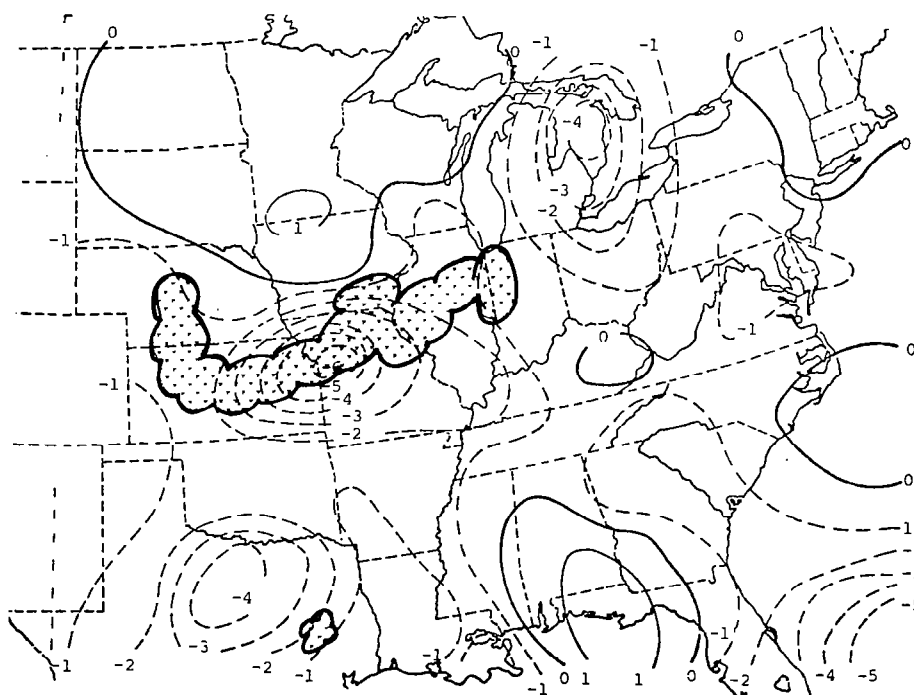
(a) LLI 1.

(b) ULI.

Fig. 31. Analyzed fields of thunderstorm indices for 0000 GMT on 24
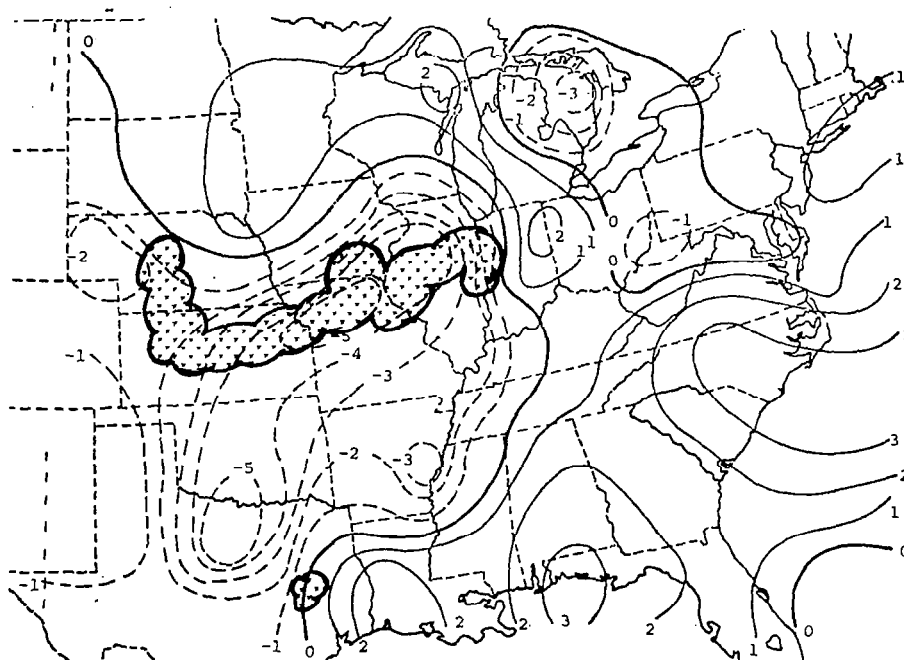April 1975 (MDR ≥ 4 superimposed).

(c) TPI 1.

(d) LLI 2.

Fig. 31. (Continued)

(e) TPI 2.

Fig. 31. (Continued)

thunderstorms in western Kansas and Nebraska were more accurately depicted. Otherwise, the patterns were similar. Thunderstorm Potential Index 2 (TPI 2) shown in Fig. 31e resembles TPI 1 with minimum values associated with maximum MDR values although over-forecasting again occurred in Texas.

Figures 32a and b show LLI 1 and LLI 2 at 0000 GMT with MDR ≥ 4 for 0600 GMT on 24 April 1975 superimposed. As expected from aver-age profiles for stability and vorticity production with a 6-h lag in MDR, there is an excellent agreement of negative centers of the indices with maximum MDR values. Convection is still absent in Texas at 0600 GMT so the indices also overforecast at a 6-h lag in that region.

The average profiles indicated that vorticity advection was poorly correlated with convection 6 h later. The MDR ≥ 4 field at 0600 GMT on 24 April 1975 superimposed on the 0000 GMT ULI field (Fig. 32c) shows little correlation between convection 6-h later and computed values of the index. This emphasizes the im-portance of upper-level conditions in triggering convective ac-tivity.

At 0600 GMT on 24 April 1975 and 1200 GMT on 24 April 1975, the major squall line continued to be active, decreasing somewhat in intensity at 1200 GMT. The various indices displayed similar characteristics as mentioned above for 0000 GMT. The correlation between lagged MDR values and the indices continued to be somewhat better than for zero lag.

Figure 33 shows TPI 1 and TPI 2 with MDR ≥ 4 superimposed at 1500 GMT on 24 April 1975. Convective activity is at a minimum at this time and is reflected in the fields of both indices. TPI 1 has minimum values slightly ahead of the prefrontal squall line moving through Tennessee. Elsewhere, values are higher than at previous times. TPI 2 has a narrow band of minimum values ahead of the squall line, but also has a large center indicating the potential for thunderstorms in Oklahoma. The overforecast in that area is primarily due to the strong inversion between 850 and 700 mb acting to suppress the lifting effect of convergence. There
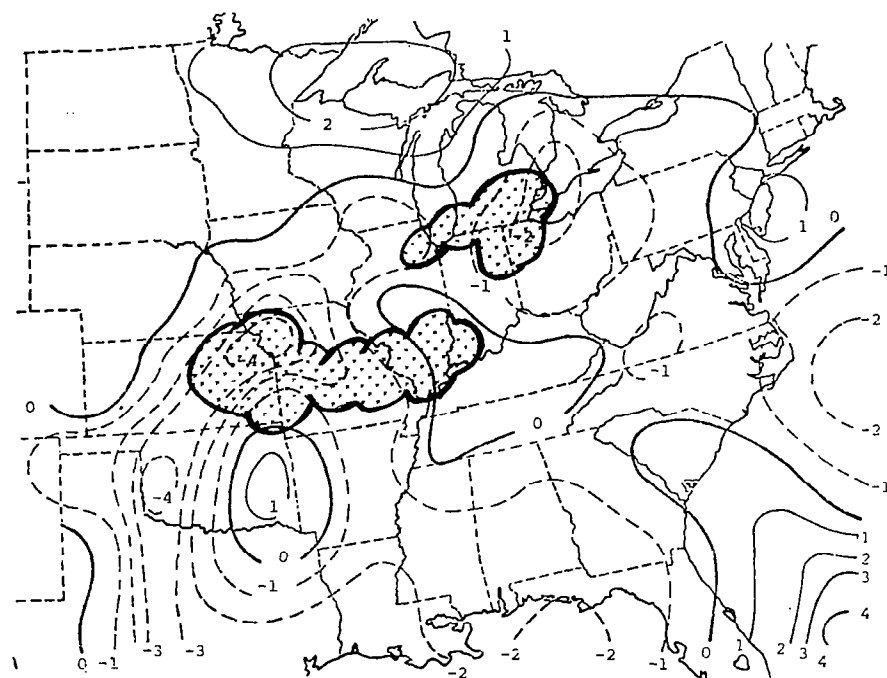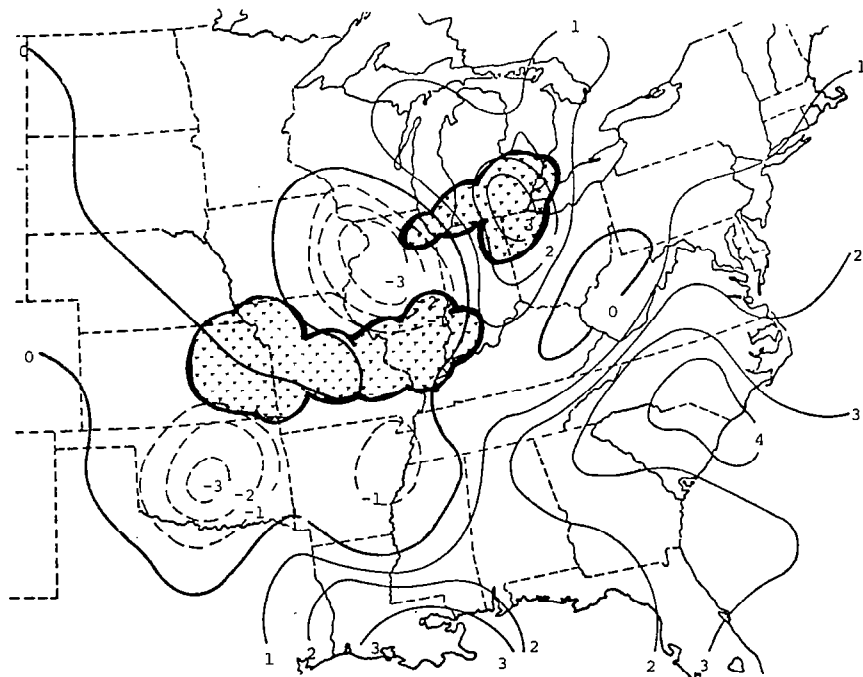
(a) LLI 1.
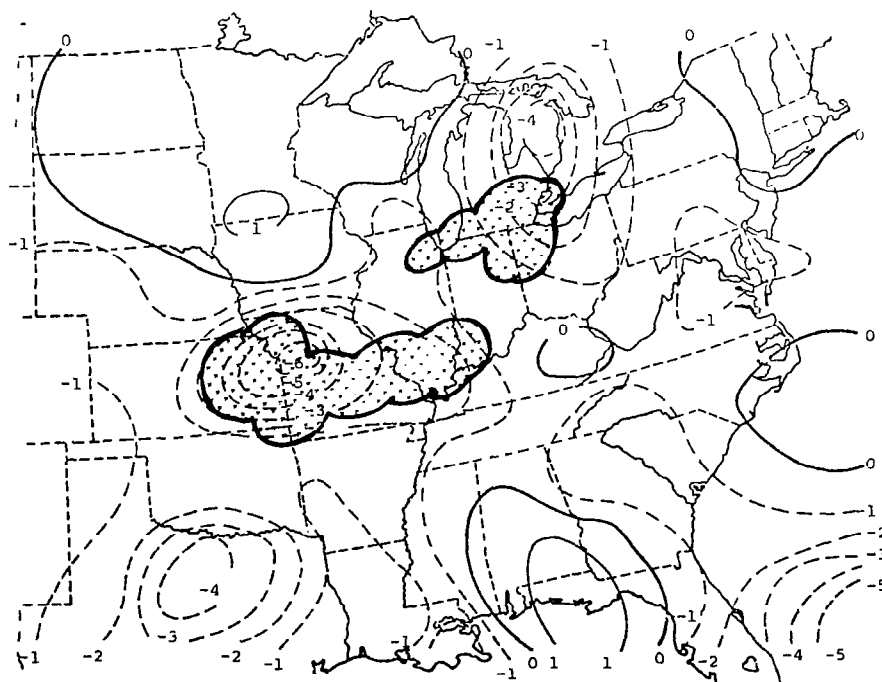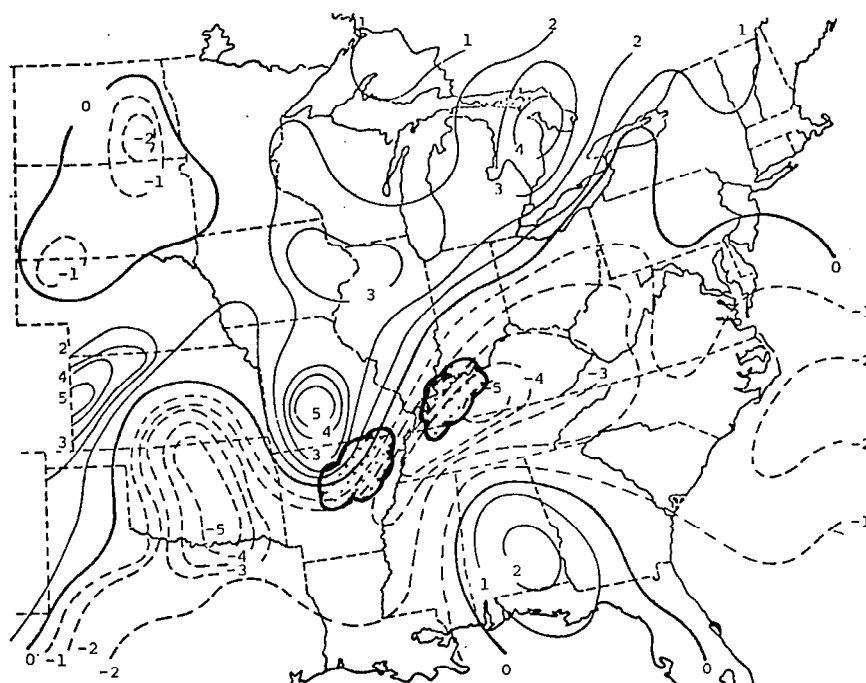
(b) LLI 2.

Fig. 32. Analyzed fields of thunderstorm indices at 0000 GMT on 24
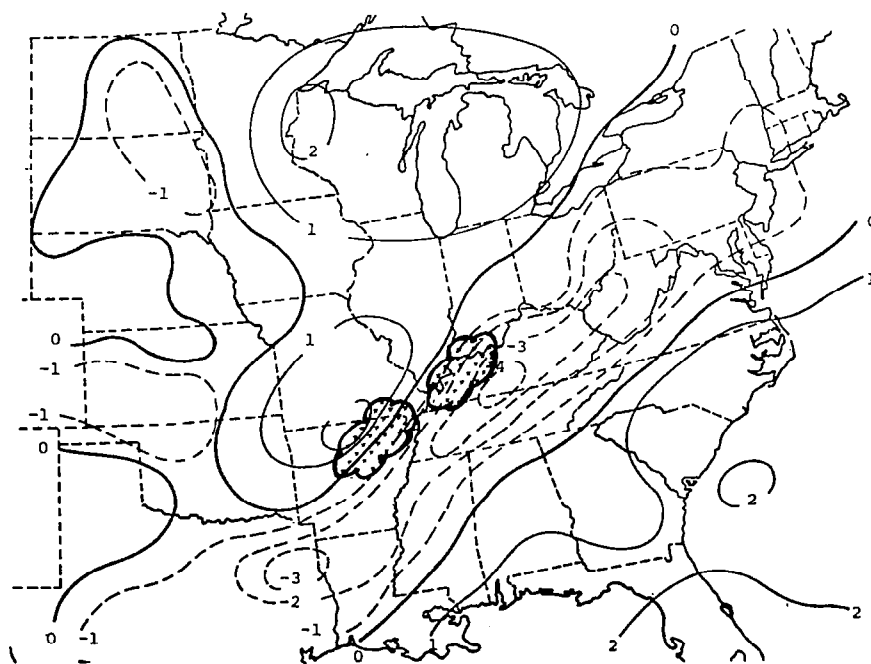April 1975 (MDR ≥ 4 at 0600 GMT superimposed).

(c) ULI.

Fig. 32. (Continued)

(a)   TPI 1.

(b)   TPI 2

Fig. 33.   Analyzed fields of Thunderstorm Potential Indices at 1500
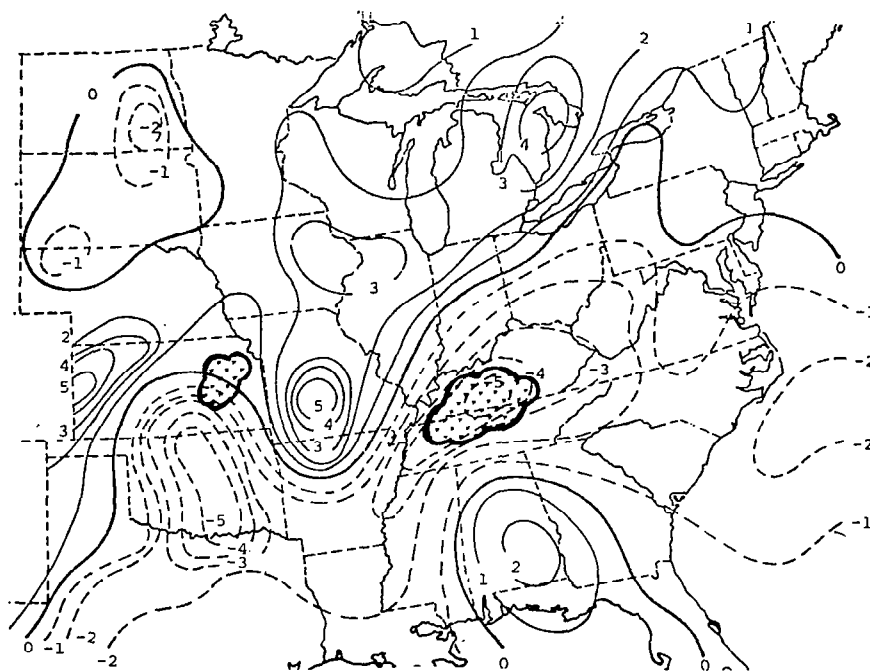GMT on 24 April 1975 (MDR ≥ 4 superimposed).

was only weak upper-level vorticity advection in that area at 1500 GMT.

Figure 34 shows the 1500 GMT values of TPI 1 and 2 with MDR ≥ 4 at 1800 GMT superimposed. The 3-h lag shows much better correlation between the indices and convection than did zero lag with the major convection area corresponding to the minimum values of both indices. Also, some severe thunderstorms (MDR ≥ 8) were beginning to develop in the negative center in Oklahoma and Kansas.
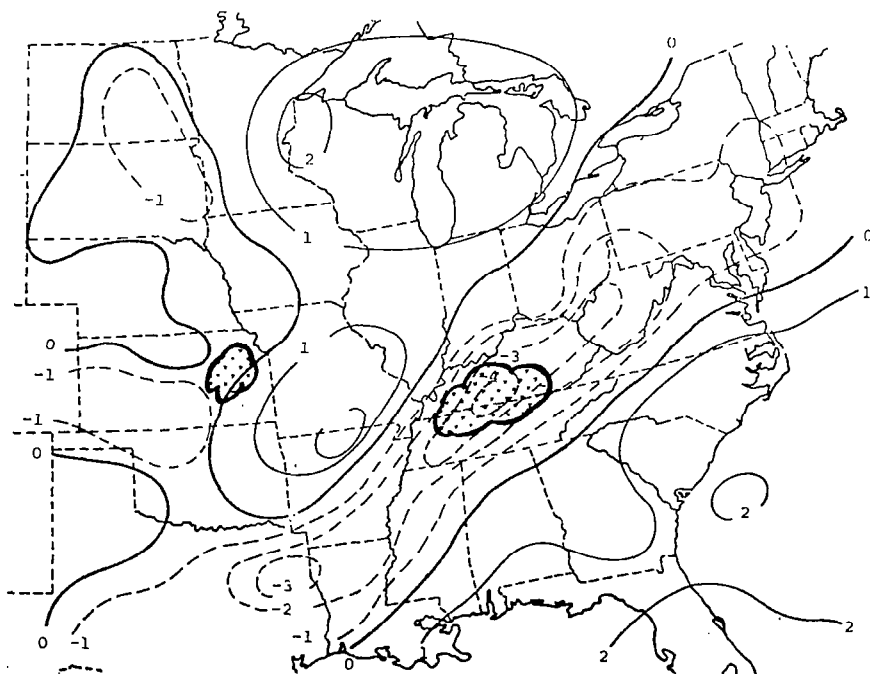
The fields of TPI 1 and 2 at 1800 GMT on 24 April 1975 differed only slightly from those at 1500 GMT. No significant changes in convective activity occurred and the lag relationships previously discussed still were evident.

At 2100 GMT on 24 April 1975 the second squall line started to form from eastern Kansas through Oklahoma. Both TPI 1 and TPI 2 show negative centers in the area where the squall line was forming (Fig. 35). The good fit at this time shows that the thunderstorms have not, as yet, interacted significantly with the synoptic-scale environment. The convective activity in the Dakotas as well as on the East Coast is near minimum centers. The remnants of the first squall line in eastern Kentucky and Tennessee are not well correlated with centers of the indices, possibly due to inter-action between the thunderstorm system and synoptic-scale temper-ature and wind fields. Overforecasting is prevalent again in east Texas where the strong subsidence inversion persisted.

Figure 36 shows the 0000 GMT, 25 April 1975 MDR ≥ 4 field superimposed on the 2100 GMT fields of TPI 1 and TPI 2. Excellent correlation with convection is evident for both indices. The most severe thunderstorms (MDR ≥ 8) are situated on the axis of minimum values of both TPI 1 and 2, emphasizing the importance of favorable synoptic-scale conditions such as low-level vorticity production and convective instability in depicting where severe activity will develop. Low-level conditions are essentially the same as at 1800 GMT, indicating the need for upper-level vorticity advection or of small-scale changes in the lower levels for trig-gering severe thunderstorms. The results in AVE IV seem to point

(a)　TPI 1.

(b)　TPI 2.

Fig. 34.　Analyzed fields of Thunderstorm Potential Indices at 1500
GMT on 24 April 1975 (MDR ≥ 4 at 1800 GMT superimposed).

(a) TPI 1.

(b) TPI 2.

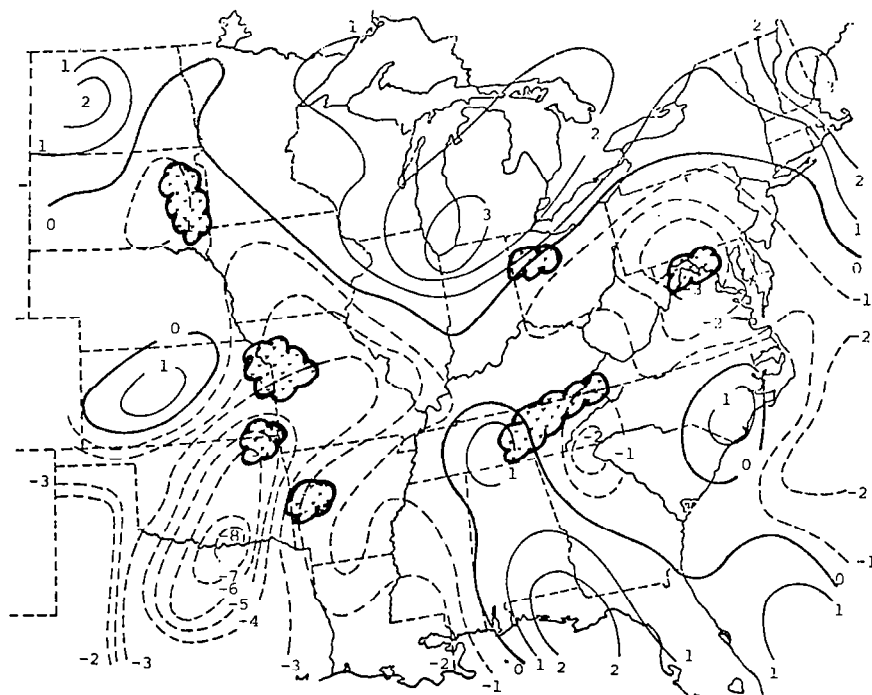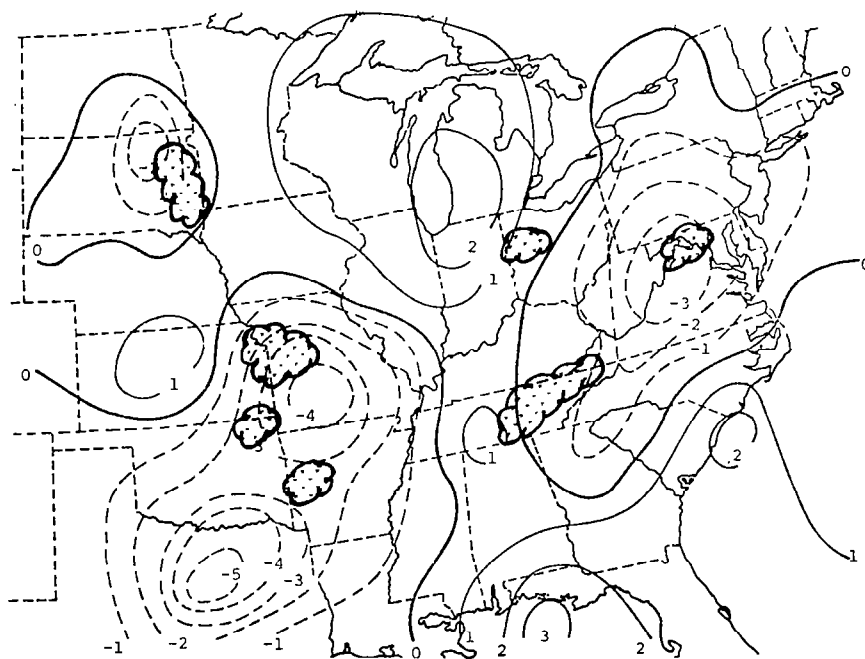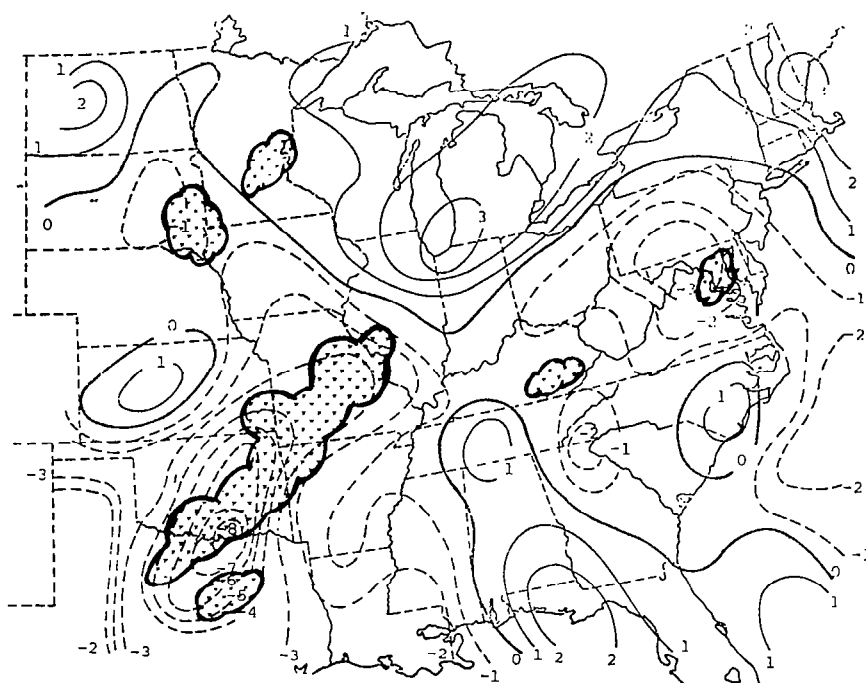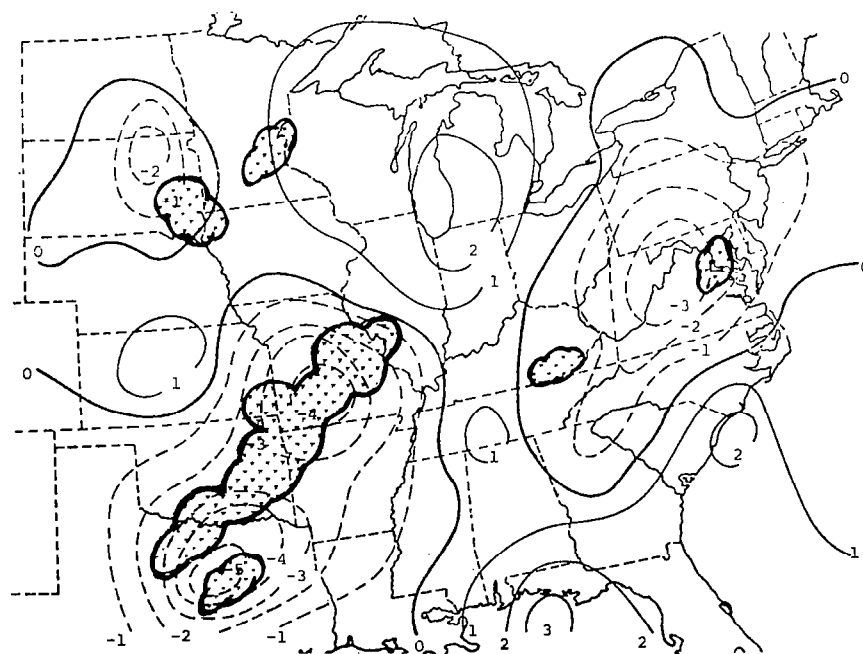Fig. 35. Analyzed fields of Thunderstorm Potential Indices at 2100 GMT on 24 April 1975 (MDR ≥ 4 superimposed).

(a) TPI 1.

(b) TPI 2.

Fig. 36. Analyzed fields of Thunderstorm Potential Indices at 2100
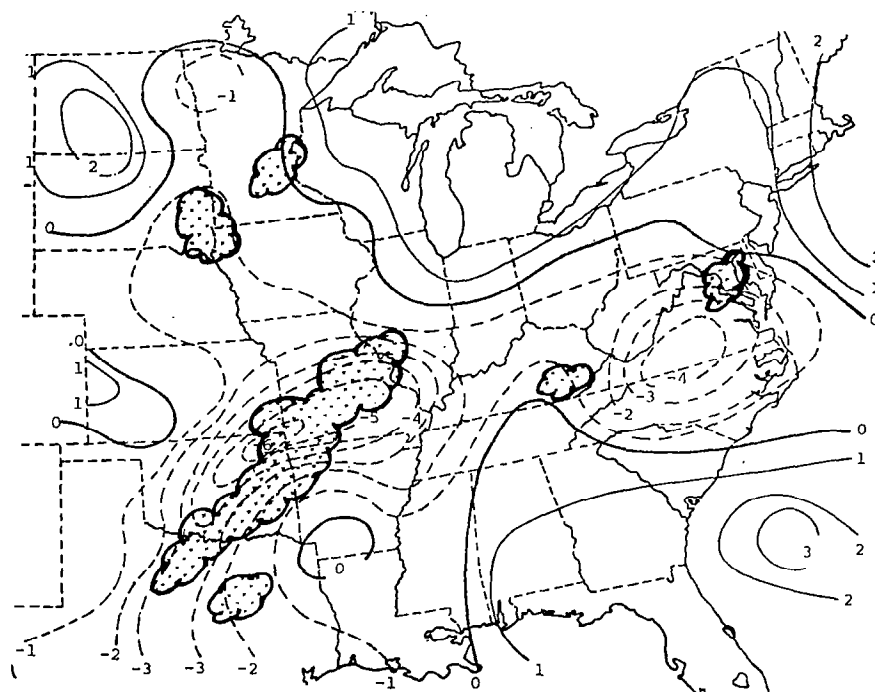GMT on 24 April 1975 (MDR ≥ 4 at 0000 GMT superimposed).

up the need for upper-level positive vorticity advection initiating thunderstorm activity, while studies of mesoscale data by Lewis et al. (1975) and Fankhauser (1969) give evidence of important local changes in initiating activity. They found large mesoscale variations in stability and vertical motion within synoptic regions that were favorable for thunderstorm development.

Both indices at 0000 GMT on 25 April 1975 show a good correlation with observed thunderstorm activity (Fig. 37). Apparently the thunderstorms have not interacted with the synoptic-scale features enough for the effect to be resolved in the data, allowing for a better correlation at zero lag in MDR values. The first squall line (at 0000 and 0600 GMT on 24 April 1975) did not show this feature since it had already developed when the experiment started. The environment in which the second squall line was imbedded still indicated a potential for further development at 0000 GMT on 25 April 1975. The large minimum in Virginia and North Carolina is almost exclusively due to strong vorticity advection at 500 mb, indicating a possible weakness in the upper-level index for strong upper-level waves. Large values of advection aloft may tend to overcompensate for neutral stability and weak vorticity production in the lower levels, as it does in this case.

The 0600 GMT on 25 April 1975 MDR values superimposed on the 0000 GMT TPI fields emphasize the non-correlation of vorticity advection with convection for 6-h lags (Fig. 38). Although most convection occurs within a band of negative values, the centers of minimum values are free of severe convection (MDR $\geq$ 8). Positive areas of the indices remain relatively free of convective activity for as much as

At 0600 GMT on 25 April 1975 the second squall line had reached maximum intensity. The fields of the Thunderstorm Potential Indices yielded similar results as at previous times. The magnitude of minimum values was less, as would be expected for the decreasing intensity of thunderstorm activity.

In general, the results of the indices indicate that in order for severe thunderstorms to develop, the large-scale conditions

(a) TPI 1.
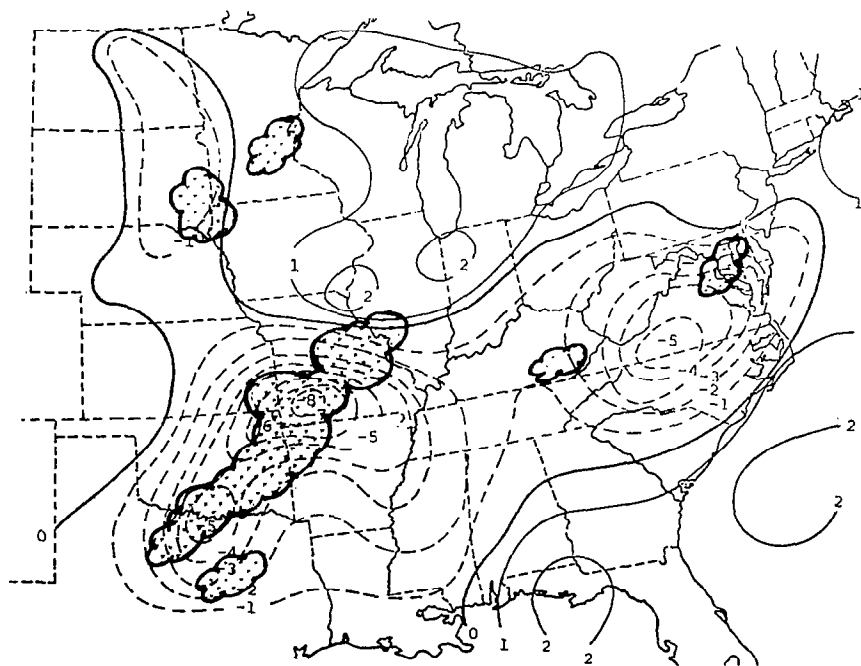
(b) TPI 2.

Fig. 37. Analyzed fields of Thunderstorm Potential Indices at 0000 GMT on 25 April 1975 (MDR ≥ 4 superimposed).

(a) TPI 1.

(b) TPI 2.

Fig. 38. Analyzed fields of Thunderstorm Potential Indices at 0000
GMT on 25 April 1975 (MDR ≥ 4 at 0600 GMT superimposed).

must include a moist, unstable lower troposphere, low-level vor-
ticity production, and upper-level vorticity advection. Although
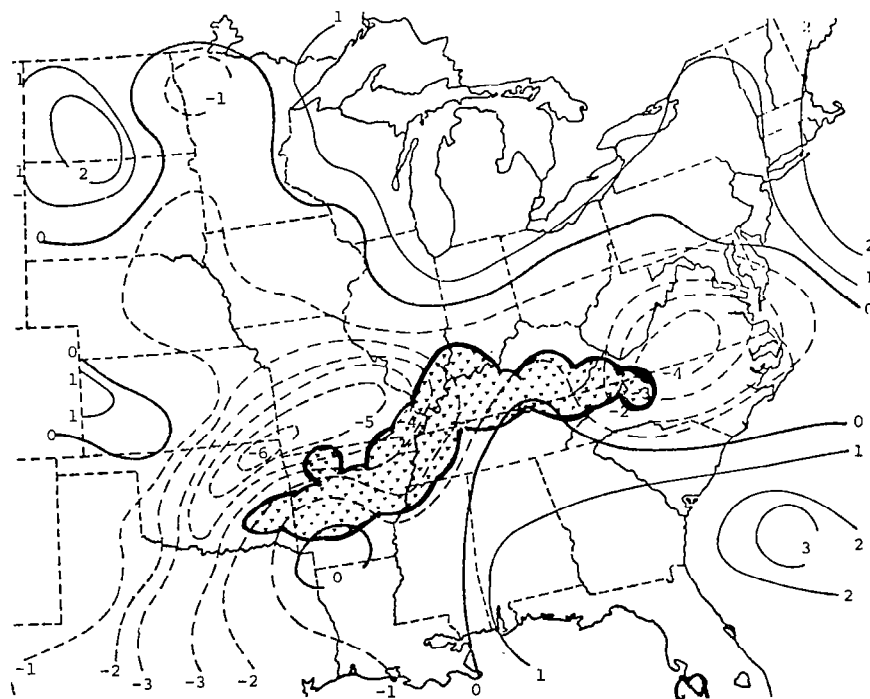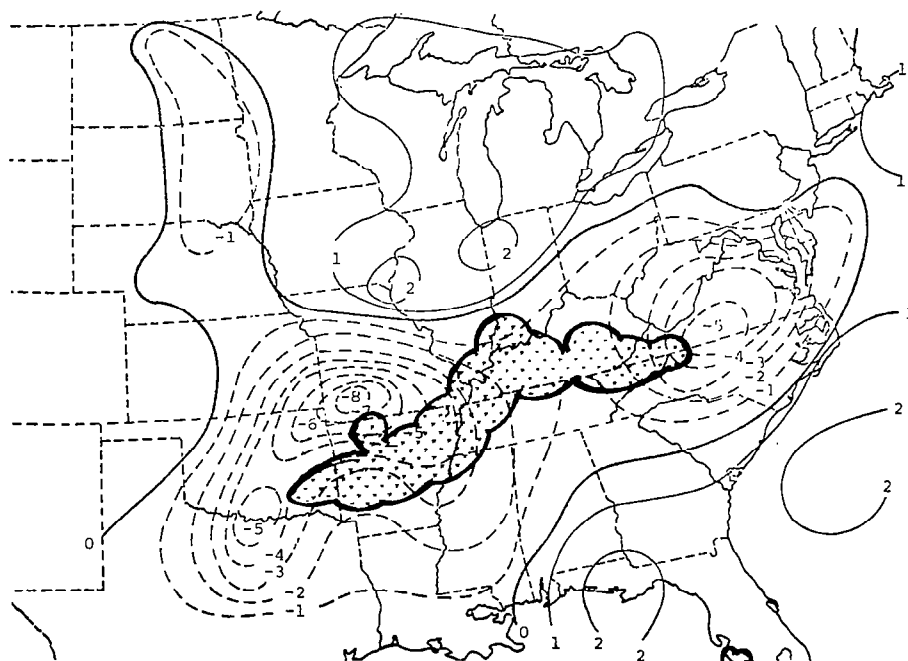low-level indices were dominant, neglect of the upper-level index
would decrease accuracy, especially for initial development. The
effect of pre-existing thunderstorms seems to reduce the synoptic-
scale potential for further development in those areas.

Table 5 summarizes the results of the indices and the para-
meters that were used to compute them. Average positive and neg-
ative values are indicated by + or - while small (sml) and large
(lge) give magnitudes relative to average values. SL1 and SL2
refer to the first and second major squall lines that developed
during the experiment. Values presented are estimated over all
grid points within the area of convection. The nonconvective
area chosen covered Alabama, Georgia, South Carolina, and Florida.
This region experienced little or no radar-observed convection
during AVE IV.

The features previously discussed are also evident in Table 5.
Low level production of vorticity, middle- and upper-level vor-
ticity advection, and an unstable layer in the lower troposphere
are evident for each time period for both squall lines. Maximum
intensity of both squall lines occurs when all factors combined
are conducive to development of thunderstorms. The indices also
accurately indicate thunderstorm activity for both squall lines.
As the intensity of the system decreases, the indices show lower
values.

The non-convective area shows the need for favorable synoptic-
scale kinematic features such as low-level vorticity production
and upper-level positive vorticity advection. This area observed
sufficient low-level instability but had no mechanism for re-
leasing it. The indices reflected the absence of thunderstorm
activity in this area.

Table 5. Summary of relationship of analyzed fields of stability and vorticity to convection.

PARAMETERS

		MDR	Sfc 1	Sfc 2	500 mb 3	500 mb 4	500 mb 1	300 mb 3	300 mb 4	300 mb 1	300 mb 2	σ_e Sfc-850 mb	σ_e 850-700 mb	σ_e 700-500 mb	TPI 1	TPI 2
SL1	00	Few Severe	lge +	lge -	+	sml -	sml -	sml +	+	+	+	sml -	lge -	sml -	lge -	lge -
	06	Maximum Intensity	+	-	+	-	+	-	lge -	lge -	+	sml +	-	sml +	lge -	lge -
	12	Moderate	+	-	+	sml -	lge +	sml -	-	-	sml -	sml -	-	sml +	sml -	0
	15	Minimum Activity	+	sml -	+	sml +	sml -	sml -	-	-	-	-	sml -	sml -	sml -	sml -
	18	Moderate	+	sml -	sml +	sml -	+	sml +	sml -	lge -	+	-	lge -	+	-	-
SL2	18	Few Strong	+	-	sml +	sml -	+	+	0	0	+	lge -	-	sml +	lge -	-
	21	Few Severe	lge +	-	sml +	-	-	+	lge -	sml -	sml -	lge -	lge -	sml +	lge -	lge -
	00	Numerous Severe	lge +	lge -	lge +	-	sml -	+	lge -	-	-	lge -	lge -	sml +	lge -	lge -
	06	Maximum Intensity	+	-	+	-	+	+	-	lge -	lge +	+	lge -	+	-	lge -
	12	Few Severe	sml +	sml -	lge +	-	lge +	sml +	lge -	-	-	+	-	+	sml -	-
NO CONVECTION	18		sml +	sml +	sml +	+	sml +	sml +	sml -	sml -	sml	lge -	-	+	sml -	sml +
	21		sml +	sml +	sml -	+	sml +	sml +	sml +	+	sml -	lge -	-	+	sml +	sml +
	00		sml -	sml +	sml +	sml +	+	-	+	sml -	+	-	-	+	sml +	sml +
	06		sml -	sml +	sml +	+	+	-	-	-	sml -	-	sml -	+	sml +	sml +
	12		sml -	sml +	sml -	sml +	-	sml -	sml +	-	+	-	sml +	+	sml +	sml +

Terms: 1 - Divergence Term, 2 - Residual, 3 - Local Derivative, 4 - Horizontal Advection

7.   SUMMARY AND CONCLUSIONS

Synoptic-scale objective analyses of terms in the vorticity equation and convective instability have been accomplished using the 3- and 6-h AVE IV rawinsonde data. Average profiles of the parameters as related to 0-, 3-, and 6-h time lags in radar-observed convection were presented to establish general relationships between thunderstorms and terms in the vorticity equation. Analyzed fields of the terms were examined to investigate changes in the fields as related to the life cycle of convective systems, and to test the validity of the average relationships on specific examples. Finally, indices were developed to aid in synoptic-scale analysis and forecasting of thunderstorm systems by combining terms of the vorticity equation and stability parameters that were related to convection.

The following conclusions were reached based on the results previously discussed:

1.   Synoptic-scale development of circulation systems, determined by computation of the vorticity budget, was related to the formation of severe thunderstorms. The observed local tendency of vorticity was usually positive in areas of observed convective activity, especially in the middle and upper troposphere. In the lower troposphere, the production of vorticity through divergence was highly correlated with convection, while in the upper levels positive vorticity advection and dilution of vorticity by divergence were important. The vertical advection and twisting terms did not attain significant values on the average in areas of convection.

2.   Averages for time lags in radar-observed convection indicate that low-level production of vorticity exists in areas of future thunderstorm development up to 6 h prior to initial formation, while in the upper troposphere positive vorticity advection is evident only 3 h before initial development.

3.   Changes occur in the terms of the vorticity equation when compared to stages in the life   of convective activity. Low-

level vorticity production is large prior to and during initial de-
velopment of thunderstorms, then decreases as the convective systems
interact with the low-level, synoptic-scale wind field. Convective
activity appears to reach maximum intensity when the positive vor-
ticity advection center at 500 mb and 300 mb are directly over the
low-level vorticity production center. Interaction between systems
of thunderstorms and the synoptic-scale flow at 300 mb creates a
diffluent zone over the activity. Within the diffluent zone,
synoptic-scale dissipation of vorticity occurs through divergence.

4. Systematic imbalance in the vorticity equation, when re-
lated to convection, was most pronounced in the lower troposphere.
Excess synoptic-scale production of vorticity was found responsible
for this imbalance. Restoration of balance at the surface and 850-
mb levels was achieved possibly through frictional dissipation and
small-scale circulations which act as turbulent mixing on the
synoptic scale. Imbalance aloft, while appearing to be systematic
on the average, showed no clear relationship to convective activity
in the spatial fields. The large imbalance in the large scale vor-
ticity equation was related to perturbations in the synoptic-
scale wind fields that could not be fully resolved in time or
space within the observational network. Large values of the residual
were evident in areas of convection, but no clear relationship
could be determined.

5. In general, convective instability was observed in areas
where thunderstorms developed. This instability was greater in
cases of higher thunderstorm intensity. Areas free of convective
storms also exhibited layers of instability, often equal to or
greater in magnitude than values in areas of severe convection.
Instability was greater 3 h, and to some extent, 6 h prior to
thunderstorm development than at the time of such development,
indicating interactions between thunderstorm systems and the
synoptic-scale environment in which they occurred. Instability
in the surface to 850-mb layer and the 850- to 700-mb layer is
important for initial development of thunderstorms while ad-
ditional instability in the 700- to 500-mb layer is related to

further intensification of the convective activity. The spatial fields verified the general stability relationships developed through averaging.

6. Development of indices as aides in analysis and forecasting proved to be a useful tool for investigating the relationships described above. The indices clearly depicted areas of convective activity. Best results were achieved when favorable upper-level and lower-level conditions coincided, confirming earlier findings based on the individual parameters.

7. The changes in the terms of the vorticity equation, stability parameters, and in the intensity of convective activity observed over 3-h periods in AVE IV show that 12-h rawinsonde data is inadequate for diagnostic studies of synoptic-scale relationships to thunderstorm development. Important development of circulation systems and instability occur on a time scale of considerably less than 12 h.

REFERENCES

Barber, D. A., 1975: A contribution to the climatology of static stability and vertical wind shear. Preprints of Papers, Ninth Conf. on Severe Local Storms, Norman, 13-17.

Barnes, S. L., 1970: Some aspects of a severe right moving thunderstorm deduced from mesonetwork rawinsonde observations. J. Atmos. Sci., 27, 634-648.

_____, 1964: A technique for maximizing detail in numerical weather map analysis. J. Appl. Meteorol., 3, 396-409.

Barr, S., W. K. Widger, Jr., I. A. Miller, and R. Stanton, 1971: Objective subsynoptic upper level analysis. J. Appl. Meteorol., 10, 410-417.

Berkofsky, L., and E. A. Bertoni, 1955: Mean topographical charts of the entire earth. Bull. Amer. Meteor. Soc., 36, 350-354.

Bjerknes, J. 1951: Extratropical cyclones. In Compendium of Meteorology, T. F. Malone, ed., Am. Meteorol. Soc. Boston, 577-598.

Charba, J. P., 1975: Operational scheme for short range forecasts of severe local weather. Preprints of Papers, Ninth Conf. on Severe Local Storms, Norman, 252-261.

Dallavalle, J. P. and L. F. Bosart, 1975: A synoptic investigation of anticyclogenesis accompanying North American polar outbreaks. Mon. Wea. Rev., 103, 941-957.

Danard, M. B., 1964: On the influence of released latent heat on cyclone development. J. Appl. Meteorol., 3, 27-37.

Danielson, E. F., 1975: A conceptual theory of tornado genesis based on macro-, meso-, and microscale processes. Preprints of Papers, Ninth Conf. on Severe Local Storms, Norman, 376-383.

Darkow, G. L., 1975: The evolution of the surface static energy fields on 3 April 1974. Preprints of Papers, Ninth Conf. on Severe Local Storms, Norman, 264-269.

Elliot, R. D. and E. L. Hovind, 1965: Heat, water and vorticity balance in frontal zones. J. Appl. Meteorol., 4, 196-211.

Endlich, R. M., and R. L. Mancuso, 1968: Objective analysis of environmental conditions associated with severe thunderstorms and tornadoes. Mon. Wea. Rev., 96, 342-350.

Fankhauser, J. C., 1971: Thunderstorm-environment interactions deduced from aircraft and radar observations. Mon. Wea. Rev., 99, 171-193.

_____, 1969: Convective processes resolved by a mesoscale rawinsonde network. J. Appl. Meteorol., 8, 778-798.

Foster, D. S. and R. M. Reap, 1975: Thunderstorms and severe local storm frequency distributions for 1974 derived from manually digitized radar data and severe local storms reports. Preprints of Papers, Ninth Conf. on Severe Local Storms, Norman, 64-67.

Fucik, N. F. and R. E. Turner, 1975: Data for NASA'S AVE IV experiment: 25-mb sounding data and synoptic charts. NASA TM X-64952, NASA Marshall Space Flight Center, Alabama, 458 pp.

Fuelberg, H. E., 1974: Reduction and error analysis of the AVE II pilot experiment data. NASA Contractor Report CR-120496. Marshall Space Flight Center, Alabama, 140 pp.

Fujita, T. T., 1963: Analytical mesometeorology: a review. Meteorol. Monograph 5. American Meteorological Society, Boston, 77-129.

Holton, J. R., 1972: An Introduction to Dynamic Meteorology. New York, Academic Press, 319 pp.

House, D. D., 1963: Forecasting tornadoes and severe thunderstorms. Meteorol. Monograph, 5. American Meteorological Society, Boston, 141-156.

Lewis, J. M., Y. Ogura, and L. Gidel, 1974: Large-scale influences upon the generation of a mesoscale disturbance. Mon. Wea. Rev., 102, 545-560.

Leverson, V. H., P. C. Sinclair, and J. H. Golden, 1975: Waterspout wind, temperature and pressure structure deduced from aircraft measurements. Preprints of Papers, Ninth Conf. on Severe Local Storms, Norman, 350-357.

Matsumoto, S., K. Ninomiya and T. Akiyama, 1967: A synoptic and dynamic study on the three dimensional structure of mesoscale disturbances observed in the vicinity of a cold vortex center. J. Meteorol. Soc. Japan, 45, 64-81.

Miller, R. C. and R. A. Maddox, 1975: Use of the SWEAT and SPOT indices in operational severe storm forecasting. Preprints of Papers, Ninth Conf. on Severe Local Storms, Norman, 64-67.

_____, 1967: Notes on analysis and severe storms fore-
casting procedures of the Air Force Global Weather Central.
Air Weather Service Technical Report 200, 102 pp.

Mogil, H. M., 1975: Pressure Change--Its use in forecasting the
Atlanta tornado of March 24, 1975. Preprints of Papers,
Ninth Conf. on Severe Local Storms, Norman, 25-32.

Newton, C. W., 1963: Dynamics of severe convective storms.
Meteorol. Monograph, 5. American Meteorological Society,
Boston, 33-58.

Ninomiya, K., 1971: Mesoscale modification of synoptic situations
from thunderstorm development as revealed by ATS III and
aerological data. J. Appl. Meteorol., 10, 1103-1121.

O'Brien, J. J., 1970: Alternate solution to the classical
vertical velocity problem. J. Appl. Meteorol., 9, 197-203.

Paine, D. A., J. W. Zack, J. T. Moore and R. J. Posner, 1975:
A theory for the conservation of three dimensional vorticity
which describes the cascade of energy momentum leading to
tornadic vortices. Preprints of Papers, Ninth Conf. on
Severe Local Storms, Norman 131-138.

Palmen, E., and C. W. Newton, 1969: Atmospheric Circulation
Systems. New York, Academic Press, 390-425.

Panofsky, H. A., 1958: Introduction to Dynamic Meteorology,
University Park, Pa., The Pennsylvania State University,
243 pp.

Reap, R. M. and D. S. Foster, 1975: New operational thunderstorm
and severe storm probability forecasts based on Model Output
Statistics (MOS). Preprints of Papers, Ninth Conf. on
Severe Local Storms, Norman 58-63.

_____, 1975: Thunderstorm and severe weather probabilities
based on model output statistics--No. 3, Technical Procedures
Bulletin No. 138, National Weather Service, Silver Springs,
Md., 4 pp.

Reed, R. J. and R. H. Johnson, 1974: The vorticity budget of
synoptic-scale wave disturbances in the tropical western
Pacific. J. Atmos. Sci., 31, 1784-1790.

Shuman, F. G., 1957: Numerical methods in weather prediction:
II Smoothing and Filtering. Mon. Wea. Rev., 85, 357-361.

Smith, P. J., 1971: An analysis of kinematic vertical motions.
Mon. Wea. Rev., 99, 715-724.

Williams, K. T., 1970: A statistical analysis of satellite-observed trade wind cloud clusters in the western North Pacific. Atmos. Sci. Paper No. 161, Colorado State University, 80 pp.

Wilson, G. S. and J. R. Scoggins, 1976: Atmospheric structure and variability in areas of convective storms determined from 3-h rawinsonde data. NASA Contractor Report CR-2678, Marshall Flight Center, Alabama, 117 pp.

Vincent, D. G. and L. N. Chang, 1975: Kinetic energy budgets of moving systems: Case studies for an extratropical cyclone and hurricane Celia, 1970. Tellus, 27, 224-235.

Young, H. D., 1962: Statistical Treatment of Experimental Data. New York, McGraw-Hill, 172 pp.

APPENDIX A
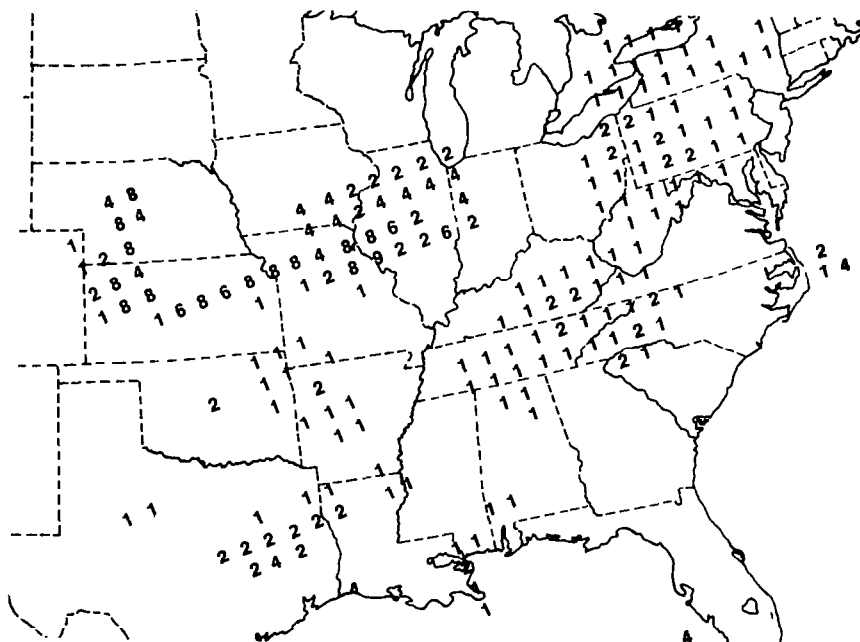
(a)   0000 GMT on 24 April 1975.
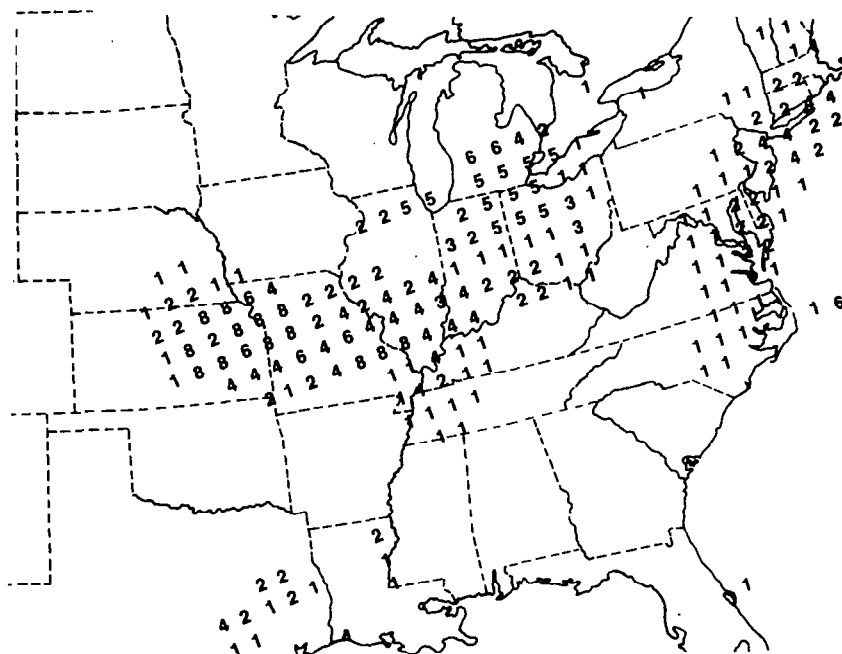
(b)   0600 GMT on 24 April 1975.

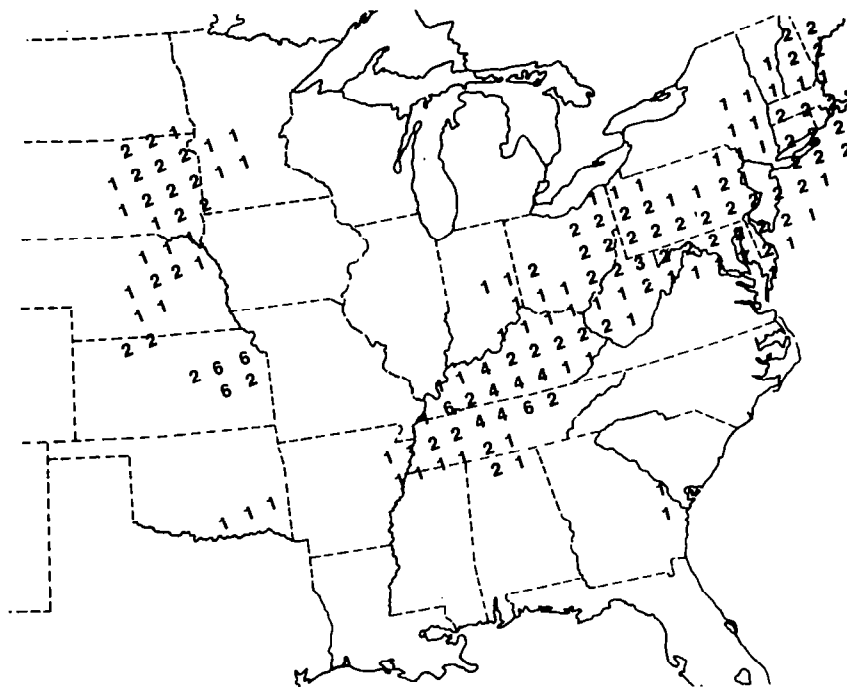Fig. A-1.   Composite fields of MDR data used for AVE IV.
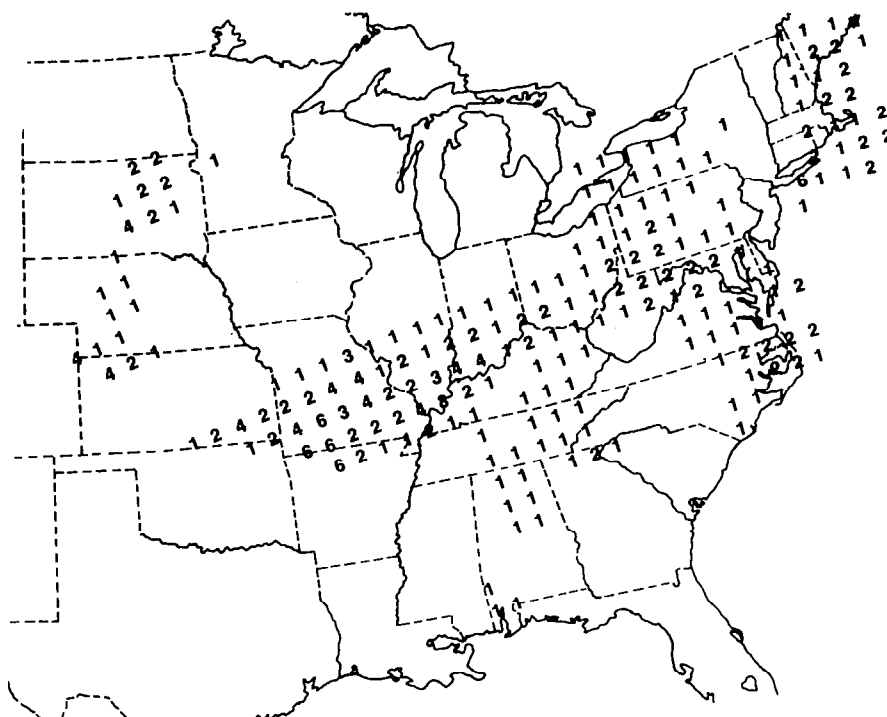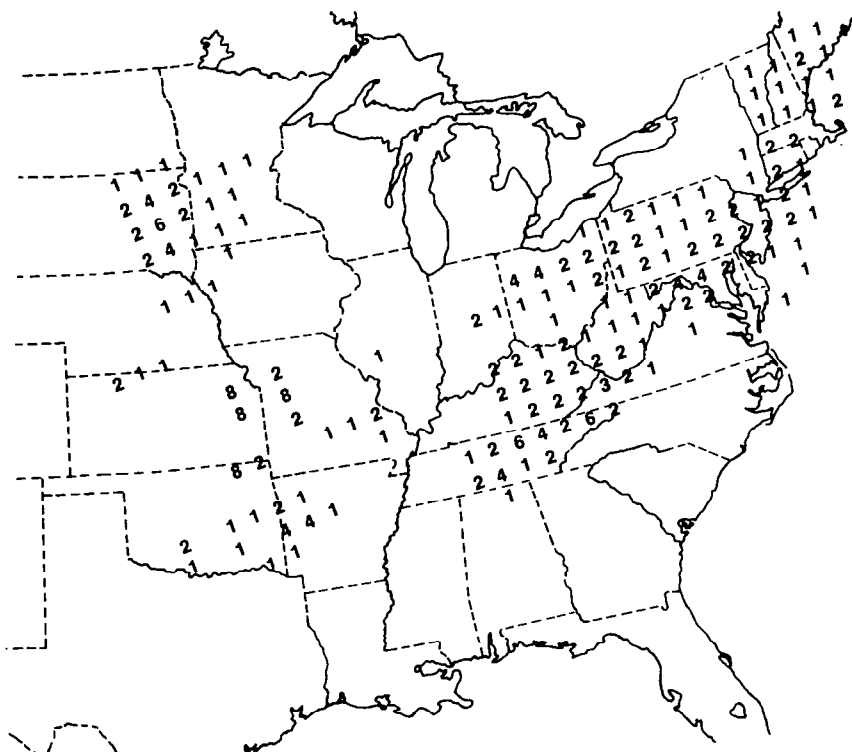
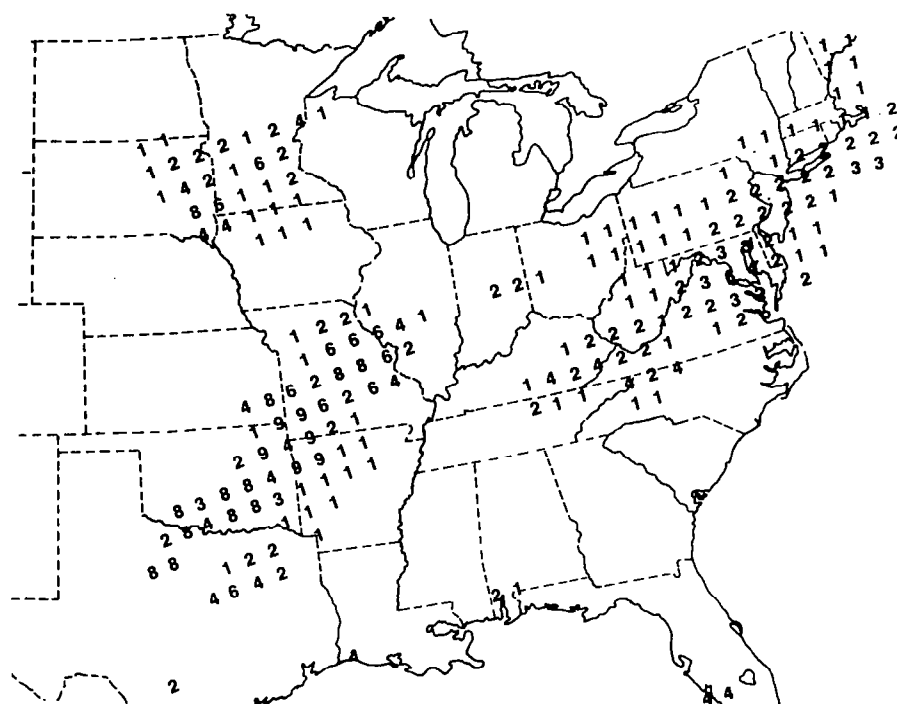(c)   1200 GMT on 24 April 1975.
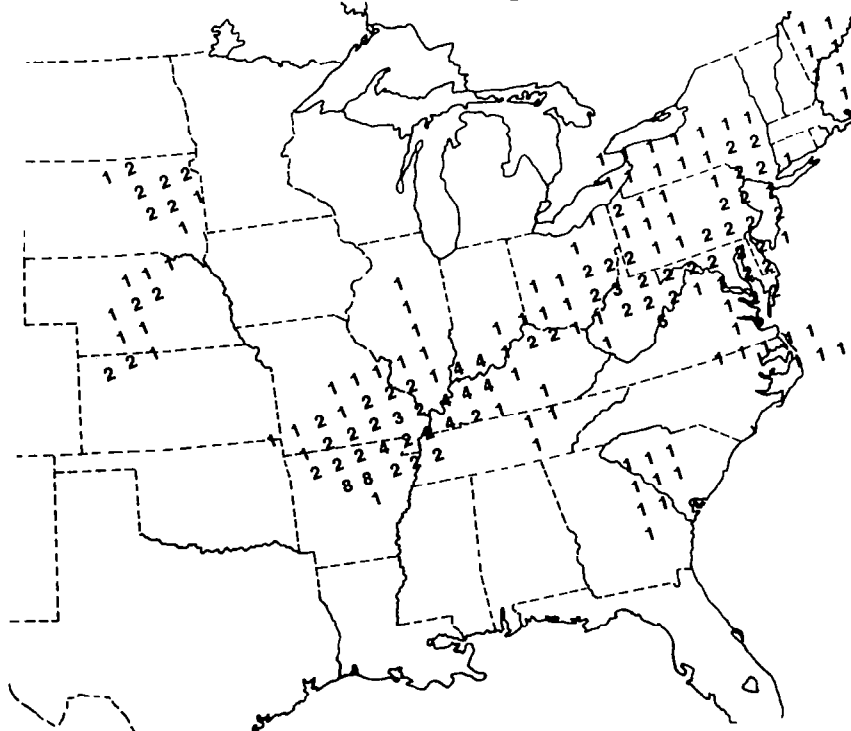
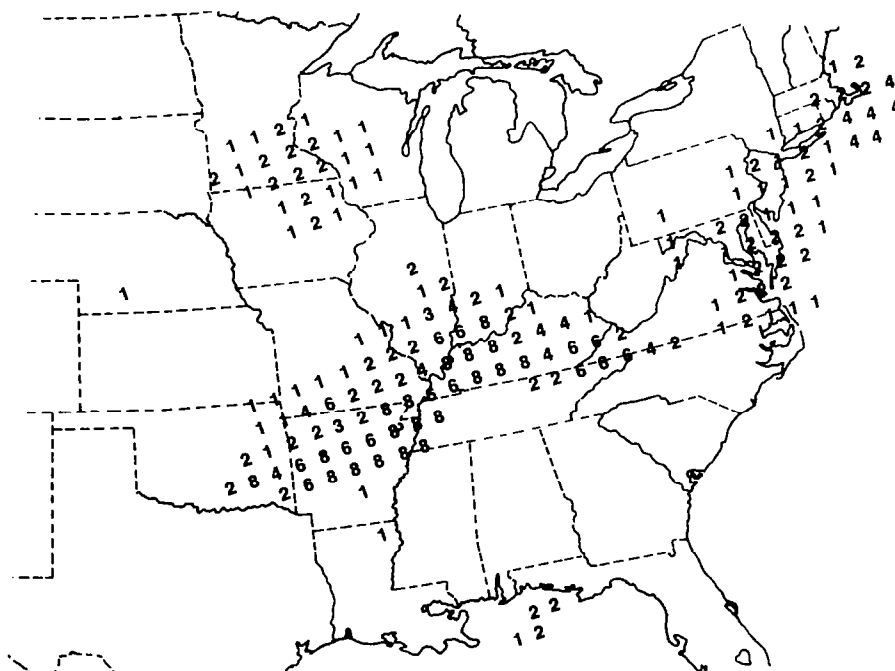(d)   1500 GMT on 24 April 1975.

Fig. A-1.   (Continued)

(e) 1800 GMT on 24 April 1975.

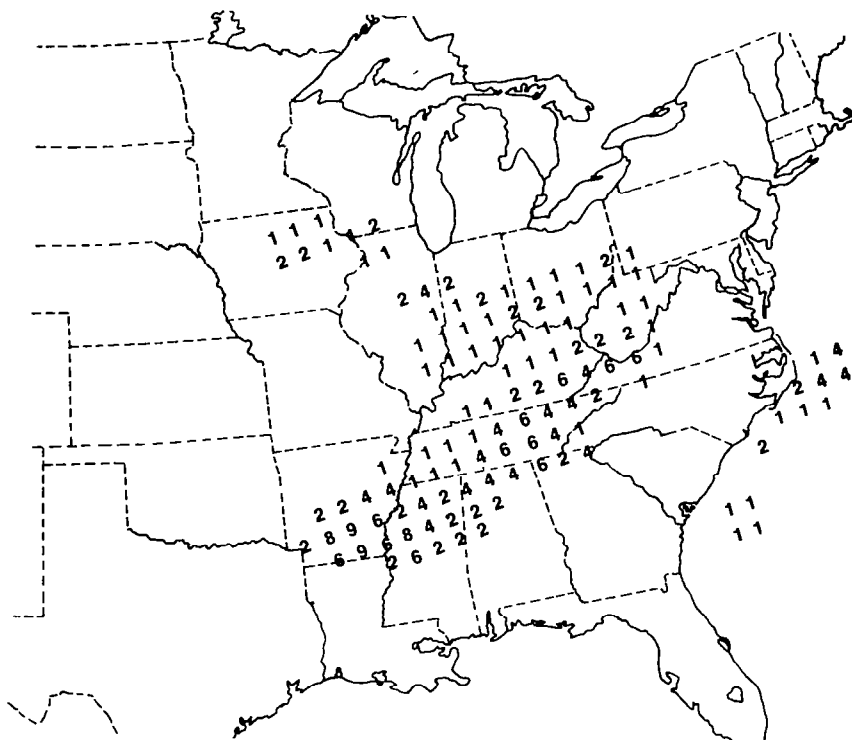(f) 2100 GMT on 24 April 1975.

Fig. A-1. (Continued)

(g)   0000 GMT on 25 April 1975.

(h)   0600 GMT on 25 April 1975.

Fig. A-1.   (Continued)

(i)   1200 GMT on 25 April 1975.

Fig. A-1.   (Continued)

APPENDIX B

SYNOPTIC CONDITIONS

In general, the AVE IV synoptic situation consisted of quasi-stationary systems at the surface, with showers and thundershowers developing along the surface front in response to short wave development in the mid and upper troposphere. Figures B-1 and B-2 give the 850-, 700-, 500-, and 300-mb synoptic charts for 0000 GMT on 24 April 1975 and 0000 GMT on 25 April 1975.

At the beginning of the experiment, 0000 GMT on 24 April 1975, three air mass types were distinguishable at the surface over the AVE IV network. A moist and warm maritime tropical air mass was moving northward over the network with strong southerly flow around a high pressure center (1030-mb central pressure) located about 500 km off the coast of the Carolinas. Maritime tropical air covered almost two thirds of the network extending from central Texas and Oklahoma eastward through all of the Gulf Coast and Middle Atlantic States and northeastward into the Ohio Valley.

A cold front, extending southwestward into Kansas from a moderately strong cyclone (1000 mb center) over northern Michigan, separated the maritime tropical air from the cooler and drier continental polar air moving southward over the northern plain states, while a warm front, extending southeastward from the cyclone into Pennsylvania, separated continental polar air over New England from maritime tropical air over the Ohio Valley. A second cyclone (1000 mb center) was located over central Kansas with a cold front or dry line extending southward into west Texas separating the very dry maritime polar air from the maritime tropical over east Texas. A third weaker cyclone was just entering the network in western Nebraska and South Dakota.

Temperatures over the AVE IV network ranged from 25° C along the Gulf Coast to 10° C in the northern plain states, and dew point temperatures ranged from 20° C to -10° C in the tropical and polar air masses, respectively.

The middle and upper tropospheric flow pattern was basically
zonal during the entire experiment with the polar jet stream ex-
tending roughly west-east from the northern plain states to the
northeast U. S., and the subtropical jet stream, located along the
Gulf Coast, both well defined. Two distinguishable short wave
perturbations (wavelengths $\sim$ 1000 km) moved through the basic
zonal flow during the experiment and were responsible for creating
most of the significant weather.

At the beginning of the experiment, the first short wave
was associated with the cyclone over northern Michigan, and the
second with the developing cyclone in western Nebraska and South
Dakota.

Light rain and rain showers with tops below 8000 m occurred
along and above the warm front associated with the first short
wave as it moved eastward as a stable wave to a position about
250 km off the coast of Maine at the end of the experiment. At
1200 GMT on 24 April, moderately strong thunderstorms formed in
the Ohio Valley along the slowly southeastward moving cold front
associated with the first short wave. By 2100 GMT on 24 April,
a strong squall line had formed from central Tennessee northeast
into western West Virginia with maximum radar tops to 15,000 m;
a tornado watch had been issued for this area three hours earlier.
By 0000 GMT on 25 April, the severe thunderstorms had dissipated
and only weaker shower and thundershower activity was present
over the central Appalachians.

A second area of severe thunderstorm activity at 0000 GMT on
24 April was associated with the cyclone in central Kansas and the
warm front extending northeastward into northern Missouri. A
tornado watch was issued in this area at 0000 GMT on 24 April
and radar tops exceeded 20,000 m. This area of thunderstorms
showed some movement and, by 1500 GMT on 24 April, had moved
about 200 km to the south and decreased in intensity to only
shower activity while the cyclone in central Kansas remained
stationary.

A third area of severe convective activity developed at 0000

GMT on 24 April in western Nebraska and South Dakota in response to the eastward movement of the second short wave. The intensity of the thunderstorm activity decreased from tops up to 16,000 m at 0000 GMT on 24 April to maximum tops of only 10,000 m at 1800 GMT on 24 April, while the entire system and associated short wave moved slowly eastward into the central and eastern Dakotas and Nebraska.

By 2100 GMT on 24 April, the cyclone in central Kansas had begun to intensify and move southeastward into northeast Oklahoma with the eastward movement of the second short wave. Severe thunderstorm activity developed rapidly within the intensifying low and southwestward along the trailing cold front or dry line. Three hours later at 0000 GMT on 25 April, a severe squall line and tornado watch area extended from central Oklahoma into southwest Missouri with maximum tops at 18,000 m.

Between 0000 GMT and 1200 GMT on 25 April the cyclone moved eastward into Kentucky with the eastward movement of the second short wave perturbation, while the associated cold front extended southwestward into Texas. The severe squall line grew in intensity and length with maximum radar tops exceeding 20,000 m and, at 1200 GMT on 25 April, extended along an arc almost 1000 km long from eastern Kentucky southwestward into northern Alabama and westward into Arkansas. Both hail and tornadoes were reported along the path of the squall line.

At the end of the experiment at 1200 GMT on 25 April, the major weather system was a strong squall line moving southeastward into the southeast U. S. while the upper-level flow pattern was developing a trough running north-south through the northern plains. With the developing trough, the surface anticyclone off the Carolinas had moved farther eastward out into the Atlantic and continental polar air was replacing maritime tropical air in the Ohio Valley and the southeast U. S. with the southeastward movement of the cold front.
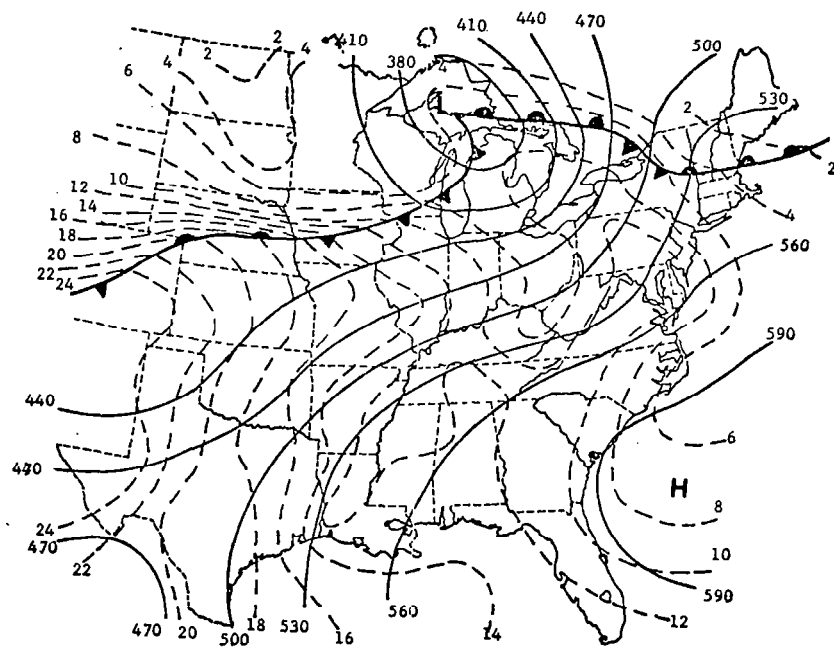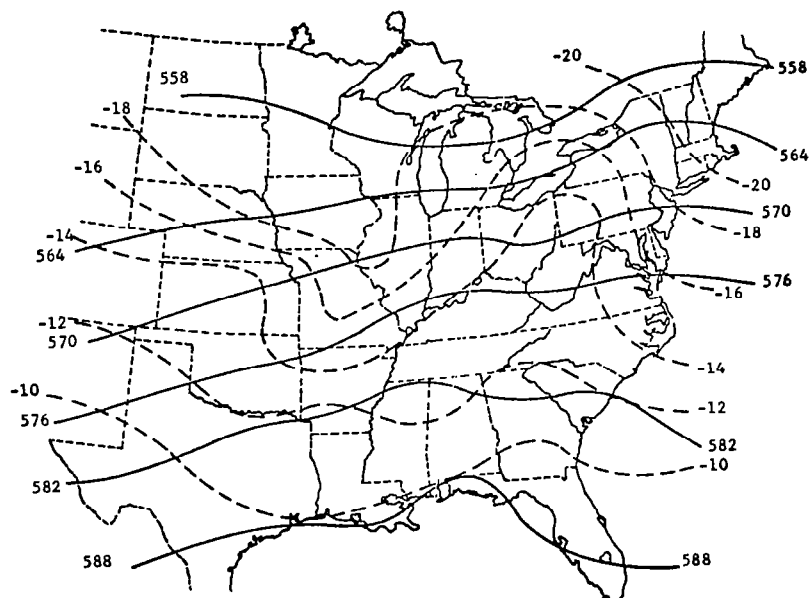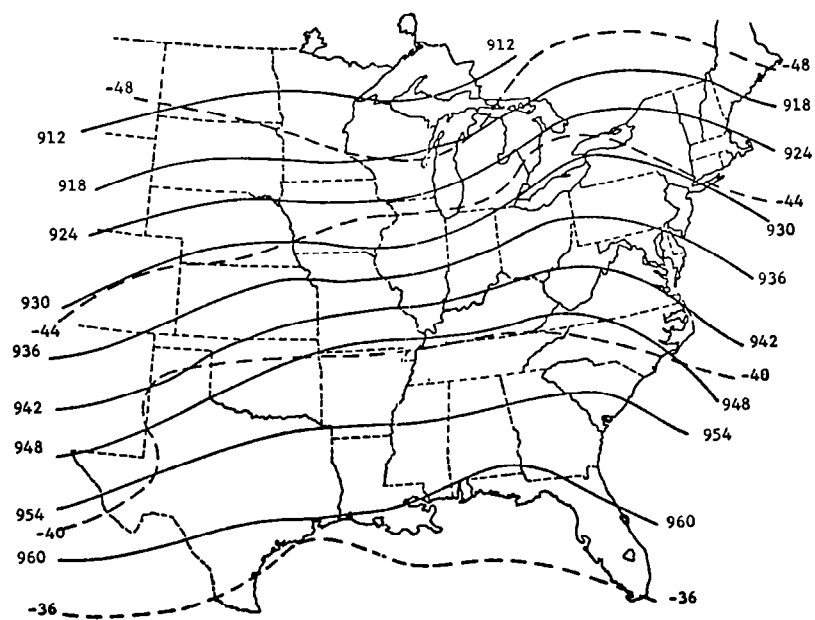
(a)   850 mb.
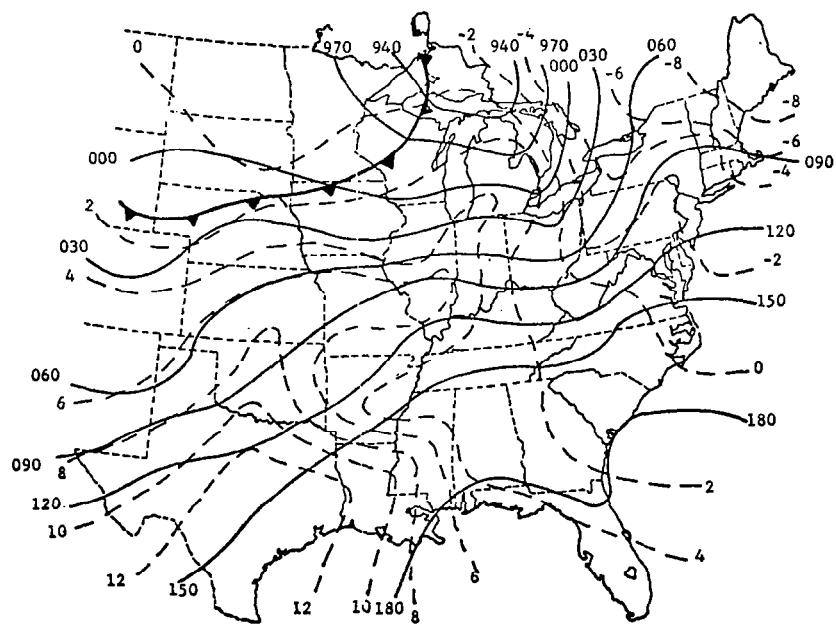
(b)   700 mb.

Fig. B-1.   Synoptic charts for 0000 GMT on 24 April 1975; solid lines, height (gpm), dashed lines temperature (°C).
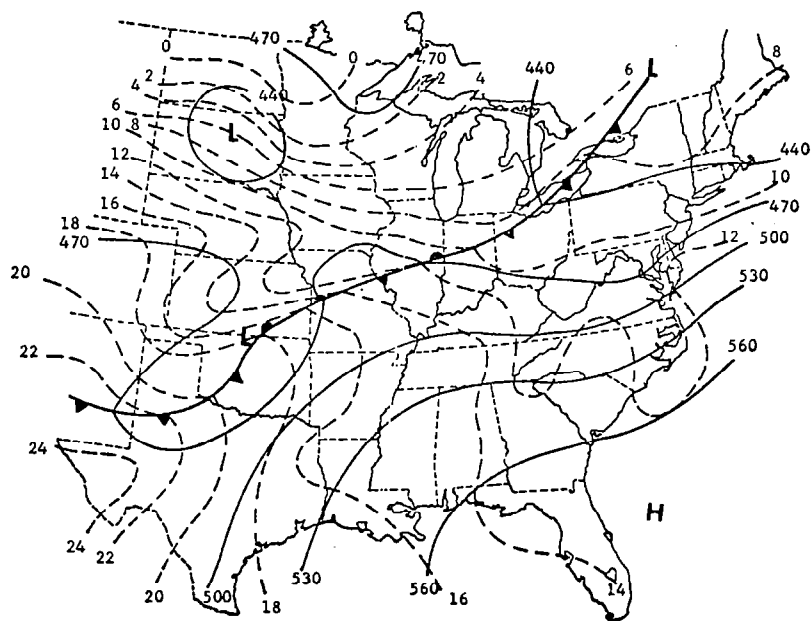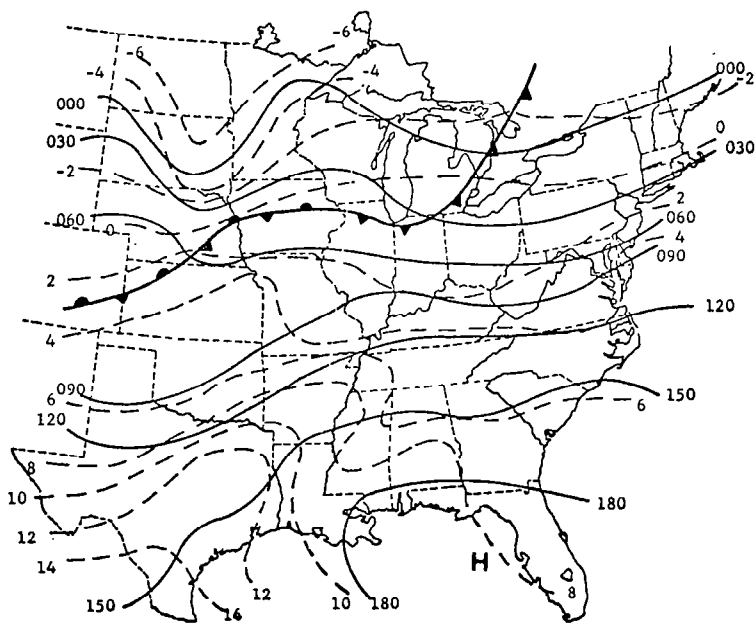
(c)   500 mb.

(d)   300 mb.

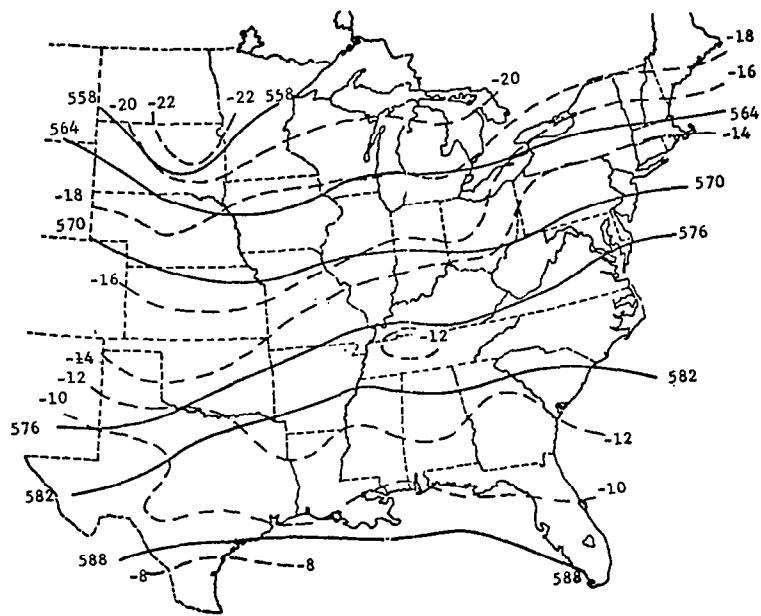Fig. B-1.   (Continued)
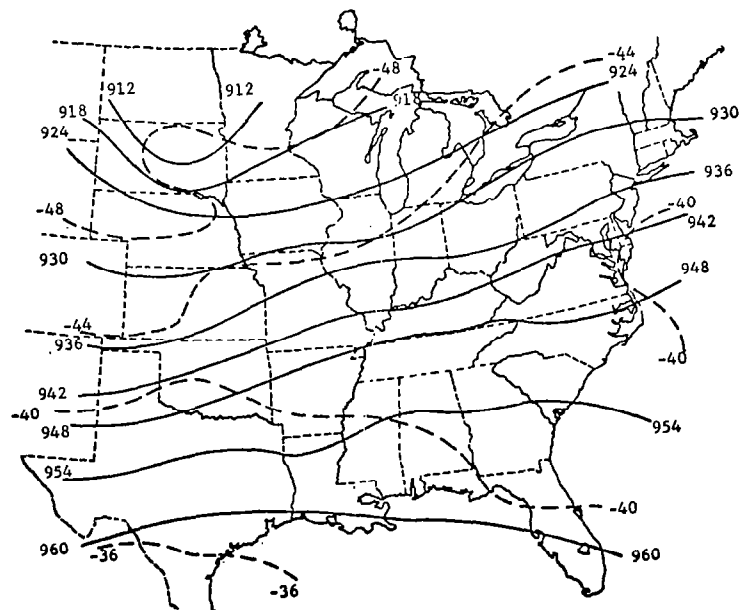
(a)   850 mb.

(b)   700 mb.

Fig. B-2.   Synoptic charts for 0000 GMT on 25 April 1975; solid lines, height (gpm), dashed lines, temperature (°C).

(c) 500 mb.

(d) 300 mb.

Fig. B-2. (Continued)